ÉCOLE POLYTECHNIQUE DE BRUXELLES
UNIVERSITÉ LIBRE DE BRUXELLES

Uncertainty Quantification and Optimization of kinetic mechanisms for non-conventional combustion regimes

Turning uncertainties into possibilities

Thesis presented by Magnus Fürst
in fulfilment of the requirements of the PhD Degree in Engineering Sciences and Technology (ULB - "Docteur en Sciences de l'ingénieur et technologie") & Industrial Chemistry and Chemical Engineering (POLIMI)

Academic year 2019-2020

Supervisor : Professor Alessandro PARENTE
Université Libre de Bruxelles
Co-supervisor : Professor Alessio FRASSOLDATI
Politecnico di Milano

Thesis jury :
Gérard DEGREZ (Université libre de Bruxelles, Chair)
Alberto CUOCI (Politecnico di Milano, Secretary)
Francesco CONTINO (Université catholique de Louvain)
Tamás TURÁNYI (ELTE Eötvös Loránd University)

European Commission

CLEAN GAS

Uncertainty Quantification and Optimization of kinetic mechanisms for non-conventional combustion regimes

A thesis presented by

Magnus Fürst

in fulfilment of the requirements of the PhD Degree in Engineering Sciences and Technology (ULB) and Industrial Chemistry and Chemical Engineering (POLIMI) 31^{st} cycle

Belgium, June 2020

Tutor :
Prof. Alberto Cuoci

Doctoral program coordinator :
Prof. Alessio Frassoldati

Supervisors :
Prof. Alessandro Parente (Univeristé Libre de Bruxelles, Belgium)
Prof. Alessio Frassoldati (Politecnico di Milano, Italy)

Doctoral Committee :
Prof. Gérard Degrez (Univeristé Libre de Bruxelles, Belgium), Chair
Prof. Alberto Cuoci (Politecnico di Milano, Italy), Secretary
Prof. Francesco Contino (Université catholique de Louvain, Belgium)
Prof. Tamás Turányi (ELTE Eötvös Loránd University, Hungary)

Acknowledgements

There are many people whom I would like to thank for their help in getting me to this point, but first and foremost I want to thank my family. My parents, Inger and Göran, for always supporting me throughout the years. It always made me feel closer to home whenever I talked with you, even when I was far away. My brother, Fredrik, for teaching me the first phrase I learned in German.

Then I would like to thank my dear friend Mattias Djerv, who was the person who actually planted the idea of doing a PhD into my head. Then of course Enrico Cresci, for the good times we had in Renningen, and for introducing me to the possibility to come here to Brussels in the first place. Then naturally I would like to thank Professor Parente, for giving me the opportunity to do this PhD, and for helping me throughout these years with building up this work from scratch. There have been moments of hardships, but you always pushed me forward and helped me grow in many ways.

Then I get to my beloved colleagues and friends. Without you, these years would not have been nearly as much fun or stimulating. I would like to thank you all in various ways, starting with Salvatore for picking me up when I first arrived in Brussels and staying a friend since that time. Simone, first of all for feeding me, but also for always giving me something to laugh about. Roberta, for always staying positive. Morabito, again for making me laugh, but also for teaching me Italian in his own special way. Cristina, for all the fun times we have spent together during these years. Guilherme, for all the good laughs and pranks we have pulled on each-other. Marco for the many good times we have spent together. You were always someone I could talk to about anything. Alice, for all of the nice times that we spent together. Riccardo, for helping out with the pranks, but also for being a good friend and colleague. Andrea, for the good times we had, both at and after work. Pedro, for being a good friend and an even better neighbour. Jan, again for all the good times we have spent together. Maryam, for being a nice colleague and caring friend. Bilal, for always staying until the very end. Mariano, for his geographical knowledge about India. Peppe, for being a good friend and an exceptional colleague. Ruggero, for bringing many laughs to the department, just for being you. Arthur, for the nice discussions we have had.

Of course any workplace would not be complete without a kind and welcoming secretary. Shirley has always brought a nice and happy atmosphere to the department. Thank you Shirley.

I would also like to thank my friends and colleagues from Milan. You made my stay there very welcoming and nice in many ways. I want to start with thanking Professor Frassoldati, for always being supportive and helpful. Alberto, for helping me out during some tough times. Isabella, for making me feel welcome from the very beginning, and always staying supportive. Giampaolo, not only for being a good office mate, but also for being a good friend. Alessandro, for all the laughs we have shared together. Giancarlo, for brining laughs to every situation. Paulo, for being supportive and a good friend. Matteo, for the good laughs about a particular rock. Sangi, for being a good colleague and friend. Ghobad, for always being a good friend. Kik, again for being a good colleague and a good friend to talk to.

Last, but definitely not least, I would like to thank with all my heart, *Amore mio*, Marianna Cafiero. You supported me through all the bad times, even before we were together, and I always felt that you were by my side, even if we were apart. I feel immensely grateful that this journey has brought us two together.

This work has received funding from the European Union's Horizon 2020 research and innovation program under the Marie Skłodowska-Curie grant agreement No 643134, and from the European Research Council (ERC) under the European Union's Horizon 2020 research and innovation programme under grant agreement No 714605.

Summary

The usage of novel combustion technologies, such as Moderate or Intense Low-oxygen Dilution (MILD) combustion, in the future energy mix provides both a flexible and reliable energy supply, together with low emissions. The implementation though is highly situational and numerical studies can help in the assessment of said technologies. However, the existing uncertainties in numerical modeling of MILD combustion are quite significant, and as detailed kinetics should be considered while modeling MILD combustion, a major part of this uncertainty can be accredited to the kinetics. Combined with the fact that existing detailed mechanisms have been developed and validated against conventional combustion targets, there exists a gap between the performance of existing mechanism and experimental findings. To handle this discrepancy, Uncertainty Quantification (UQ) and Optimization are highly viable techniques for reducing this misfit, and have therefore been applied in this work.

The strategy applied consisted of first determining the reactions which showed the largest impact towards the experimental targets, by not only considering the sensitivity, but also the uncertainty of the reactions. By using a so-called impact factor, the most influential reactions could be determined, and only the kinetic parameters with the highest impact factors were considered as uncertain in the optimization studies.

The uncertainty range of the kinetic parameters were then determined using the uncertainty bounds of the rate coefficients, by finding the lines which intercepts the extreme points of these maximum and minimum rate coefficient curves.

Based on this prior parameter space, the optimal combination of the uncertain parameters were determined using two different approaches. The first one utilized Surrogate Models (SMs) for predicting the behavior of changing the kinetic parameters. This is a highly efficient approach, as the computational effort is reduced drastically for each evaluation, and by comparing the physically viable parameter combinations within the pre-determined parameter space, the optimal point could be determined. However, due to limitations of the amount of uncertain parameters and experimental targets that can be used with SMs, an optimization toolbox was developed which uses a more direct optimization approach. The toolbox, called `OptiSMOKE++`, utilizes the optimization capabilities of `DAKOTA`,

and the simulation of detailed kinetics in reactive systems by OpenSMOKE++. By using efficient optimization methods, the amount of evaluations needed to find the optimal combination of parameters can be drastically reduced. The tool was developed with a flexibility of choosing experimental targets, uncertain kinetic parameters, objective function and optimization method. To present these features, a series of test cases were used and the performance of OptiSMOKE++ was indeed satisfactory.

As a final application, the toolbox OptiSMOKE++ was used for optimizing a kinetic mechanism with respect to a large set of experimental targets in MILD conditions. A large amount of uncertain kinetic parameters were also used in the optimization, and the optimized mechanism showed large improvements with respect to the experimental targets. It was also validated against experimental data consisting of species measurements in MILD conditions, and the optimized mechanism showed similar performance as that of the nominal mechanism. However, as the general trend of the species profiles were captured with the nominal mechanism, this was considered satisfactory.

The work of this PhD has shown that the application of optimization to kinetic mechanism, can improve the performance of existing mechanism with respect to MILD combustion. Through the development of an efficient toolbox, a large set of experimental data can be used as targets for the optimization, at the same time as many uncertain kinetic parameters can be used contemporary.

Contents

CHAPTER 1

Introduction

The role of energy production is not something often thought about in our daily lives. The fact that the light turns on when we flip the switch is considered undisputable. But where does this energy come from? Depending on where you live, the energy can be produced by many different means, such as wind, solar, hydro, nuclear power or through combustion of hydrocarbons. The implementation of hydro power is extremely case dependent and nuclear power has many drawbacks, not only considering social acceptance. The highly intermittent nature of renewable energy sources, referring to wind and solar, makes it difficult to rely on only these sources for a stable energy supply.

One measure to solve this, is by storing the surplus energy produced in some form. The more direct way would be battery storage, however, this is very expensive and not suitable for long term storage. What instead is appealing is the concept of using the surplus energy from wind and solar to produce fuels through electrolysis. These fuels can then be utilized in combustion, which is very flexible, in a sense that a combustion facility can be turned on/off relatively easily, and constructed at locations most suitable for the end use. However, one drawback of combustion is fuel flexibility. When a facility is designed, normally it is designed for the combustion of one specific fuel, and changing the fuel could be very problematic. As fuels created from electrolysis can consist of a variety of both gaseous and liquid fuels, a flexible combustion process is needed.

Another major drawback of energy production through combustion is related to emissions. By burning hydrocarbons, carbon dioxide (CO_2), nitrogen oxides (NO_x), soot, and other harmful compounds are formed, and if not treated properly, released into the atmosphere. Instead of investing in expensive flue gas treatment facilities, that clean the flue

gases from these harmful compounds, primary measures can be applied, i.e. changing the conditions in the combustion chamber in order to produce less emissions. CO_2 can in one sense be considered as a complete product of the combustion of hydrocarbons, together with water (H_2O). Soot emissions can easily be controlled by ensuring that either non-sooting conditions are used in the combustion zone, i.e. not extremely fuel-rich conditions, or by ensuring that the soot formed is completely oxidized before the flue gases are released into the atmosphere. NO_x emissions on the other hand originate from nitrogen (N_2) from the combustion air which reacts with oxygen (O_2) and intermediate species to form NO_x. It is therefore more difficult to reduce the NO_x emissions from a combustion process, as it is necessary to use air for burning the fuel.

One way to counteract this, is by removing the N_2 from the combustion air, and only feed O_2 into the combustion chamber for the oxidation of the fuel. This is referred to as oxy-fuel combustion, and it is a very effective approach for reducing NO_x emission. However, due to the removal of N_2, the concentration of O_2 in the combustion chamber is increased, which in turn increases the combustion temperature to infeasible values. To circumvent this problem, Exhaust Gas Recirculation (EGR) can be applied to dilute the O_2 stream with combustion products, effectively reducing the combustion temperature. However, these added controls present extra complexity and costs to the facility, as the removal of N_2 from the air, and the EGR, requires additional instruments and energy. There is therefore an overall reduction of efficiency related to oxy-fuel combustion.

Other primary measures for the reduction of NO_x emissions can be considered as following [1]:

— reducing availability of O_2 in the reaction zone

— reducing combustion temperatures

— avoiding peak temperatures

— decreasing residence times at high temperatures

— NO_x reburning

By reducing the availability of O_2 in the reaction zone, the oxidation of the fuel is inhibited which reduces the efficiency of the combustion process. Also a reduced combustion temperature directly affects the efficiency of the process. There is therefore often a trade-off between emission reduction and process efficiency for conventional combustion. To instead achieve all of the five measures listed above, and still keep a high combustion efficiency, non-conventional conditions such as MILD combustion needs to be applied.

MILD stands for Moderate or Intense Low-oxygen Dilution, and was introduced by Cavaliere and de Joannon [2], but the same phenomena was reported using different techniques and names, such as; FLOX (Flameless Oxidation) [3], HiTAC (High Temperature Air Combustion) [4] and Colorless Distributed Combustion (CDC) [5]. According to the definition of MILD combustion, it is reached when the inlet temperature of the reacting mixture is above that of the auto-ignition temperature of the mixture, and when the maximum temperature increase in the system is lower than the auto-ignition temperature of the mixture. A relatively simple way to achieve this is by recirculating the hot combustion products back towards the injected stream, which both preheats and mixes the injected mixture with combustion products, thus also diluting the mixture. These criteria ensures that both the combustion temperatures and peak temperatures are reduced, as well as the

residence time at high temperatures are reduced. Moreover, as the name entails, the concentration of O_2 in the reacting zone is reduced due to the dilution of the reacting mixture. The first criteria in the list above is therefore also satisfied. NO_x reburning is a concept where already formed NO_x react with intermediate species from the fuel combustion at intermediate to high temperatures [6, 7]. Again these conditions are present in MILD combustion due to the effect of the recirculation, and already formed NO_x are recirculated back into the reacting zone, where fuel intermediates are present. The combination of all these facts therefore results in extremely low NO_x emissions from MILD combustion processes.

Furthermore, due to the improved mixing between the fuel and oxidizer, the combustion efficiency is also higher for MILD combustion, compared to conventional conditions.

It should also be noted that as the reaction zone is highly diluted in MILD combustion, the combustion occurs during lean conditions, which directly counteracts the formation of soot, and the emissions of soot are also negligible.

As previously mentioned, future perspectives include having a fuel flexible combustion system. Due to the high inlet temperature and good mixing between the fuel and the oxidizer, ignition of the fuel is assured, as well as a very stable and efficient combustion process. MILD combustion therefore presents a very promising solution to the problem at hand, i.e. flexible energy production with low emissions.

The implementation of such a system is of course situational, and to assess this, numerical modeling, in the form of Computational Fluid Dynamics (CFD) simulations, can be employed. Rather than the more traditional trial-and-error approach, CFD allows for a faster and more cost-effective evaluation of a system. However, numerical modeling of combustion is quite a challenging task, as it is a multiphysics problem and it is commonly subjected to estimations. The predictability is therefore highly dependent on modeling accuracy of the geometry, flow field, heat transfer and/or chemistry. The modeling of chemical kinetics is a particularly challenging task, and as mentioned by Lu and Law [8] the overall simulation cost can roughly be allocated only to the kinetics, as all other components are insignificant with respect to the computational cost of solving the kinetics. The overall simulation cost (C) can be estimated as $C = C_0 + aK + bK^2 + cK^3$, where C_0 is the computational overhead, a, b and c are coefficients related to the rate evaluation, diffusion and Jacobian factorization respectively, and K the number of species in the mechanism. The coefficients (a, b and c) are all case specific, but the strong correlation between the size of the mechanism K and C can still be appreciated from this correlation.

Whether detailed kinetics should be used in CFD simulations depends mostly on which conditions that are simulated. A common criteria to evaluate this, is by estimating the Damköhler number (Da), defined as the ratio between the mixing and chemical time scales [9]. For many conditions, the mixing time scale is significantly higher than the chemical time scale, i.e. the Da is high for these conditions, and detailed kinetics can therefore be neglected. However, in MILD conditions the strong recirculation results in lower mixing time scales due to the good mixing, and at the same time, the dilution increases the chemical time scales, resulting in Da numbers close to unity. This directly indicates that detailed kinetics is important for MILD conditions.

As the usage of detailed chemical kinetics is important for modeling MILD combustion, a lot of uncertainty in numerical predictions can be allocated only to the kinetics. Since each kinetic parameter were determined from experimental measurements, theoretical calculations and/or expert estimations, they could all be considered uncertain to

some degree [10]. For each reaction in a kinetic mechanism, the modified Arrhenius law ($k = AT^{\beta}e^{-E_a/RT}$, where A is the pre-exponential factor, β the temperature exponent, E_a the activation energy, T the temperature and R the ideal gas constant) states that between 1-3 Arrhenius parameters can be added to the pool of uncertain parameters. Considering that pressure dependent reactions, such as fall-off reactions, are included in a kinetic mechanism as well, the amount of uncertain parameters are increased even more. A fall-off reaction is a reaction where the effective rate coefficient is calculated as a blend between the behavior at high and low pressures. At high pressures a fall-off reaction can show one specific trend that can be described by one set of Arrhenius parameters, while at low pressures the behavior is significantly different. Another set of Arrhenius parameters are therefore needed to describe the low pressure behavior. In most cases, additional energy is also needed at low pressures for the specific reaction to occur, which is extracted from a so called third body collision. A species is considered a third body if it stays inert through the reaction process, and only transfers energy to the process. The total amount of uncertain parameters in a kinetic mechanism, considering both pressure dependent and non-pressure dependent reactions, can therefore roughly be estimated as 3 times the number of reactions.

Additionally, as our knowledge of chemical kinetics increases, the size of kinetic mechanisms are growing. The development of kinetic mechanisms of different groups over recent years can be seen in Figure 1.1, where the trend for each group shows an increase of the number of species/reactions, and therefore also the number of uncertain parameters.

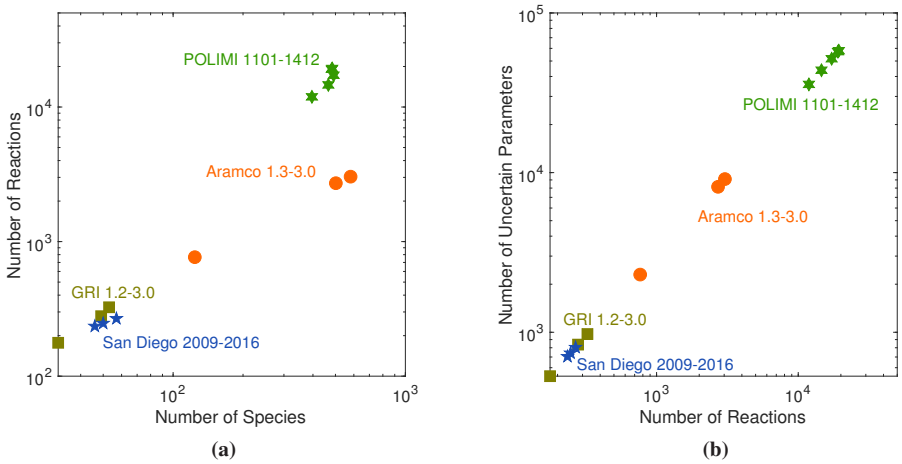

Figure 1.1: *Displaying number of species vs number of reactions (a) for some chemical mechanisms (adapted from [8]), as well as number of reactions vs number of uncertain parameters (b), estimated as 3 × number of reactions. This is applied for several versions of mechanisms from different groups [11–14].*

The problem does not only lie with the number of uncertain parameters, but also the fact that MILD combustion behave chemically differently compared to conventional com-

bustion. Detailed kinetic mechanisms developed and validated for conventional conditions, and are therefore not performing satisfactorily in MILD conditions, and there have been several studies that highlight this. Such as the work from Wang et al. [15], where the chemical and thermal effects of CO_2 and H_2O on methane counter-flow diffusion flames were studied. They saw an especially large thermal effect of CO_2 on the flame temperature in this study.

In both the works from Sabia et al. [16] and Lubrano Lavadera et al. [17], the effect of CO_2 and H_2O on propane oxidation in MILD conditions were evaluated. They saw a strong effect of CO_2 on the system, and not only considering the thermal effect, due to the high heat capacity of CO_2, but also a large impact of the interaction of CO_2 and H_2O as third body species, at low to intermediate temperatures. It was also highlighted in Lubrano Lavadera et al. [17] that there exists a large discrepancy between the values of the third body efficiencies of CO_2 in different detailed chemical mechanism. In the work of Sabia et al. [18], the difference in chemical pathways between conventional and MILD conditions were highlighted for the oxidation of biomass pyrolysis products, as well as the effect of third body efficiencies. These are but some works that highlights the discrepancy between the performance of existing detailed chemical mechanism in MILD conditions, and experimental findings.

Considering all these open issues, i.e. need for detailed kinetics while simulating MILD combustion, large number of uncertain parameters in detailed kinetics, and finally the fact that existing detailed kinetic mechanisms are under-performing in MILD conditions, a promising approach would be to use Uncertainty Quantification (UQ) and/or Optimization techniques, in order to improve the performance with respect to these conditions.

1.1 UQ and Optimization of kinetic mechanisms

Imagining that a simulation code can be considered as a black box, where one set of input parameters results in one output value, as illustrated in Figure 1.2a (where the input parameters in this case refers to kinetic parameters). The model output can then be compared to the experimental value in the output space and a quantitative evaluation of the mechanisms performance can be made, for one specific design point.

However, in the case of kinetic mechanisms, the values of the input parameters are not fixed and there exists an uncertainty in the input parameter space. This uncertainty can be propagated towards the output space (Figure 1.2b), and the accuracy of the mechanism can be evaluated, considering the uncertainty of the input parameters. This is referred to as forward UQ and can be used to determine which parameters contribute to the largest discrepancy in the predictions, as well as to determined the accuracy of the mechanism, considering also the uncertainty of the parameters. Consequently, this information can be used to evaluate which parameters needs further analysis, in order to reduce the output uncertainty of the mechanism.

Instead of propagating the input parameter uncertainty to the output space, the information regarding the experimental data can be used to restrict the input parameters in order to ensure that the predictions lay within the experimental uncertainty. This can be done by solving what is mathematically called an inverse problem, or in this case inverse UQ. Here the experimental data, with corresponding uncertainty, is used to determine which

combination of input parameters that predict the experimental data within the experimental uncertainty (Figure 1.2c). For a simple case, this may be feasible to achieve, but as the number of experimental data increases, so does the number of input parameters that are influential for these conditions. The problem therefore quickly arrives with more input parameters than constraints, and no single combination of the parameters can satisfy all the experimental constraints [19]. Nevertheless, an inverse UQ procedure can be used to derive useful statistical information regarding the input parameters, constraining the uncertainty range of the input parameters and providing useful information for further kinetic mechanism development.

Rather than constricting the uncertainty range of the input parameters, it would be useful to find one optimal point in the input parameter space, with respect to the experiments. This optimal point would allow the model to predict the experimental data "best", considering both the uncertainty of the input parameters and the experimental data (see Figure 1.2d). This optimal point can be found through many different methods, but in principle the optimal point is that which allows for a minimum or maximum of a specified objective function (see Section 2.3). Depending on the problem at hand, the absolute optimum is very difficult to find, if not impossible for some cases.

All the concepts described above, i.e. black box modeling, forward UQ, inverse UQ and optimization, are illustrated graphically in Figure 1.2.

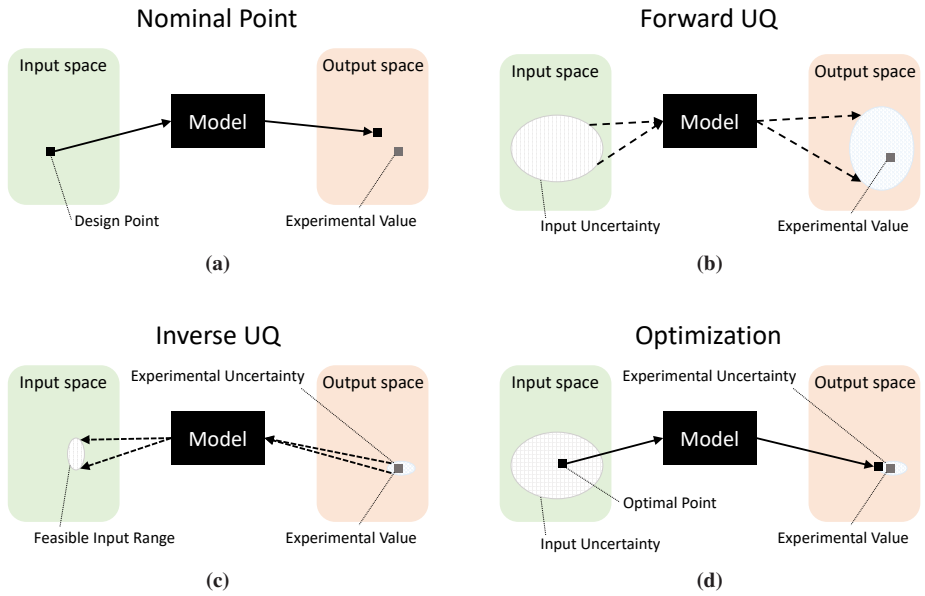

Figure 1.2: *Graphical representation of a black box model (a), forward Uncertainty Quantification (b), inverse Uncertainty Quantification (c) and Optimization (d). Adapted from Tamás Turányi [20].*

It should also be mentioned that the cases described above, i.e forward UQ, inverse UQ and optimization, considers that the kinetic mechanism used is complete and is able

to physically predict the output. However, if a kinetic mechanism is incomplete, i.e. some crucial reaction pathways are missing, then the aforementioned approaches should be used with caution, as it is easy to arrive with an unphysical mechanism. Nevertheless, these approaches can still be used in order to determine if a mechanism is complete or not. By using experimental targets of similar nature, the inability to predict some experimental targets can in many cases be explained by missing reaction pathways. It is therefore important to always use a mechanism which has been developed and validated for fuels and conditions similar as to that of the targets.

1.1.1 Literature review

Forward UQ, inverse UQ and optimization of kinetic mechanisms have been applied in numerous works for different fuels, conditions, and experimental targets. Listed here are but a few of them, but they still represent the application of aforementioned techniques on kinetic mechanisms. For simplicity they are divided into forward UQ and inverse UQ/optimization, as the later two often are combined.

Forward UQ

The work of Habib Najm and co-workers [21–24] has applied forward UQ on kinetic mechanisms for several different systems and for different fuels, by using Polynomial Chaos Expansion (PCE) methods for propagating the uncertainties of the kinetic parameters. Through this, they were able to highlight how the uncertainty of some specific kinetic parameters contributes to the uncertainty of the mechanism as a whole, and also providing information regarding which reaction rates could use further experimental investigation, for reducing this prediction uncertainty.

The application of forward UQ of kinetic mechanisms has also been applied by Turányi and co-workers [25] where the effect of kinetic and thermodynamic parameter uncertainties were evaluated for methane flames. They later extended this to both local and global uncertainty analyses of different systems in [26–29]. In these works they were able to determine the key kinetic and thermodynamic parameters, which were significantly influencing the simulation results.

Another application of forward UQ to combustion chemistry can be found in the works of Alison Tomlin and co-workers [30–34], where global sensitivity analysis studies of kinetic mechanisms in different systems, were performed. By using a High Dimensional Model Representation (HDMR), they determined the combined effect of changing parameters from more than one reaction. Through these studies they were able to identify key reactions which needed further studies and through high level quantum chemistry and transition-state theory calculations for these reactions, they were able to improve the performance of existing mechanisms.

Inverse UQ/Optimization

The application of inverse UQ to kinetic mechanisms has been performed in numerous works available in the literature, but one of the first can undoubtedly be accredited to Michael Frenklach [35–40]. Frenklach applied Surrogate Models (SM) (see Section 2.4) for predicting the behavior of the model with respect to a large set of experimental

targets, and a feasible set was found in the parameter space by solving an inverse UQ problem. This was developed into the Bound-to-Bound Data Collaboration (B2B-DC) approach [38] where not only the feasible set was found, but also the optimal point within this set (see Figure 1.2d). The target parameters, called active parameters, consisted mostly of pre-exponential factors (A), some enthalpies of formation and third body efficiencies. This resulted in the widely known GRI mechanisms [41–43]. The relatively small size of the GRI mechanisms, and their performance for natural gas in conventional combustion conditions, proved to be a very effective combination, as they are still used today in a large extent.

Building on the approach established by both Frenklach and Najm, Hai Wang and David Sheen developed the Method of Uncertainty Minimization using Polynomial Chaos Expansions (MUM-PCE) [44,45]. The approach is again based on representing the parameter uncertainties through a set PCE, and by combining this with a model representation using SMs, they were able to solve the inverse-UQ problem. By applying a least-squares optimization approach (normalized with the standard deviation of the experimental targets) they were able to determine an optimal mechanism, with new restricted input parameter uncertainties. The MUM-PCE approach has been applied in several works [46–50] for the optimization of kinetic mechanisms for different conditions, but still the optimization was restricted to only A factors. Only in recent works [49,50] has some third body efficiencies and activation energies (E_a) been added to the optimization procedure.

Liming Cai and Heinz Pitch [51–54] utilized the MUM-PCE approach for the optimization of rate rules. As rate rules are used for sorting reactions which behave in a similar way, the change of one rate rule will bring a direct change to several reactions, and it is a very efficient approach for the development of mechanisms for fuels with large molecules and therefore also many reactions. In these works [51–53], only the A factors were used in the optimization, and the optimal point was found based on the least-squares, normalized with the standard deviation of the experiment, and a secondary term that penalized large changes to the A factors. This ensured that optimization was achieved with minimal changes to the nominal parameters. Recently, in vom Lehn et al. [54], they extended their work to additionally optimize some thermochemical quantities, such as enthalpies of formation for some species, in combination with some A factors.

By considering all three Arrhenius parameters (A, β and E_a), as well as third body efficiencies, Turányi and co-workers [55–61] have also had success in optimizing kinetic mechanisms. By first determining the joint probability distribution of each uncertain reaction they try to find the optimal combination of parameters by sampling these distributions, and the combination which results in the lowest so-called Error function [62] is considered the optimum. Their approach is based on using both direct and indirect experimental data for the optimization, where direct data refers to experimental and theoretical estimations of a single rate coefficients, and indirect data refers to experimental measurements which are influenced by several reactions, e.g. Ignition Delay Time (IDT) and Laminar Flame Speed (LFS). Depending on the complexity of the target fuel and simulation, they used a combination of direct simulations and SMs in the form of orthonormal polynomials [56–59], for the optimization.

Although SMs present a highly efficient approach for optimization, the highly complex, and non-linear nature of mechanism optimization presents challenges in accurately predicting the response with SMs. The above mentioned applications which used SMs,

used mainly A factors as uncertain variables. The SMs therefore only had to predict the linear nature of the Arrhenius law at the most, which is feasible. However, as the SMs have to start predicting the highly non-linear nature several β and E_a parameters adds to the problem, a SM quickly starts to loose accuracy. Rather than using SMs for representing the response of the mechanism, each change to the mechanism can be evaluated directly, thus removing the approximation error that the SMs adds. However, the amount of evaluations needed to find the global optimum can add up to millions if the full parameter space should be covered completely. Sophisticated optimization algorithms can be used instead, which finds potential optimums within the parameter space, based on the information given by previous evaluations. This drastically reduces the number of evaluations needed to find the global optimum. One such algorithm which is very suited for global optimization of such complexity is Genetic Algorithms (GA) or Evolutionary Algorithms (EA). It is a global non-gradient based optimization approach, which will be described in more detail in 2.5.2. The first application of GA to mechanism optimization was Polifke et al. [63], which optimized two- and three-step mechanisms for lean-premixed laminar methane flames, by matching the performance of the global mechanisms with a detailed mechanism. Elliott and co-workers thereafter applied GA for the optimization of kinetic parameters for different fuels [64–67]. They even applied GA for optimizing a reduced mechanism, targeting the performance of the original mechanism [68]. Building on the approach of Elliott [68], Perini et al. [69] developed an automated mechanism reduction and optimization approach, where a reduced and optimized mechanism was determined iteratively by first reducing and then optimizing the reduced mechanism using GA, targeting the performance of the full mechanism. Sikalo et al. [70] also applied a similar approach of mechanism optimization of a reduced mechanism. However, in order to reduce drastic changes to kinetic parameters, a penalty function was introduced, which increased the objective function value if large changes to the kinetic parameters were foreseen. By doing this, they were able to arrive with a reduced optimized mechanism, with minimum amount of changes to the kinetic parameters.

The application of optimization techniques in different forms has also been applied with respect to global mechanisms for MILD combustion [71–75]. Kim et al. [71] and Tu et al. [73] compared different existing global mechanisms and applied some manual modifications to some reactions to achieve better agreement with respect numerical predictions of MILD combustion using CFD. Wang et al. [72] and Hu et al. [74] used results with the GRI 3.0 mechanism [43] from a Plug Flow Reactor (PFR) to manually tune the kinetic parameters in global mechanisms to improve the performance with respect to MILD and MILD oxy-combustion, where MILD oxy-combustion is a combination of oxy-fuel and MILD combustion. More recently, Si et al. [75] used a Artificial Neural Network (ANN), trained with respect to changes in the kinetic parameters of a global mechanism, and optimized to match the species profiles of the GRI 3.0 mechanism [43] in different PFR simulations. In this work, rather than changing kinetic parameters manually, the training data for the ANN was achieved with random samples from the parameter space. However, no systematic control of the consistency of the kinetic mechanism was performed in Si et al. [75], which can result in infeasible rate coefficient values for the optimized mechanism. This is further discussed in Section 2.2.1.

1

1.2 Objectives of this work

In order to strive towards more flexible, and less polluting energy production, non-conventional combustion technologies such as MILD combustion can be used. To evaluate the feasibility of such a technology, numerical simulations are needed for cost-efficient performance predictions. However, detailed kinetic mechanisms are needed to accurately predict the complex behavior of MILD combustion. This brings a large amount uncertainty to the simulations in the form of kinetic parameters, which are all uncertain to some extent. The work in this thesis has therefore focused on developing a strategy for the Uncertainty Quantification (UQ) and optimization of detailed kinetic mechanisms with respect to non-conventional, or MILD, combustion.

As with any UQ or optimization works, key reactions for the conditions at hand has to be determined, considering mainly their influence on the numerical predictions. Additionally, the uncertainty range of each kinetic parameter has to be defined, and the optimal combination of the uncertain parameters has to be found within this parameter space.

The feasibility of this was evaluated using a Surrogate Model (SM) based optimization approach (see Chapter 3). However, the application of optimization with respect to a larger set of uncertain kinetic parameters and experimental data requires a more efficient approach. A toolbox was therefore developed for the optimization of kinetic mechanisms (see Chapter 4). The toolbox was validated for a series of different conditions, considering different types of experimental targets. Finally, the application of the toolbox to a large set of experimental targets of propane combustion in MILD conditions was applied (see Chapter 5).

CHAPTER 2

Methodology

This chapter aims to briefly discuss the different methodologies applied in this work. The optimization strategies applied can be divided into two different categories; surrogate model based UQ and optimization, and direct optimization. With direct optimization referring to methodologies which does not utilize surrogate models for estimating the behavior of the model, but instead directly evaluates the effect of each change of the uncertain parameters. The later strategy was realized by developing a toolkit called `OptiSMOKE++`, which will be discussed in detail in Chapter 4.

2.1 Selection of uncertain parameters

The first step in any UQ or optimization study is always to determine which parameters that should be considered. For some cases, where a mechanism consist of only a small amount of parameters, such as global mechanisms which consist of only a few reactions, the complete set of parameters can be considered in the study. However, for larger chemical mechanisms, the amount of parameters quickly increases, and it would be infeasible to consider all parameters in an UQ/optimization study. It is therefore necessary to distinguish which parameters that are most influential for the conditions at hand.

2.1.1 Local sensitivity analysis

The most straightforward approach for determining if a parameter is influencing the results or not, is that of a brute force sensitivity analysis. Here each parameter is changed

slightly and the response with respect to the Quantity of Interest (QoI) is evaluated. This is what is referred to as local sensitivity analysis [10], and can be formulated as:

$$S_{ij} = \frac{\partial Y_i}{\partial x_j} \tag{2.1}$$

where S_{ij} is the sensitivity coefficients, Y_i is the QoI of condition i and x_j is a kinetic parameter of index j. However, the unit of these sensitivity coefficients are not universal, as they depend on both Y_i and x_j. It is therefore not possible to compare two sensitivity coefficients if either the QoI, or the kinetic parameter considered, is different. To circumvent this problem, the normalized sensitivity coefficients should be used. Here the sensitivity coefficients (calculated with Eq. 2.1) is normalized with the nominal values of Y_i and x_j as:

$$S_{ij} = \frac{\partial Y_i}{\partial x_j} \cdot \frac{x_j}{Y_i}. \tag{2.2}$$

This ensures that each sensitivity coefficient in the sensitivity matrix S_{ij} are comparable and the parameters which are most influential for each condition can be determined.

As already mentioned in Chapter 1, the number of parameters in a kinetic mechanism quickly increases with the number of reactions, which consequently increases the computational effort of the sensitivity analysis. To avoid this drastic increase in computational cost, only the pre-exponential factor (A) of each reaction is commonly used for the sensitivity analysis of kinetic mechanisms. This saves a lot of computational effort, and still gives an indication of which reactions that are most influential for the conditions at hand. Eq. 2.2 therefore becomes:

$$S_{ij} = \frac{\partial Y_i}{\partial A_j} \cdot \frac{A_j}{Y_i} \tag{2.3}$$

where the index j in this case represents the reaction number in the mechanism used.

It should also be mentioned that for some conditions, it is more beneficial to normalize the sensitivity coefficients with respect to the maximum value of the QoI. This is especially applicable for when the QoI consists of mass or mole fractions of species, which can approach values close to/or zero. The sensitivity coefficient is therefore artificially increased due to the normalization, which is unwanted, and the maximum value of the QoI should be used instead:

$$S_{ij} = \frac{\partial Y_i}{\partial A_j} \cdot \frac{A_j}{max(Y_i)} \tag{2.4}$$

Global sensitivity analysis

A local sensitivity analysis considers only the linear effect of changing one kinetic parameter at a time. For most cases, as mentioned above, only the pre-exponential factor is considered in local sensitivity analyses of kinetic mechanisms. However, to capture the non-linear response of changing other kinetic parameters, as well as the effect of changing more than one kinetic parameter, a global sensitivity analysis is needed. A global sensitivity analysis does not only take into account small changes to one single parameter, but changes several parameters at the time, and through the response with respect to the QoI, the parameters specific, or joint, contribution to the prediction uncertainty of the mechanism can be determined. This is of course a very computationally expensive procedure, as each added kinetic parameter increases the number of combinations that should

be evaluated by a factor of three (considering that each parameter can assume a nominal value, $\pm$ a percentage change). The number of possible combination of parameters in a global sensitivity study can therefore be determined as 3^j, where j is the number of kinetic parameters. This quickly becomes infeasible due to the large amount of parameters in a kinetic mechanism (see Figure 1.1b). The total number of evaluations can be reduced by only considering a subset of the total amount of parameter combinations as done in Valkó et al. [76]. Here response surface techniques (see Section 2.4) were also used to reduce the computational effort needed. However, when comparing the results of the local and global sensitivity analyses, the same set of influential reactions could be found using both approaches. Although the specific order of the reactions were not the same, the qualitative information regarding which reactions that are important could still be considered the same. Similar results were obtained by Zádor et al. [27], where both local and global uncertainty analyses were compared for methane flames.

An efficient approach for determining global sensitivity coefficients was also proposed by Bruno Sudret [77], where he used a Polynomial Chaos Expansion model to analytically determine the variance of the model and attribute that to the input parameters. This approach of variance-based sensitivity analysis is often called Sobol' indices [78] and the approach of Sudret [77] has been used in several works in the scope of UQ and optimization [79, 80]. However, Sudret [77] mentioned that this approach is particularly efficient for a low number of input parameters, specifically less than 10. The application of this approach to kinetic mechanisms was therefore not considered, as the amount of uncertain parameters quickly reaches the limit of 10, proposed by Sudret [77].

Considering all this, it was considered sufficient to use the information from only the local sensitivity analysis in this work, in order to save both computational effort and to include a large set of parameters. However, it should be mentioned that the additional information gained from global sensitivity analysis could prove important as the complexity of the optimization increases and it will be more crucial to restrict the optimization only to the most influential kinetic parameters. This can partly be seen in Chapter 5, were some parameters used in the optimization did not prove to be influential.

2.1.2 Impact factor

The sensitivity indices indicates which reactions that have the largest influence with respect to the QoI, but this effect is based on only a small change in the pre-exponential factor (for local sensitivity analysis) of the reaction. Considering that the influence is also proportional to the change of the parameter, the effect of changing a specific parameter is also correlated to the physical limits of the parameter. If a reaction is highly sensitive to the QoI, but the allowed change of the reaction parameters are small with respect to other reactions, the total effect would not necessarily result in a large change of the QoI. The total impact of a specific reaction is therefore not only related to the sensitivity, but also to the uncertainty correlated to that reaction.

Warnatz [81] introduced another index, which also considers the uncertainty of the reaction by multiplying the absolute value of the sensitivity coefficient with the uncertainty parameter for each reaction:

$$I_{ij} = |S_{ij}| \cdot f_j \tag{2.5}$$

where I_{ij} is referring to this index for condition i and reaction j, S_{ij} are the normalized

sensitivity coefficients and f_j the uncertainty parameter for reaction j. Warnatz used this measure for determining which reactions that needed more experimental work, but later Frenklach [40] started using this measure for determining which reactions that should be considered in an optimization study. He referred to this index as "impact factor", but it has also been referred to as "sensitivity uncertainty index" [25] and "optimization potential" [51, 52]. In this work it will be be referred to as impact factor from now on, and as will be seen, also used to determine the reactions for the optimization studies.

2.1.3 Cumulative function

With either the sensitivity coefficients, or the impact factors, the important reactions for each condition i can be determined. However, to narrow down the list to a set of overall important reactions either the average index for each reaction can be considered (see Section 3.2.1), or a cumulative function of either the sensitivity or the impact factor indices can be constructed. The cumulative function is constructed by summing up the indices of each reaction over the complete set of conditions, and by normalizing all these values with the maximum, a value between 0-1 can be assigned to each reaction. By specifying a cut-off threshold ϵ, each reaction with a normalized cumulative value above ϵ will be considered in the optimization. An example of such a curve can be seen in Figure 2.1 below.

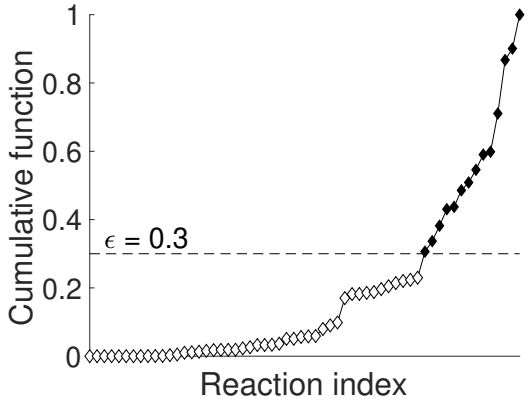

Figure 2.1: *Example of a cumulative function, where the white and black diamond scatter represents the reactions which are below and above the cut-off of ϵ=0.3, respectively. It should be noted that the Reaction indexes are not necessarily ordered in ascending order on the x-axis, but according to the reactions specific cumulative function value.*

2.2 Uncertainty range of the kinetic parameters

After the most influential reactions with respect to the conditions at hand are determined, the next step would be to determine the limits of these parameters. The direct

upper and lower bounds of the Arrhenius parameters are not normally given, instead the limits of the rate coefficient (k_{min} and k_{max}) are often specified for specific temperature ranges. These can be determined using the spread of available direct experimental data or theoretical estimations of the rate coefficient value, available in the literature. The nominal rate coefficient value (k_0) is determined such that the limits are symmetrically located around k_0 on a logarithmic scale. Based on this, the uncertainty parameter (f) can be defined as:

$$f = log_{10}\left(\frac{k_0}{k_{min}}\right) = log_{10}\left(\frac{k_{max}}{k_0}\right) \tag{2.6}$$

or by only using the extreme values of the rate coefficient (k_{min} and k_{max}), f can be determined as:

$$f = 0.5 \cdot log_{10}\left(\frac{k_{max}}{k_{min}}\right). \tag{2.7}$$

Based on this, the physically viable values of the rate coefficient for each reaction can be determined. To correlate this to the Arrhenius parameters on the other hand is not as straightforward as it would seem. As the parameters are strongly correlated, the combined effect of changing two parameters could either enhance, or cancel out, the effect of the change on the rate coefficient. However, by considering the extreme curves of the rate coefficient, Fürst et al. [82] defined a procedure which can be utilized for determining the extreme values of each Arrhenius parameter:

(a) Firstly, only the pre-exponential factor A is considered uncertain, which then corresponds to an uncertainty range equal to the extreme curves k_{min} and k_{max}.

(b) If either β or E_a are equal to zero, the range of the second non-zero parameter can simply be determined with the extreme points, $k_{min}(T_{max})$ with $k_{max}(T_{min})$ and $k_{max}(T_{max})$ with $k_{min}(T_{min})$, where T_{min} and T_{max} were taken as a large range (300 - 2500 K) to ensure a large validity of the mechanism.

(c) Otherwise the range of β is evaluated by fixing the activation energy E_a to its nominal value, as well as letting A be unknown. Then by using the extreme points defined by the temperature range and the maximum and minimum rate coefficient curves, the maximum and minimum β values can be found. The range of A determined in this step is not considered, because the range determined in step (a) is used for this parameter.

(d) Finally, the range of the activation energy E_a, is determined similarly as for β in step (c), using the extreme points. However, this time the temperature exponent β is fixed to its nominal value and A is still considered unknown. Again, the range of A determined in this step is not considered.

An example of this procedure can be seen in Figure 2.2, where the extreme curves (determined through steps (c) and (d) above) for the rate coefficient for reaction CH_4 + $OH \rightarrow H_2O$ + CH_3 are plotted, as well as the k_0, k_{min} and k_{max} curves.

It should be noted that this approach of determining the specific parameter bounds assumes no correlation between the different parameters.

2.2.1 Ensuring physically viable values

Although the ranges of each parameter can be determined through the approach described above, a change in two or more parameters can still result in a rate coefficient

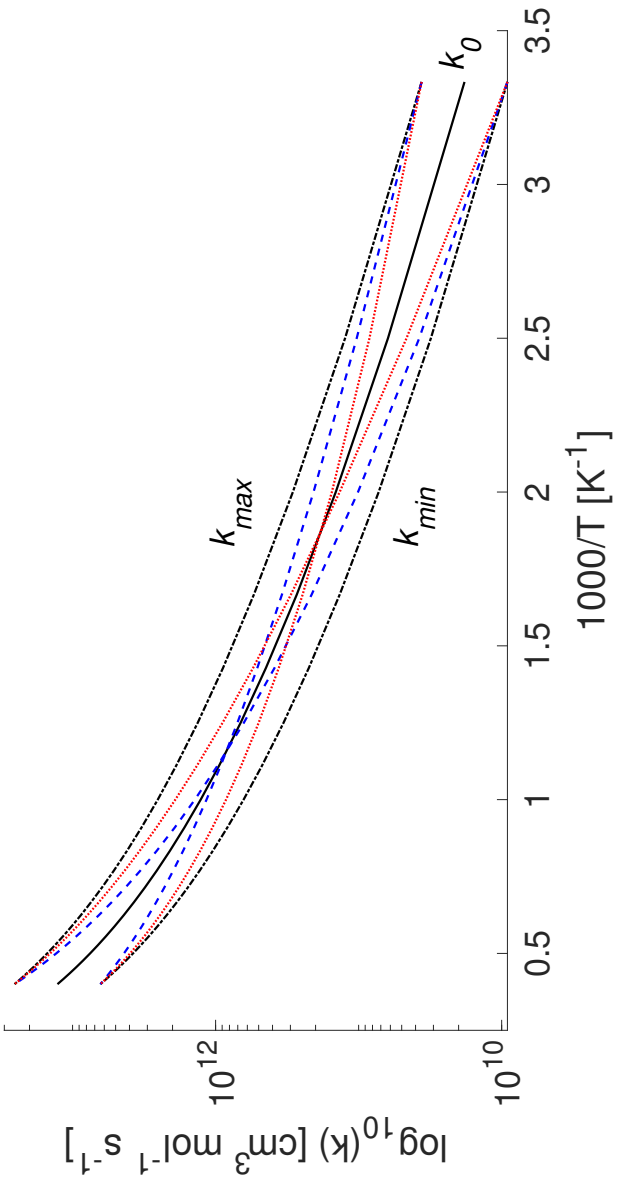

Figure 2.2: *Rate coefficient for reaction CH_4 + OH $\rightarrow$ H_2O + CH_3 where the black solid line (—) corresponds to the nominal curve from the POLIMI C1-C3 [83] mechanism and the black dashed-dotted lines (-·) corresponds to the extreme curves k_{min} and k_{max}, while the blue dashed lines (- -) corresponds to the extreme curves for the temperature exponent β and the red dotted lines (···) corresponds to the extreme curves for the activation energy E_a, derived from the approach described in the text.*

value outside of the extreme curves (k_{min} and k_{max}). It is therefore important to always double check the rate coefficient, to ensure that the suggested combination of parameters allows for physically viable values. An *a posteriori* check of the rate coefficient is therefore necessary, and only the combination of parameters which satisfy this criteria should be considered viable candidates for the optimal solution.

2.3 Objective function

In any optimization problem, the optimal solution is always determined based on the objective function (Obj). This is a measure which determines how close the current evaluation (Y^{sim}) is to the experimental targets (Y^{exp}). There exists many different ways to calculate the objective function in an optimization problem, but arguably one of the most common is the L2-norm, also referred to as Least Squares (LS). Here the residual between between the experimental data Y^{exp} and the simulated value Y^{sim}, are squared for each data point (j) in each data set (i):

$$Obj = \sum_{i}^{N} \sum_{j}^{N_i} (Y_{ij}^{exp} - Y_{ij}^{sim})^2 \tag{2.8}$$

where N refers to the total number of data sets and N_i the number of data points in data set i.

This approach has been used in many works, but this is basically weighing each experimental point equally against each-other. Instead if one experimental data point has a large uncertainty correlated to it, it would be beneficial to say that this experimental target should have less weight in the objective function, and vice versa for experimental points with small uncertainty. This effect can of course be achieved by a weighted LS definition, and as first introduced in [84], the weight can be directly correlated to the experimental uncertainty by dividing the residual in Eq. 2.8 with the standard deviation (σ), giving:

$$Obj = \sum_{i}^{N} \sum_{j}^{N_i} \left(\frac{Y_{ij}^{exp} - Y_{ij}^{sim}}{\sigma_{ij}} \right)^2 \tag{2.9}$$

By weighing the residuals with σ, experimental data with large uncertainty have a lower impact in the overall sum.

In order to avoid that data sets with a large number of data points becomes overly important, it is also important to weigh the objective function based on the number of data points in each data set. The objective function for each data set is therefore divided by the number of data points in each specific data set (N_i), thus removing the bias towards data sets with many experimental targets. Eq. 2.9 therefore becomes:

$$Obj = \sum_{i}^{N} \frac{1}{N_i} \sum_{j}^{N_i} \left(\frac{Y_{ij}^{exp} - Y_{ij}^{sim}}{\sigma_{ij}} \right)^2 \tag{2.10}$$

The determination of the standard deviation is in this approach is crucial for the value of the objective function. As stipulated by Olm et al. [59], the standard deviation can be

estimated as a combination of the standard deviation based on the reported experimental errors (σ_{exp}) and the standard deviation calculated based on the experimental scatter (σ_{stat}):

$$\sigma = \sqrt{\sigma_{stat}^2 + \sigma_{exp}^2} \tag{2.11}$$

where σ_{exp} is calculated based on how many standard deviations the experimental error represents, i.e.

$$\sigma_{exp} = \frac{Y^{exp} \cdot \varepsilon}{X} \tag{2.12}$$

where ε is the reported relative experimental error and X is the number of standard deviations that the experimental error represents. If no specific information regarding how many standard deviations the experimental error represents was given, it was assumed to be 2 standard deviations in this work.

For many cases, only the experimental error is given together with the experimental values. With no repetition of the experimental points, the statistical standard deviation cannot be determined, and the total standard deviation can then be estimated as only the σ_{exp}.

Another common definition of the objective function is the L1-norm, or also called Least Absolute Deviation (LAD). Here the absolute value of the residual is used instead of the square of the residual. This approach has been used in several works [65–67, 69] with some modifications, but to stay consistent, the following form of the L1-norm was used:

$$Obj = \sum_{i}^{N} \frac{1}{N_i} \sum_{j}^{N_i} \frac{\mid Y_{ij}^{exp} - Y_{ij}^{sim} \mid}{\sigma_{ij}} \tag{2.13}$$

As mentioned in Olm et al. [85], for experimental targets that have a scatter proportional to the experimental value itself (more specifically data such as Ignition Delay Time (IDT)) the objective function should be calculated using the natural logarithm of the experimental and simulated values, i.e. $Y_{ij}^{exp} = ln(y_{ij}^{exp})$ and $Y_{ij}^{sim} = ln(y_{ij}^{sim})$, where y_{ij}^{exp} and y_{ij}^{sim} refers to the absolute experimental/simulated value for data set i and point j. This ensures that the objective function is more evenly distributed between the data points, and it will be easier to achieve overall improvements for each point, rather than only for some. For other experimental targets, such as species concentrations and laminar flame speeds, the objective function is calculated directly based on the absolute value of the experimental and simulated values, i.e. $Y_{ij}^{exp} = y_{ij}^{exp}$ and $Y_{ij}^{sim} = y_{ij}^{sim}$. For the specific cases where $Y^{exp} = 0$, which can occur for species concentrations, the σ_{exp} from Eq. 2.12 is assumed to be one in order to avoid numerical issues in Eq. 2.10 and 2.13.

2.4 Surrogate models

An optimization study usually consists of hundreds or thousands of evaluations. By comparing them based on the objective function value (see 2.3), the evaluation which shows the lowest value can be considered the optimal one. Due to the large amount of evaluations needed, also a large computational cost should therefore be expected. One way to speed up this process is by reducing the computational effort for each single evaluation by utilizing Surrogate Models (SMs), also referred to as Response Surface Models (RSMs)

or solution mapping, approaches. SMs are approximations of how the actual model would behave with specific parameter changes, and the computational cost is just a fraction of the time needed by the actual model for one evaluation. It is therefore very common to use SMs in combination with optimization studies.

A SM is built up by using a set of known model outputs and parameter values, and based on these, the SM can predict what the model output would be at another location in the parameter space. The accuracy of these predictions can be more or less precise depending on both the number of samples used for the construction, and the strategy used for creating the SM. Some common strategies for SMs are; Polynomial Chaos Expansion (PCE) [86], Gaussian Process interpolation (GP)/Kriging [87, 88] and High-Dimensional Model Representation (HDMR) [89]. In this work, the application of Kriging for the optimization of a chemical mechanism has been performed (see Chapter 3). A more detailed description of the Kriging approach is therefore presented below.

2.4.1 Kriging

The basic concept of Kriging states that the target $y(\mathbf{x})$ can be described as a combination of a regression (or trend) function $f(\mathbf{x})$, and a residual function $Z(\mathbf{x})$ [90] as:

$$y(\mathbf{x}) = f(\mathbf{x}) + Z(\mathbf{x}) \tag{2.14}$$

where $\mathbf{x}$ represents the variable vector. The regression function $f(\mathbf{x})$ can universally be expressed as a weighted linear combination of a set of polynomials:

$$f(\mathbf{x}) = \sum_{i=1}^{p} \alpha_i b_i(\mathbf{x}) \tag{2.15}$$

where b represents the basis functions with power base of p and α the weights, which are determined by Generalized Least Squares (GLS). However, as choosing the regression function is quite challenging, one can assume a constant known regression function, called *Simple* Kriging, where it is usually set to zero, i.e. $f(\mathbf{x}) = 0$. Another common approach is to assume a regression function of order zero, called *Ordinary* Kriging, giving $f(\mathbf{x}) = \alpha$.

The residual function $Z(\mathbf{x})$ is modelled as a Gaussian process with mean 0, variance σ^2 and a correlation matrix $\mathbf{\Psi}$:

$$\mathbf{\Psi} = \begin{bmatrix} \Psi(x^1, x^1) & \cdots & \Psi(x^1, x^n) \\ \vdots & \ddots & \vdots \\ \Psi(x^n, x^1) & \cdots & \Psi(x^n, x^n) \end{bmatrix} \tag{2.16}$$

where Ψ are the correlation functions and n represents the number of observations. A common description of the correlation function is the so called powered-exponential:

$$\Psi(x, x') = exp\left(-\sum_{i=1}^{d} \theta_i \mid x_i - x_i' \mid^{\gamma} \right) \tag{2.17}$$

where x and x' represents two points in the input parameter space, with d dimensions. The correlation therefore only depends on the distance between these two points, and the rate

of which the correlation is related to the distance is defined by both γ and θ. γ determines how the initial drop in the correlation changes with the distance, and $\gamma = 2$ (also called Gaussian correlation function) is often used, assuming a smooth change in the correlation function. θ on the other hand determines the rate of which the correlation changes with the distance, and consists of a set of hyper-parameters that are usually determined using Maximum Likelihood Estimation (MLE).

Finally, the prediction of the target at any point $\mathbf{x}^*$ in the input parameter space can be expressed as:

$$y(\mathbf{x}^*) = \mathbf{b}(\mathbf{x}^*)^\intercal \alpha + \mathbf{r}(\mathbf{x}^*)^\intercal \mathbf{\Psi}^{-1}(y(\mathbf{x}) - \mathbf{F}\alpha) \tag{2.18}$$

where$\mathbf{b}(\mathbf{x}^*)$ is the vector of basis function evaluations at point $\mathbf{x}^*$, α is the vector of weights used for the regression function in Eq. 2.15, $\mathbf{r}(\mathbf{x}^*)$ is the correlation vector between the observed points $\mathbf{x}$ and point $\mathbf{x}^*$, $\mathbf{\Psi}$ is the correlation matrix from Eq. 2.16, $y(\mathbf{x})$ is the vector of observed targets at $\mathbf{x}$ and $\mathbf{F}$ is a matrix of the basis functions evaluated at the observed locations, i.e:

$$\mathbf{F} = \begin{bmatrix} b_1(\mathbf{x}^1) & \cdots & b_p(\mathbf{x}^1) \\ \vdots & \ddots & \vdots \\ b_1(\mathbf{x}^n) & \cdots & b_p(\mathbf{x}^n) \end{bmatrix} \tag{2.19}$$

One thing to note is that once $\mathbf{\Psi}$, $\mathbf{F}$ and α have been determined based on the observed values, they remain constant and Eq. 2.18 can be simplified to:

$$y(\mathbf{x}^*) = \mathbf{b}(\mathbf{x}^*)^\intercal \alpha + \mathbf{r}(\mathbf{x}^*)^\intercal \mathbf{g} \tag{2.20}$$

where $\mathbf{g}$ contains these constants.

2.5 Optimization algorithms

In order to reduce the amount of evaluations needed in a direct optimization approach, sophisticated optimization algorithms can be used. An optimization algorithm tries to find the optimal point in the parameter×objective function space based on existing evaluations, with the smallest amount of total evaluations possible. There exists many different approaches in the literature, some more suited for the problem at hand, i.e. kinetic mechanism optimization, than others. In this sections two global optimization approaches used in this work (see Section 4.6.1) will be described in more detail.

2.5.1 DIviding RECTangles (DIRECT) algorithm

As the name entails, the DIRECT [91] algorithm divides the parameter search space into different rectangles. Each rectangle is then evaluated based on the center point, and the different rectangles are divided into promising and non-promising regions (promising where the objective function is small). In the promising regions, local optimization approaches are used, i.e. one parameter is changed at the time, while for the non-promising regions, a global approach is still applied to ensure that a global optimum is not overseen. The procedure of dividing the rectangles are then repeated each iteration and further division into promising and non-promising regions are made until a stopping criteria has

been reached. A graphical representation of how three iterations steps with the DIRECT algorithm in a 2D parameter space can be seen in Figure 2.3.

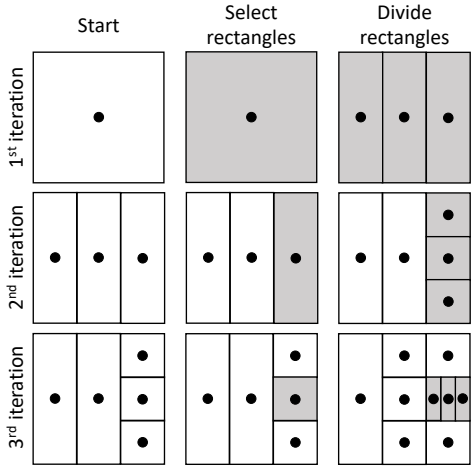

Figure 2.3: *Three iteration steps in a 2D parameter space of the DIRECT algorithm. The shaded and white areas represent the promising and non-promising regions respectfully. Adapted from [92].*

Here the shaded areas represent the promising regions, where a local optimization approach is used, and the white areas are the non-promising areas where a global optimization approach is applied. In the last step, it can be seen that even-though the central rectangle is not considered as a promising region, it is still divided into sub-rectangles. This is done to keep a global aspect of the optimization, which can also be controlled by specifying a so-called global balance parameter. This parameter determines if a small rectangle can be subdivided or not, based on the ratio between the size of the small rectangle and the size of the largest rectangle. If this ratio is greater than this specific threshold, the small rectangle can be subdivided. This further ensures that no region is overlooked, and that a global minima is found. This combination of local and global optimization approaches has proven to be highly efficient for engineering optimization problems.

2.5.2 Evolutionary Algorithm (EA)

Based on the evolutionary theory by Darwin, EA follows the rule of survival of the fittest, and a logical workflow can be seen in Figure 2.4. EA starts off by creating an initial population of individuals from random samples. Each individual consists of a parameter combination which are evaluated and the objective function (see Section 2.3) is calculated. Each individual is thereafter ranked against each-other, and the "best" individuals are kept in the population, and through crossover and mutation new individuals are created from the "best" individuals. These new individuals are then added to the population, replacing the worst ranking ones from the previous population. This is repeated until a predetermined stopping criteria has been reached. Crossover refers to the procedure of combining the

features of two individuals, called parents, and create children which potentially have a lower objective function value than the parents. Mutation, or small changes, to the children is added in order to increase the diversity of the population and to avoid falling into local minima.

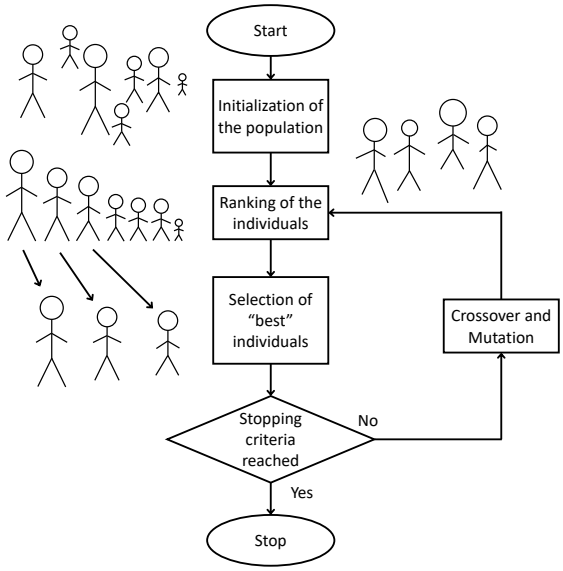

Figure 2.4: *A graphical representation of the workflow of an Evolutionary Algorithm.*

CHAPTER 3

Optimization of a chemical mechanism for MILD conditions

This chapter describes the application of UQ and optimization on a kinetic mechanism with respect to MILD combustion. These results were published in Fürst et al. [82] and it was the first time a large scale optimization study was performed on a detailed kinetic mechanism with respect to MILD combustion conditions.

3.1 Experimental data

The experimental targets used in this chapter are from Sabia et al. [93] and Sabia et al. [18]. The data consists of Ignition Delay Time (IDT) data from a Plug Flow Reactor (PFR) for two different fuels, methane (CH_4) and biomass pyrolysis products. The reference composition of the biomass pyrolysis products was: 1% C_2H_4, 2% C_2H_6, 10% CH_4, 25% CO, and 62% CO_2. The PFR has a length of 1.4 m and internal diameter of 0.01 m. The experiments were performed at C/O ratios between 0.025-0.2 and oxygen ratios (Ω) [94] between 0.9-1, and each condition was evaluated at different inlet temperatures ranging from 1130 to 1400 K.

The PFR was enclosed inside a heater to reduce heat losses, and the surrounding temperature was set to that of the inlet. The overall heat transfer coefficient was estimated in Sabia et al. [93] to be 100.4 W/(m^2K). The mixture of fuel and combustion air was diluted with nitrogen (N_2) to a total of 85% for the CH_4 cases and 90% for the biomass pyrolysis product cases. The usage of Ω for the biomass pyrolysis products data was due to the

presence of partially oxidized compounds in the fuel, and according to Mueller et al. [94], gives a more accurate description of the characteristics of the mixtures.

In the experiments, the ignition delay time was calculated as the ratio between the distance where the temperature was 10 K higher than the inlet temperature and the velocity. The same definition was applied in the present work for a direct comparison between the experimental data and the simulation results. The temperature was measured along the reactor axis with thermocouples of type N every 0.05 m. The experimental uncertainty was estimated on the basis of the displacement of the thermocouples and the inlet velocity of the mixture [18, 93].

The experimental conditions were simulated using the open-source software OpenSMOKE++ [95] for non-isothermal and non-adiabatic conditions. According to Sabia et al. [93] the Reynolds number is higher than 3000 for the experiments, which verifies the plug flow assumption in the model.

As mentioned by Sabia et al. [93], some of the experimental conditions for the methane data showed a transitional ignition behavior, where a first stable ignition condition was established experimentally, and then a shift towards slower ignition occurred. This behavior was more prominent at high C/O ratios and at high inlet temperatures, and is the reason why two significantly different IDT values are presented for some conditions in Figure 3.1d. The average value between the two IDTs were used as targets in the optimization for these data.

3.2 Choice of mechanism

As there are many different detailed chemical mechanisms available in the literature, an initial screening was performed in this work in order to find the mechanism which is predicting the trend of the experimental data most accurately. The mechanisms used for this study are listed in Table 3.1, together with reference, number of species, number of reactions and average deviation from the experimental data. The deviation was calculated as the absolute difference between the experimental and the simulated values, for each experimental point, divided by the experimental value in that point.

Table 3.1: *List of chemical mechanism used in this work with, reference, number of species, number of reactions and average absolute deviation from experimental data [18, 93].*

Mechanism	Reference	Nr species	Nr reactions	Av. abs. dev. [%]
Aramco1.3	[96]	124	766	50.06
Aramco2.0	[97]	502	2716	43.97
Galway Natural Gas	[98]	293	1593	44.19
GRI 2.11	[42]	49	279	67.53
GRI 3.0	[43]	53	325	67.86
POLIMI C1C3 LT	[83]	107	2642	39.66
San Diego 2016-12-14	[14]	57	268	77.86
Zhukov	[99]	549	2518	66.57

The results from the simulations can be appreciated in Figures 3.1-3.2 in so-called

Arrhenius plots, where the IDT is presented in the logarithmic scale on the y axis and the x axis is represented by 1000 divided by the inlet temperature of the mixture.

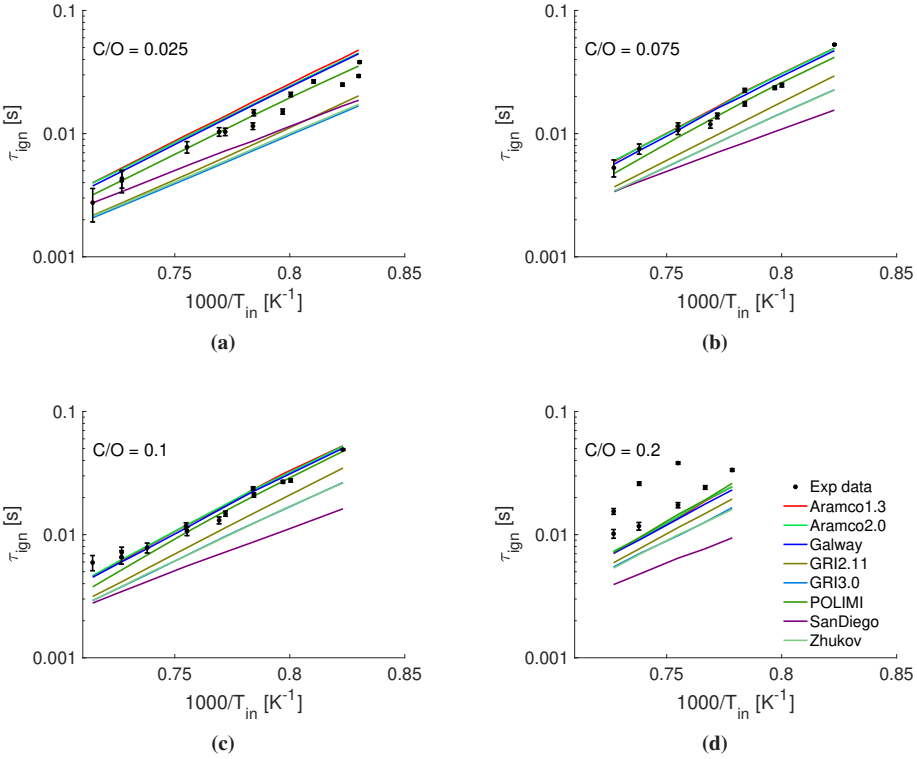

Figure 3.1: *IDT for methane at different inlet temperatures for C/O = 0.025-0.2. Experimental data are represented by points with corresponding error bars, while simulation results for the different mechanisms are presented by the colored lines.*

Based on the average deviation, the POLIMI [83] mechanism was chosen for the continued evaluation.

3.2.1 Parameter selection

As mentioned in Chapter 2, the choice of which parameters to consider in the optimization study is an important task. In this chapter the selection of parameters were done by ranking the reactions from the mechanisms based on an averaged impact factor (see Section 2.1.2). An initial screening of the 20 reactions with the highest absolute value of the sensitivity coefficients, at each of the conditions considered, resulted in 42 different reactions. The sensitivity indices were determined with respect to temperature, and the uncertainty parameters were primarily extracted from the Baulch et al. [100] database, but if a reaction was not listed in [100], estimations of the uncertainty parameter based on data from the NIST Chemical Kinetics Database [101] were made. The average impact factor

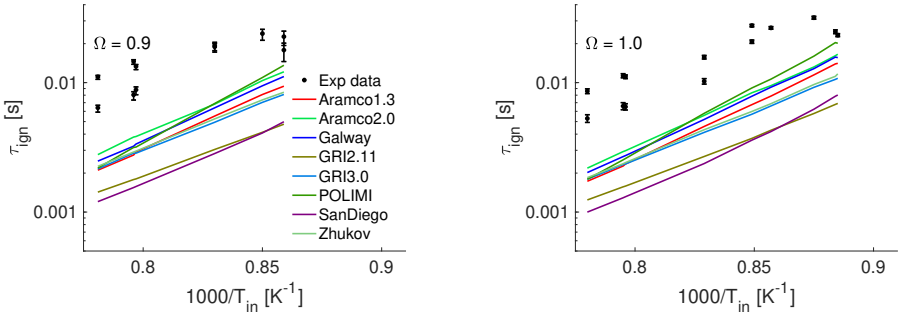

(a) **(b)**

Figure 3.2: *IDT for biomass pyrolysis products at different inlet temperatures for* Ω = *0.9 and 1. Experimental data are represented by points with corresponding error bars, while simulation results for the different mechanisms are presented by the colored lines.*

for these 42 reactions can be seen in Figure 3.3, where they are ranked in descending order.

To reduce the number of parameters evaluated in this study, an initial evaluation of the top five reactions was performed, to determine if the prior uncertainty range for each reaction was enough to cover the complete range of the experimental uncertainty. This was performed in a so-called forward UQ study, where the individual uncertainty of each reaction was propagated to the output of the model, which in this case refers to the IDT. If the prior uncertainty range for a specific reaction was not sufficient enough, that reaction was not considered in the optimization process.

This study showed that reactions R229 ($O_2 + CH_3 \Leftrightarrow O + CH_3O$) and R513 ($CH_3OO \Leftrightarrow CH_2O + OH$) had very small impact on the prediction of the IDT, especially for the biomass pyrolysis products cases, even though their global impact factor ranking was high. Reactions R1 ($O_2 + H \Leftrightarrow O + OH$), R271 ($HO_2 + CH_3 \Leftrightarrow OH + CH_3O$) and R405 ($CH_4 + H \Leftrightarrow H_2 + CH_3$) on the other hand showed large prior uncertainty ranges on the IDT predictions with respect to all of the experimental data.

Reaction R1 ($O_2 + H = O + OH$) is indeed very influential in the ignition process as it is a branching reaction which creates two highly reactive radicals (O and OH), and although the uncertainty parameter for this reaction is quite low, i.e. $f = 0.2$, even small changes to the kinetic parameters has a large impact on the prediction on the IDT.

Reaction R271 ($HO_2 + CH_3 \Leftrightarrow OH + CH_3O$) is an oxidation route for methyl and it is also highly influential for the IDT in MILD conditions, which is discussed in [93]. This reaction consists only of a value for the pre-exponential factor A, while the other Arrhenius parameters are zero. The uncertainty parameter f for this reaction is therefore very high, i.e. $f = 1$, hence also the impact factor is high.

Reaction R405 ($CH_4 + H \Leftrightarrow H_2 + CH_3$) is a propagation reaction, which creates the methyl radical, already mentioned before to be highly influential for the IDT in MILD conditions.

The complete forward UQ evaluation of these reactions can be found in Appendix A.

Using the approach described in Section 2.2, the uncertainty range for the kinetic pa-

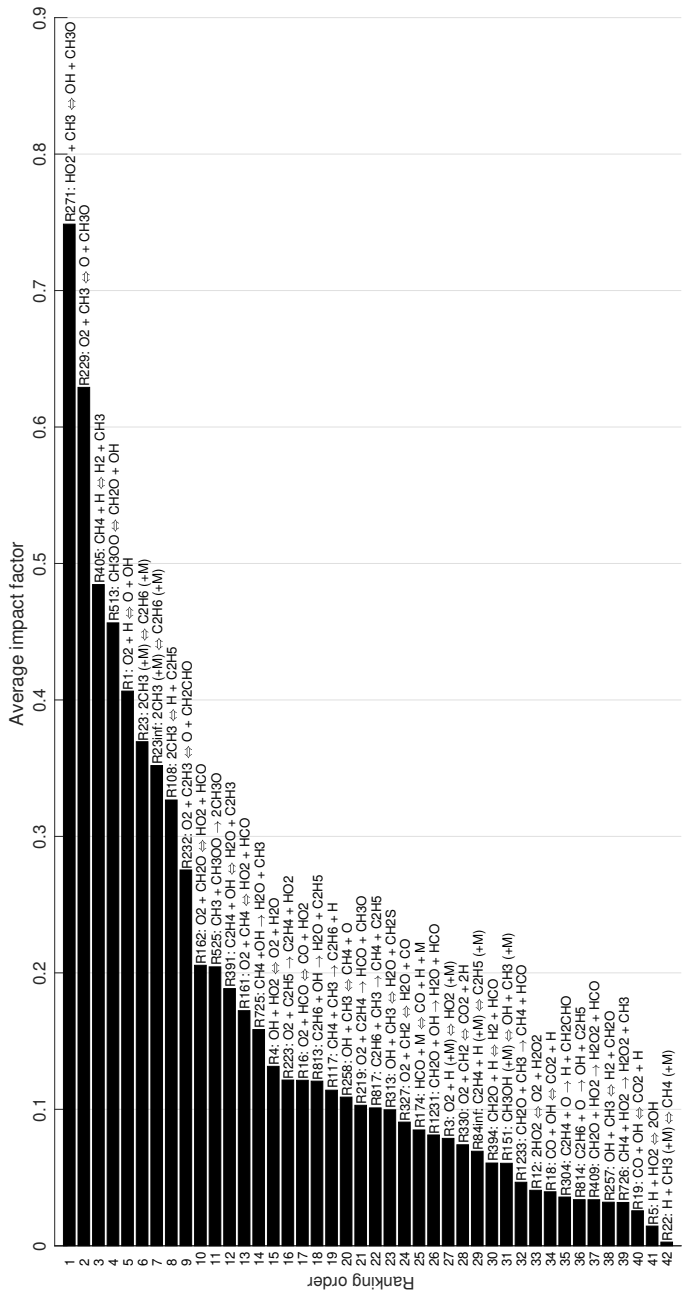

Figure 3.3: *Average impact factor for the 42 reactions which occurred in the top 20 most sensitive reactions for at least one simulated condition. The reactions are presented in descending order based on this averaged impact factor.*

rameters of each of the reactions considered was determined and can be found in Table 3.2, together with the nominal values from the POLIMI mechanism [83].

Table 3.2: *Uncertain parameters for considered reactions with nominal values from the POLIMI C1-C3 [83] mechanism and prior uncertainty range of each parameter. The units of the different kinetic parameters are as follows: A [s - cm^3 - mol], β [-] and E_a [cal/mol].*

Kinetic Parameter	Nominal value	Minimum value	Maximum value
R1 (O_2 + H $\Leftrightarrow$ O + OH)			
A	9.6×10^{14}	6.1×10^{14}	1.5×10^{15}
β	-0.2	-0.6	0.2
E_a	16 625	16 001	17 249
R271 (HO_2 + CH_3 $\Leftrightarrow$ OH + CH_3O)			
A	6.00×10^{12}	6.00×10^{11}	6.00×10^{13}
R405 (CH_4 + H $\Leftrightarrow$ H_2 + CH_3)			
A	3.0×10^{7}	1.2×10^{7}	7.54×10^{7}
β	2.0	1.13	2.87
E_a	10 000	8 752	11 248

3.3 Optimization study

In this study, the application of Surrogate Models (SMs) was used for determining the optimal combination of parameters. The SMs were created with the help of the Matlab toolbox ooDace [90, 102]. This toolbox uses the so-called Kriging method [87, 88], which is described in detail in Section 2.4.1. So called *Ordinary* Kriging, i.e. a regression function of order zero, was used, with a Gaussian correlation function. One SM was created with respect to each experimental point to reduce further estimation errors with respect to either inlet temperature, C/O ratio, or Ω value.

An initial set of samples were produced in order to fit the SMs. These samples were determined using Latin Hypercube Sampling (LHS), which ensures a good spread of the samples over the complete parameter space, which is crucial for having accurate predictions from the SMs. Only some of these samples created with LHS were used for building the SMs, while the rest were used to evaluate the fitting error of the SMs, with respect to the total set of samples. Then rather than adding other random samples to reduce the fitting error, the samples which showed the highest fitting error were added to the SM building process in an iterative way until the maximum fitting error reached a converged value strictly lower than 10%. This so-called adaptive sampling procedure reduces the number of samples needed for building the SMs, as well as the size of the initial sample pool needed, including both samples used for building the SMs and the samples used for evaluating the fitting error. In order to ensure a good estimation of the fitting error, the total sample pool were at least twice the size of the number of final samples used to build the SMs. It should be noted that the size of the sample pool could not be determined *a priori*,

instead a sufficiently large number of samples were included. For the cases evaluated in this study, a set of 600 samples were initially created and used for building the SMs and the fitting error evaluation.

The final SMs were then used to evaluate several thousands of combinations of the uncertain parameters, in order to find the optimal combinations of values with respect to the experimental data. However, as mentioned in Section 2.2.1, to ensure that a specific combination of parameters allowed the rate coefficient to stay within its uncertainty limits, an *a posteriori* evaluation of the kinetic parameter combinations was performed, and only the combinations which gave k values within the uncertainty limits were considered. More specifically, a total number 544 480 valid evaluations were performed and compared using the least squared residual (described in Section 2.3) as objective function. As the experimental data used in this work can be considered as one data set, the division with the number of data points, as mentioned in Section 2.3, was not performed. Additionally, the standard deviation of the experimental data can be considered constant for the whole data set, and the division with the standard deviation (as seen in Eq. 2.9) can also be disregarded. The objective function can therefore be formulated as:

$$Obj = \sum_i (Y_i^{exp} - Y_i^{sim}(\mathbf{X}))^2 \tag{3.1}$$

where Obj is the sum of the square of the residual in each point i, and $\mathbf{X}$ the combination of uncertain parameters considered in this study.

It should be noted that non-linear optimization problems such as this, could consists of several local minima of the objective function, and finding the global minimum is difficult. However, using the approach described in this chapter ensures that each viable combination within the pre-determined uncertainty range were evaluated and compared against each other, and therefore allows the determination of the optimum out of all the evaluated parameter combinations.

The optimal combination of parameter was therefore determined and the performance of this optimized mechanism, with respect to the nominal POLIMI C1-C3 [83] mechanism, can be seen in Figures 3.4-3.5.

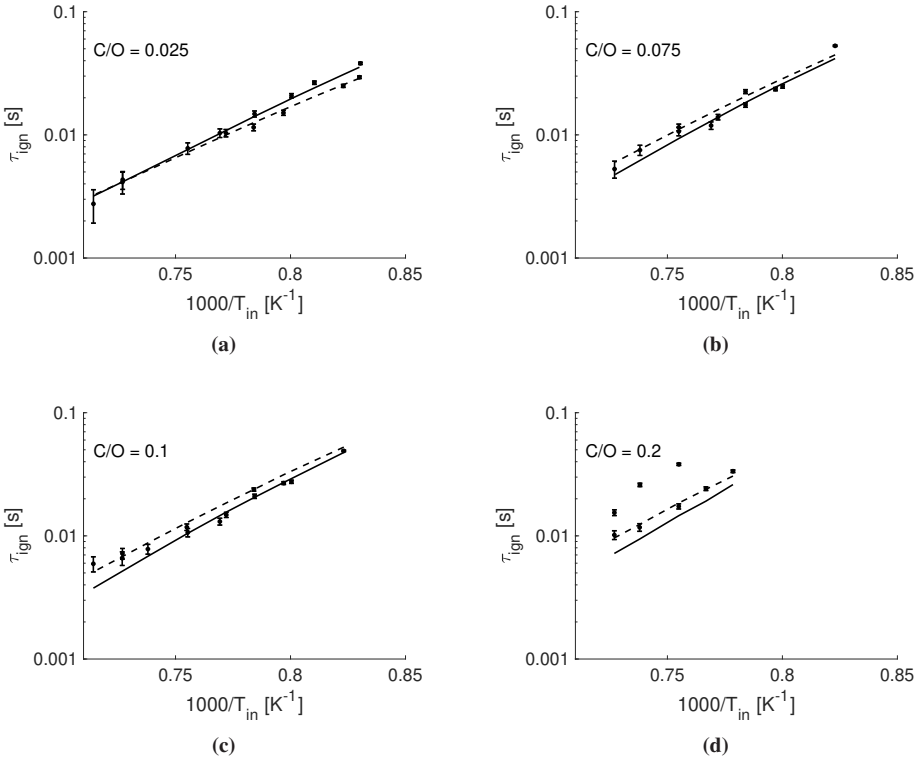

Figure 3.4: *IDT for methane at different inlet temperatures for C/O = 0.025-0.2. Experimental data are represented by points with corresponding error bars, while simulation results for the POLIMI mechanism are presented by the solid lines (—) and the optimized mechanism by the dashed lines (- -).*

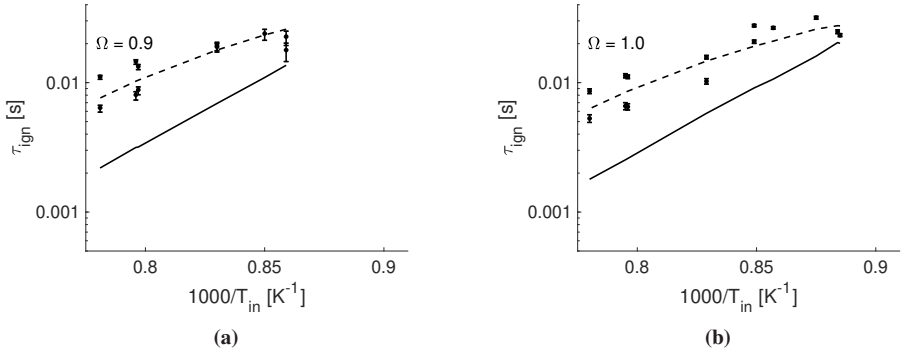

Figure 3.5: *IDT for biomass pyrolysis products at different inlet temperatures for Ω = 0.9 and 1. Experimental data are represented by points with corresponding error bars, while simulation results for the POLIMI mechanism are presented by the solid lines (—) and the optimized mechanism by the dashed lines (- -).*

The corresponding parameters for the optimized mechanism are presented in Table 3.3, as well as the objective function value, calculated using Equation 3.1. For comparison the nominal POLIMI C1-C3 [83] mechanism parameters are also presented in Table 3.3, together with its calculated objective function value.

Table 3.3: *Nominal and optimal values for the parameters from R1 (O_2 + H ⇔ O + OH), R271 (HO_2 + CH_3 ⇔ OH + CH_3O) and R405 (CH_4 + H ⇔ H_2 + CH_3). The nominal values are from the POLIMI C1-C3 [83] mechanism. Also the Obj value is presented at the end of the table for both the mechanisms. The units of the different kinetic parameters are as follows: A [s - cm^3 - mol], β [-] and E_a [cal/mol].*

Reaction Nr	Parameter	Nominal values	Optimized values
1	A	9.6×10^{14}	6.1×10^{14}
	β	-0.2	-0.2
	E_a	16 625	16 556
271	A	6.0×10^{12}	2.56×10^{13}
405	A	3.0×10^{7}	7.54×10^{7}
	β	2	2
	E_a	10 000	10 139
Obj [-]		2.03×10^{-3}	4.99×10^{-4}

3.3.1 Validation against conventional conditions

To ensure that the performance of the optimized mechanism did not diminish for conventional conditions, a validation against ignition delay time for methane in conventional conditions was also performed. This validation showed that the optimized mechanism gave improved predictions also for conventional conditions, with respect to the nominal POLIMI mechanism [83]. This validation was performed using data from Hu et al. [103] and consists of the IDT for methane-air mixtures in a shock-tube at different temperatures, an equivalence ratio (ϕ) of 0.5 and pressures ranging from 1-10 atmosphere (atm). As no experimental uncertainty was mentioned in [103], it was assumed to be $\pm 28 \times 10^{-6}$ s, which was estimated for the same facility by Zhang et al. [104]. As mentioned by Hu et al. [103], the ignition delay time was simulated as the time before the maximum derivative of the temperature increase could be observed. The simulations were performed by means of a NonIsothermal-UserDefinedVolume batch reactor with the OpenSMOKE++ [95] software. The initial mixture was exposed to a pressure wave to emulate the pressure increase from the shock. Both the experimental data and the simulation results are presented in Figure 3.6. A comparison between the original POLIMI C1-C3 [83] mechanism and the optimized mechanism showed that especially for low pressure (1 atm), the optimized mechanism gave better agreement with respect to the experimental data. This improvement can be seen in Table 3.4, where the objective function (calculated using Eq. 3.1) is presented. The objective function was calculated for each pressure condition, as well as the overall case. Although there is a slight increase in the overall objective value with the optimized mechanism, a large improvement can be seen specifically at 1 atm, where the objective function value is reduced by more than a factor of 20. Considering that all the experimental targets in the optimization study were also at a pressure of 1 atm, it is logical that the largest change is at those conditions. However, interestingly enough there is a slight reduction in the objective function also at a pressure of 10 atm, which is due to the increase of the IDT at intermediate temperatures.

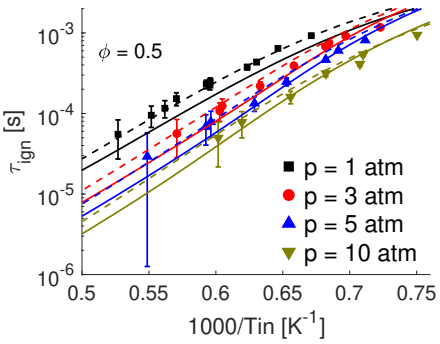

Figure 3.6: *Ignition delay time for methane-air mixture at ϕ = 0.5, and at different inlet temperatures and pressures. The solid lines (—) represents the predictions with the nominal mechanism and the dashed lines (- -) represents the predictions with the optimized mechanism from this work.*

Table 3.4: *Comparison of objective function value between the nominal and optimized mechanisms. The objective function values were calculated using Eq. 3.1.*

Pressure	1 atm	3 atm	5 atm	10 atm	Overall
POLIMI	1.21×10^{-7}	1.30×10^{-7}	1.62×10^{-8}	7.62×10^{-8}	3.43×10^{-7}
Optimized	5.69×10^{-9}	3.97×10^{-7}	9.31×10^{-8}	6.74×10^{-8}	5.64×10^{-7}

3.4 Concluding remarks

This chapter has presented an optimization study of a kinetic mechanism with respect to MILD combustion targets. It shows the discrepancy between the prediction of several existing detailed mechanisms with respect to the IDT of MILD combustion, for both methane [93] and biomass pyrolysis products [18]. Based on the average deviation from the experimental targets, the POLIMI mechanism [83] was chosen for the optimization study, and by performing a forward UQ study on the top five reactions with the highest averaged impact factor, a total number of three reactions and seven parameters were used for the optimization. The prior uncertainty range for each of the seven parameters were determined using the approach described in Section 2.2 and SMs were used for predicting the behavior of the model. The SMs were built up using LHS and the fitting error was reduced using an adaptive sampling approach, which ensured fitting errors strictly below 10%. The SMs were then used to evaluate many different feasible combinations of the parameters, and the least squared residual formulation (see equation 3.1) was used to determine the optimal combination of the uncertain parameters.

The optimized mechanism showed only slight improvements for most of the methane cases, but large improvements could be found for all the biomass pyrolysis products cases. However, improvements for the methane cases could be seen for high inlet temperatures, and for the C/O=0.2 case, where the optimized mechanism showed improvements for all inlet temperatures.

For each of the reactions considered in this optimization study, the following modifications to the kinetic parameters are needed in order to improve the performance with respect to the experimental targets:

— The pre-exponential factor and the activation energy for reaction R1 (O_2 + H $\Leftrightarrow$ O + OH) should be decreased slightly, while the temperature exponent should be kept to the same value.

— The pre-exponential factor for reaction R271 (HO_2 + CH_3 $\Leftrightarrow$ OH + CH_3O) should be increased by almost a factor of 2.

— For reaction R405 (CH_4 + H $\Leftrightarrow$ H_2 + CH_3), the pre-exponential factor should be increased by a factor of 2.5, while the temperature exponent should be kept to its nominal value, and the activation energy should be reduced slightly.

In order to ensure that the optimized mechanism did not lose predictability for conventional conditions, a validation against IDT for methane-air mixtures in conventional conditions was also performed, and showed an improved performance also for these conditions.

The results from this study clearly indicate that the approach of mechanism optimization with respect to non-conventional conditions is feasible, and by only using the kinetic

parameters of three reactions, quite significant improvements could be achieved. However, in order to arrive with a more comprehensive mechanism, more experimental targets should be added to the optimization process. This would not only require a larger set of SMs to be built with respect to the expansion of the experimental targets, but also increase the complexity of the SMs with respect to an increased number of kinetic parameters, as this would naturally also increase. The limitations of the approach described in this chapter therefore drives us towards the implementation of a more efficient approach, which can handle both more uncertain parameters and experimental targets. This was realized through the development of an optimization toolbox called `OptiSMOKE++`, which will be described in detail in Chapter 4.

CHAPTER 4

OptiSMOKE++

In order to facilitate the optimization of kinetic mechanisms with respect to a large number of experimental data, and using many uncertain parameters, a toolbox was created using the capabilities of DAKOTA [105] and OpenSMOKE++ [95]. The aim of this work was to ensure a flexible interaction, where the choice of optimization procedure, objective function formulation and optimization targets could easily be managed by the user. This chapter aims to describe the different features of this code as well as it presents some test cases which exemplifies them.

4.1 Workflow

A graphical representation of how the code operates can be appreciated in Figure 4.1, and it conveys the following logic:

The code starts by reading the specified input file, then changes the parameters in the kinetic scheme (for the first evaluation the kinetic parameters from the starting kinetics are used). The code then double checks if the rate parameters (k), for all specified reactions are within the uncertainty bounds, using a non-linear constraint, i.e. $k_{min} \leq k \leq k_{max}$ (see section 2.2.1). If yes, OpenSMOKE++ is used for running the simulations, and the results are used to calculate the objective function value. If at least one of the rate parameters are outside of the uncertainty bounds, a penalty function is applied to that evaluation and the simulations are not carried out. A more thorough explanation regarding the uncertainty bounds can be found in section 2.2, while the penalty function implemented in the code is discussed further in section 4.4.

Based on the objective function value, DAKOTA suggests a new set of parameter values and the process is repeated until at least one of the stopping criteria has been reached. These stopping criteria can depend on the optimization methodology used, but some typical universal ones are; maximum number of evaluations, maximum number of iterations, solution target and convergence criteria. These criteria, and method specific ones, are explained in further detail in the Reference Manual of DAKOTA [106].

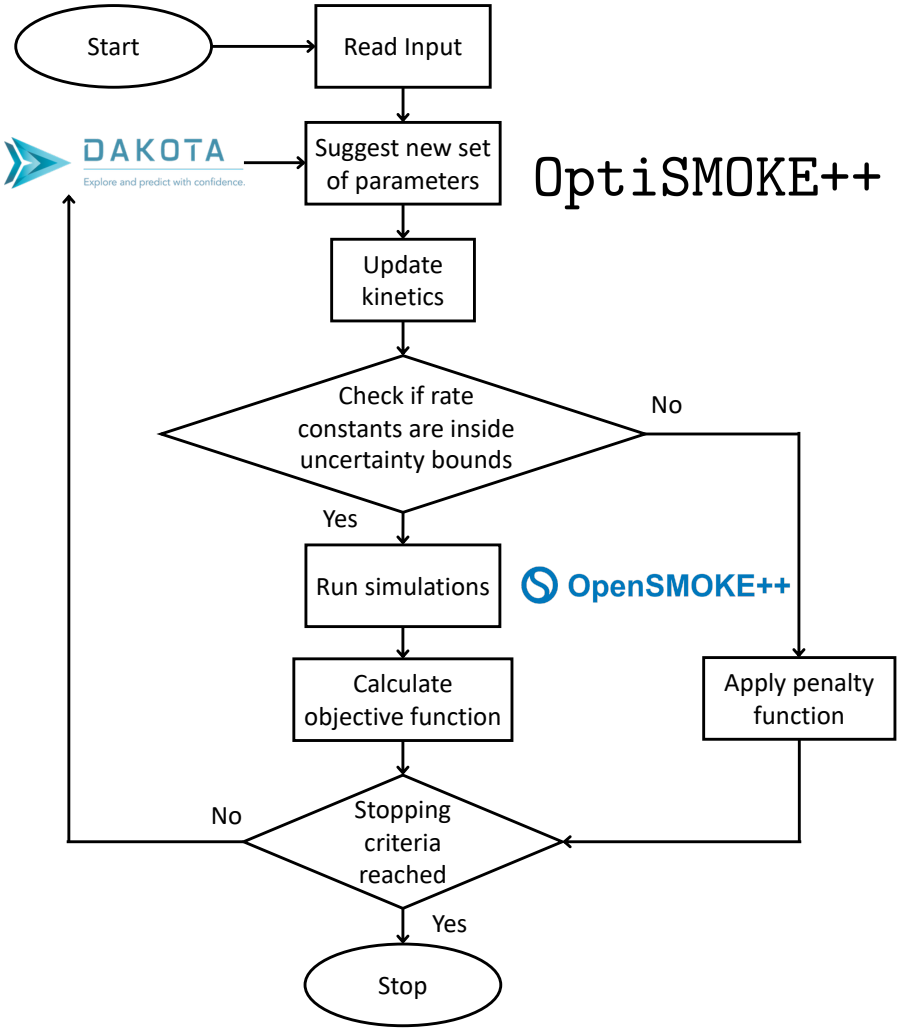

Figure 4.1: *Schematic workflow of OptiSMOKE++.*

As OptiSMOKE++ uses the different features of OpenSMOKE++ and DAKOTA, a short description of these codes will follow.

4.1.1 OpenSMOKE++

The OpenSMOKE++ framework [95] was developed specifically for solving reacting systems with thousands of species and reactions. It consists of a series of solvers for 0D reactors (Batch Reactors, Plug Flow Reactors (PFR), Perfectly Stirred Reactors (PSR), Shock-Tube (ST) Reactors, Rapid Compression Machines (RCM)) and 1D laminar premixed and counterflow diffusion flames. The code was written exclusively in object-oriented C++, which facilitated the coupling with DAKOTA, also written in C++. OpenSMOKE++ utilizes advanced numerical techniques to reduce the computational cost of the simulation, without sacrificing accuracy or robustness. A more extensive description of the code and its utilities can be found in [95].

4.1.2 DAKOTA

Design Analysis Kit for Optimization and Terascale Applications (DAKOTA) is a framework developed at and distributed by Sandia National Laboratories [107]. It is a toolkit used for iterative parameter evaluations, such as optimization, sensitivity analysis, forward and inverse uncertainty quantification, etc. The toolkit consists of many different optimization methodologies which can be divided into the following sub-categories: Gradient-Based and Derivative-Free Local Methods and Gradient-Based and Derivative-Free Global Methods.

The DAKOTA User's Manual [105] provides useful suggestions regarding which methodology to use depending on the case at hand, as well as listing the specific algorithms available in the different sub-categories.

As DAKOTA was intended to be used together with a separate application, it is considering the simulation code as a "black box", i.e. it is working completely independently, only relying on the objective function value for finding new combinations of the uncertain parameters which could potentially reduce the value of the objective function. There exists many cases in literature where DAKOTA has been coupled with different simulation software for this purpose [108–110]. The OptiSMOKE++ toolbox was written following the instructions provided in the *PluginSerialDirectApplicInterface.cpp* file available in the DAKOTA source code. This allowed for an easy coupling between the two codes, which was one of the reasons why DAKOTA was chosen. The tight coupling between OpenSMOKE++ and DAKOTA also allows the user to utilize any of the optimization methodologies available in the DAKOTA package with OptiSMOKE++. However, due to the problem at hand, i.e. mechanism optimization, some optimization methodologies are less suited than others, due to the highly irregular behavior of the objective function. Gradient based methodologies can have problems to determine the optimum because of the complex structure of the objective function [67], and their use in this context is not recommended.

There are also applications of Surrogate Model (SM) based optimization using DAKOTA, with methods such as `efficient_global`. This method works in a very similar way as what was presented in Chapter 3, i.e. first a certain number of samples are used to create a SM using a Gaussian Process (see Section 2.4.1), which is then used for a subsequent optimization study. The `efficient_global` approach then uses the NCSU_DIRECT approach, which is based on the DIRECT algorithm described in Section 2.5.1 for finding the optimum. The issue with this in the case of kinetic mechanism optimization, is

that the SM is created based on the response of the model, i.e. the objective function. As already mentioned, the objective function in kinetic mechanism optimization in general is multi-modal and highly irregular. It is therefore very difficult to create an accurate representation of the objective function using SMs. This approach can therefore result in infeasible parameter combinations, and is therefore also not recommended for this specific application.

4.2 Optimization targets

Finding the optimal combination of a set of uncertain kinetic parameters with respect to some experimental targets requires an optimization process typically involving several thousand evaluations before the global optimum is found. Even if response surface techniques are used, several hundred evaluations are needed initially for creating the response surface, as has been seen in Chapter 3. It is therefore important that the numerical simulations are fast, to assure that the optimization reaches convergence within a reasonable time frame. In the field of kinetic mechanism optimization, it is therefore common to use experimental data from so-called 0D or 1D reactors as targets. OptiSMOKE++ therefore focuses on the use of the following solvers: Batch Reactor, PFR, PSR, RCM, ST and premixed laminar flames. Experimental data from any of these types of reactors can therefore be used as targets in the optimization. However, it should be mentioned that only experimental data for which 0D or 1D simplifications of the system can be made should be used as targets. Mayor facility effects and epistemic uncertainties cannot be taken into account by the simple 0D and 1D solvers.

4.2.1 Ignition Delay Time (IDT)

In order to accurately predict the onset of reactions in a system, the Ignition Delay Time (IDT) is used. It is a physico-chemical property of a specific mixture [111], and as the ignition determines the consecutive combustion process, it is a crucial target for accurately predicting the behavior of a combustion system. IDT is therefore commonly used for both mechanism development, validation and optimization. However, there does not exist one single criteria for determining the IDT of a mixture. As the IDT shows the onset of reactions, a common definition relates to the maximum concentration of OH, which is generally used as a marker for the flame front. Even the maximum change of OH is used for determining the IDT [112] in some cases. Other definitions relate to a change in pressure, commonly used in Rapid Compression Machines (RCMs) [113], or temperature [93]. As mentioned in Cuoci et al. [95], the IDT data from both ST and RCMs can be reproduced using a transient closed homogeneous batch reactor simulation, where facility effects can be accounted for using a volume history profile. OptiSMOKE++ utilizes this for the simulation of STs and RCMs.

To facilitate all this, OptiSMOKE++ utilizes the built in definitions of the IgnitionDelayTimeAnalyzer available in OpenSMOKE++. The user can therefore easily chose the definition of the IDT as needed, and several different definitions, e.g. one per each data set, can be used simultaneously.

However, there could be some experimental data which has been derived at conditions which does not support the 0D simplification for the evaluation of IDT. This was for exam-

ple seen in Bourgeois et al. [114], where a comparison between 0D and CFD simulations for the IDT of n-heptane in a RCM was performed. The results showed that specifically at low temperatures a significant discrepancy was found in the IDT predictions. The application of the 0D assumption can therefore not be applied to this case.

4.2.2 Species profiles

The evolution of different species in a transient system does not only indicate if a mechanism predicts the onset of reactions in a system, but also the behavior of intermediate species as well as the behavior of the system after ignition has occurred. It is therefore an important quantity in the prospect of mechanism optimization. The utilization of species profiles is therefore supported in `OptiSMOKE++` and several species can be used as targets at the same time. It is also possible to combine an optimization study, utilizing both IDT and species profiles as targets. This will be demonstrated in 4.6.4.

4.2.3 Laminar Flame Speed (LFS)

As a key quantity for describing the combined effect of a mixtures diffusivity, reactivity and exothermicity [83], the LFS is often used as a target for the development, validation and optimization of a kinetic mechanism. The LFS describes at which speed the flame front is propagating back towards the unburned gases. When the inlet velocity of the mixture is equal to the LFS, a stable flame front is established. The numerical evaluation of the LFS are mostly done using a 1D premixed flame simulations, and by finding the stable condition, the LFS can be determined for a specific mixture. The numerical solution of such a system depends on the kinetic and thermodynamic parameters, as well as the transport properties, which is why it is commonly used for the validation of a kinetic mechanism. `OptiSMOKE++` supports the application of LFS as targets for the optimization by using the premixed laminar flame solver of `OpenSMOKE++`.

4.3 Choice of objective function

`OptiSMOKE++` has two different formulations of the objective function implemented, the L1-norm (Eq. 2.13) and the L2-norm (Eq. 2.10). The user is free to choose the formulation which suits the application the best. However, while performing optimization with several different data sets, it is important that the objective function values for each data set are somewhat comparable. If there is a significant difference between the objective function of two different data sets, the optimizer will naturally work on trying to reduce the objective function of the data set with a higher value. To demonstrate this, a comparison between L1-norm (Eq. 2.13) and the L2-norm (Eq. 2.10) can be observed in Figure 4.2, where the localized objective function value is presented, using both of the definitions, for two different test cases; test case 1 and 3. These two test cases consists of experimental targets of IDT for test case 1 and species profiles from a Jet Stirred Reactor (JSR) for test case 3. More detail about these test cases will follow in sections 4.6.1 and 4.6.3. The difference between the two y-axis scales of the objective function values in Figure 4.2a for test case 1 and 3, clearly shows that using the L2-norm definition would give more weight to the data in test case 3, since the values of the objective function are several

orders of magnitude higher than for test case 1. Using the L1-norm definition (Figure 4.2b) allows, on the other hand, to obtain local objective function values showing a more uniform distribution and more comparable numerical values (only 10^3 difference rather than 10^6). In this case, the optimizer would more quickly seek to optimize the mechanism with respect to both data sets, rather than just for test case 3, as would happen using the L2-norm definition. This fact will be demonstrated further in Section 4.6.4.

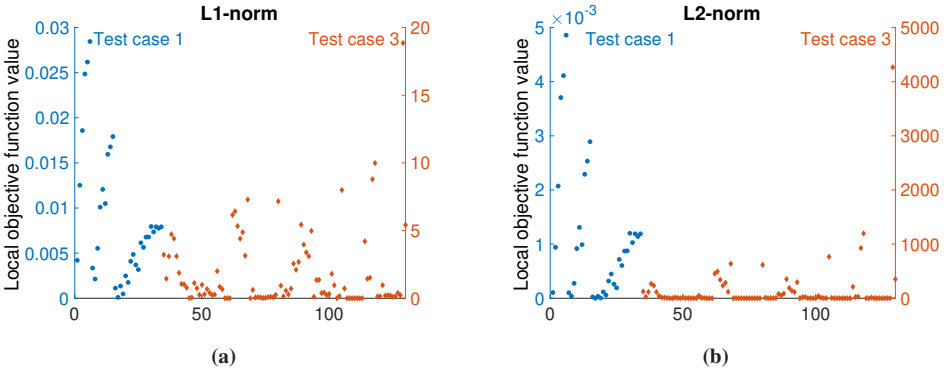

Figure 4.2: *Local objective function values for test cases 1 and 3, using the L1-norm (Eq. 2.13) and the L2-norm (Eq. 2.10) objective function formulations.*

4

4.4 Penalty function

Based on the non-linear nature of the modified Arrhenius curve, it is not guaranteed that a change of several kinetic parameters, within their specific uncertainty range, ensures that the rate constant is within its initially prescribed bounds for the complete temperature span (normally considered 300-2500 K). This was already discussed in 2.2.1, and in Chapter 3 only the combination of parameters that satisfied this criteria were considered for evaluation. However, when using a so-called direct optimization strategy, the optimizer decides on-the-fly which new combination of parameter that should be evaluated. The approach used in Chapter 3 is therefore not suitable in this case. Instead a secondary constraint on the rate constant can be applied. If this secondary constraint is violated for a specific parameter combination, it should not be considered as a good combination. `OptiSMOKE++` utilizes a so-called penalty function to ensure this. Penalty functions are very common for handling constrained optimization problems and can be used for many purposes. For example, Sikalo et al. [70] used a penalty function for keeping the optimized parameters close to the original values as possible. However, in `OptiSMOKE++` the penalty function is implemented to forcefully increase the objective function value, to a fixed value, for parameter combinations which do not respect the uncertainty limits of the rate constants, for all of the reactions considered. This ensures that the optimizer does not choose a parameter combination which violates this restriction, and finds the optimal combination of parameters which satisfies this constraint.

However, it is important that the evaluations that are issued the value of the penalty

function are not considered as possible "good" evaluations. If for example the Evolutionary Algorithm approach (see Section 2.5.2) is used, and the evaluations with the penalty function value as objective function are considered as good evaluations, they will become parents and create new children through crossover and mutation. This directly contradicts the purpose of the penalty function. To ensure that this does not happen, the value of the penalty function needs to be very high. Specifically much larger than any potential objective function values that can be encountered during the optimization process, of parameter combinations that satisfy the constraint on the rate coefficient. The value of the penalty function was therefore set to 10^{12} in this work, to ensure that this problem did not occur.

The combination of a penalty function and non-gradient based global optimizers is very efficient for problems where a secondary constraint is applied on the optimization. However, for gradient based optimization approaches, penalty functions are not a good choice, as these algorithms depend on the prior evaluations for the estimation of the slope of the objective function. The use of penalty functions disrupts the natural slope of the objective function and gradient based algorithms would then face issues in finding the optimal solution.

There exists many variations of penalty functions for optimization problems, such as increasing the objective function value linearly for the cases that violates the constraints, or adaptively changing the penalty function. However, as seen in Figure 4.1, by applying a fixed value of the penalty function, and not running the simulations and calculating the objective function, large computational savings could be achieved.

It should also be mentioned that the problem with the secondary constraints can be avoided by only considering the linear nature of a kinetic mechanism, i.e. considering only the pre-exponential factors. By removing the degrees of freedom in the optimization in such a way, you can also ensure that the secondary constraint is never violated.

4.5 Uncertain parameters

The strategy described in 2.2 is also applied in `OptiSMOKE++` for determining the ranges of each kinetic parameter. However, specific limits for each kinetic parameter can also be specified independently.

As mentioned by Cuoci et al. [95], the computational effort of calculating a rate coefficient ($k = AT^{\beta}e^{-E_a/RT}$) involves two expensive functions, namely a power (T^{β}), and an exponential ($e^{-E_a/RT}$). By instead using the linearized form of the Arrhenius equation ($ln(k) = ln(A) + \beta ln(T) - \frac{E_a}{R}T^{-1}$), and evaluating the rate coefficient as $k = e^{(ln(A)+\beta ln(T)-\frac{E_a}{R}T^{-1})}$, only one expensive function evaluation is needed, in the form of an exponential, as the only other expensive function $ln(A)$ can be evaluated only once and stored. It is therefore beneficial for `OptiSMOKE++` to work directly with the linearized kinetic parameters ($ln(A)$, β and E_a/R), rather than with the Arrhenius parameters themselves. However, to stay consistent, the Arrhenius parameter values are presented for the different test cases that follows.

4.6 Test cases

In this section, some test cases, which illustrates the functionality of the OptiSMOKE++ toolbox, will be presented. The different optimization methods, and the cases, were not necessarily chosen based on efficiency or any specific interests, instead they were chosen in order to show the different features available in the OptiSMOKE++ toolbox. A final comparison between the runtime and number of evaluations performed for each specific test case is presented in Section 4.6.6.

4.6.1 Test case 1: Ignition Delay Time for MILD conditions in a Plug Flow Reactor

Similarly to the work presented in Chapter 3, the experimental target data used in this test case are from Sabia et al. [18], where the IDT of biomass pyrolysis gas in a PFR was evaluated during MILD conditions, i.e. high inlet temperature and diluted conditions. The IDT were evaluated as the time when the mixture reaches a temperature 10 K higher than the inlet temperature. The experimental uncertainties were evaluated with respect to the displacement of the thermocouples and the inlet velocity from the experimental measurements [18]. This experimental data set consists of fuel diluted with nitrogen at different oxygen ratios (Ω) [94]. The nominal mechanism used for this test case was the POLIMI C1-C3 V1412 [83] mechanism, consisting of 107 species and 2642 reactions. The choice of which reactions to optimize was done using only a ranking of sensitivity coefficients in this work. As the OptiSMOKE++ toolbox allows for more kinetic parameters to be used in the optimization study, without a drastic increase in computational effort, a larger set of reactions could be used and the screening based on only the sensitivity coefficients was considered sufficient for the work in this chapter. A cumulative sensitivity function (see 2.1.3) was created for the complete test case, and a threshold of 0.6 of the maximum cumulative sensitivity value was used for arriving with a feasible amount of reactions. This resulted in 11 reactions, and only the non-zero parameters were used in the optimization in order to stay as consistent as possible with the nominal mechanism. A total of 26 uncertain parameters were therefore considered in the optimization, which can be found in Table 4.1.

The optimization was performed using two different global optimization methodologies available in DAKOTA; coliny_direct, which is based on the DIRECT algorithm described in 2.5.1, and coliny_ea, which is based on an Evolutionary Algorithm (EA) approach (see 2.5.2).

More information about both these methods can also be found in the Reference Manual of DAKOTA [106]. The specific settings used for the two algorithms, that were not the default settings, are listed in Table 4.2. For the other method specific settings, please look in the Reference Manual of DAKOTA [106].

The maximum number of function evaluations/iterations tells the optimizer how many evaluations/iterations it is allowed to run. An iteration is very method specific, and for example with the coliny_ea methodology an iteration consists in the creation of each new complete population, i.e. after mutation, crossover and replacement is performed. The reason why these values are different for the two methods, is that the more random aspect of coliny_ea generally gives parameter combinations which does not satisfy the

Table 4.1: *List of the reactions and corresponding kinetic parameters (from the POLIMI C1C3 V1412 [83] mechanism) considered in the optimization for Test case 1.*

Reaction Nr	Reaction Formula	A	β	E_a
1	$O_2 + H \Leftrightarrow O + OH$	✓	✓	✓
23	$2CH_3\ (+M) \Leftrightarrow C_2H_6\ (+M)$	✓	✓	✓
23 [inf]	$2CH_3\ (+M) \Leftrightarrow C_2H_6\ (+M)$	✓		
223	$O_2 + C_2H_5 \rightarrow C_2H_4 + HO_2$	✓		✓
258	$OH + CH_3 \Leftrightarrow CH_4 + O$	✓		✓
271	$HO_2 + CH_3 \Leftrightarrow OH + CH_3O$	✓		
391	$C_2H_4 + OH \Leftrightarrow H_2O + C_2H_3$	✓		✓
405	$CH_4 + H \Leftrightarrow H_2 + CH_3$	✓	✓	✓
725	$CH_4 + OH \rightarrow H_2O + CH_3$	✓	✓	✓
813	$C_2H_6 + OH \rightarrow H_2O + C_2H_5$	✓	✓	✓
817	$C_2H_6 + CH_3 \rightarrow CH_4 + C_2H_5$	✓	✓	✓

Table 4.2: *List of specific settings used for the two optimization algorithms.*

`coliny_direct`		`coliny_ea`	
Max function evaluations	5 000	Max function evaluations	1 000 000
Max iterations	5 000	Max iterations	1 000 000
Convergence tolerance	10^{-8}	Convergence tolerance	10^{-8}
Solution target	10^{-6}	Solution target	10^{-6}
Seed	1000	Seed	1000
Global balance parameter	0.1	Population size	300
		Mutation rate	0.6
		Crossover rate	0.4
		Replacement size	10

non-linear constraint on the rate coefficients. In order to have a more fair comparison between the two methods (in the sense of "good" function evaluations), a larger number of evaluations and iterations were used for the `coliny_ea` methodology. The convergence tolerance determines if the optimization should stop if the relative change in objective function is lower than the specified value. The solution target specifies that the optimization should stop if the objective function is lower than the specified value. The random seed used for the initialization of the algorithms is specified using the Seed keyword.

The global balance parameter was mentioned in Section 2.5.1, and specifies if a small rectangle should be subdivided based on the ratio between the size of the small rectangle and the largest rectangle. If this ratio is smaller than the specified value, the small rectangle is not subdivided further. This ensures that a more global approach is achieved in the optimization.

The population size, used for the `coliny_ea` approach, was considered roughly 10 times the number of uncertain parameters considered in the optimization. The mu-

tation/crossover rate controls the probability of mutation/crossover to be performed to create new individuals in the `coliny_ea` approach. The replacement size specifies how many individuals that should be replaced from the previous population to generate a new population.

For both the methodologies, the L2-norm formulation of the objective function (Eq. 2.10) was used.

The optimized values of each kinetic parameter, together with the nominal values and the objective function values, for the three mechanisms are presented in Table 4.3.

Table 4.3: *List of values for the kinetic parameters considered in test case 1. The nominal values refer to the values from the POLIMI C1C3 V1412 [83] mechanism. Also the Obj value is presented at the end of the table for each mechanism. The units of the different kinetic parameters are as follows: A [s - cm^3 - mol], β [-] and E_a [cal/mol].*

Reaction Nr	Parameter	Nominal values	`coliny_direct`	`coliny_ea`
1	A	9.6 $\times 10^{14}$	6.07 $\times 10^{14}$	7.95 $\times 10^{14}$
	β	-0.2	-0.2	-0.23
	E_a	16 625	16 625	16 634
23	A	2.33 $\times 10^{34}$	1.71 $\times 10^{34}$	2.12 $\times 10^{34}$
	β	-5.03	-5.03	-5.07
	E_a	-1 200	-1 408	-1 118
23 [inf]	A	2.5 $\times 10^{13}$	1.35 $\times 10^{13}$	2.13 $\times 10^{13}$
223	A	1.0 $\times 10^{12}$	2.27 $\times 10^{12}$	1.28 $\times 10^{12}$
	E_a	3 000	3 000	3 326
258	A	2.0 $\times 10^{12}$	5.57 $\times 10^{12}$	3.37 $\times 10^{12}$
	E_a	8 000	8 000	8 194
271	A	6.0 $\times 10^{12}$	1.23 $\times 10^{13}$	1.25 $\times 10^{13}$
391	A	2.0 $\times 10^{13}$	4.31 $\times 10^{13}$	2.09 $\times 10^{13}$
	E_a	6 000	6 000	5 632
405	A	3.0 $\times 10^{7}$	6.80 $\times 10^{7}$	4.26 $\times 10^{7}$
	β	2	2	2.03
	E_a	10 000	10 000	9 872
725	A	2.796 $\times 10^{6}$	2.40 $\times 10^{6}$	2.58 $\times 10^{6}$
	β	2	2	2.03
	E_a	1 566.11	1 358	1 938
813	A	3.595 $\times 10^{6}$	2.93 $\times 10^{6}$	4.66 $\times 10^{6}$
	β	2	2	1.97
	E_a	-238.2	-238.2	-230.9
817	A	3.513 $\times 10^{5}$	2.33 $\times 10^{5}$	4.59 $\times 10^{5}$
	β	2	2	1.92
	E_a	7 622	7 483	7 744
Obj [-]		3.74 $\times 10^{-2}$	1.94 $\times 10^{-3}$	3.15 $\times 10^{-3}$

The difference between the nominal and the two optimized mechanisms can be appreciated in Figure 4.3.

It can clearly be seen that both the optimized mechanisms outperform the nominal mechanism, and that both the optimized mechanisms show very similar performance. Only

for the case where $\Omega = 1.67$ (Figure 4.3c) the two optimized mechanisms show slightly different performance. This can also be noticed in the slight difference of the Obj values for the two mechanisms (Table 4.3).

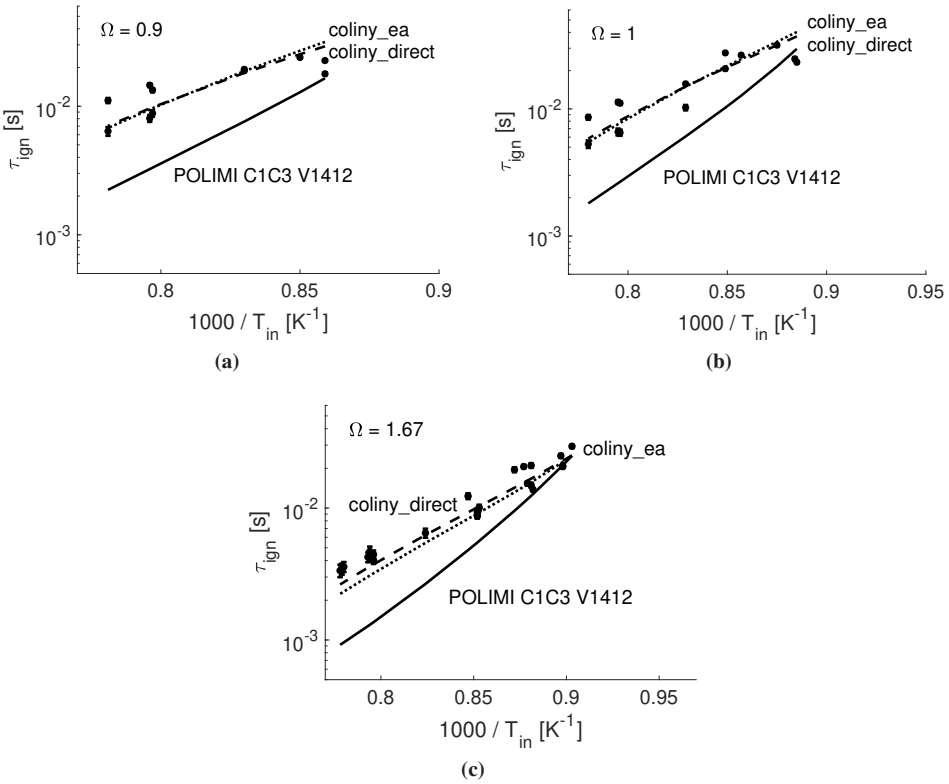

Figure 4.3: *IDT for Ω=0.9, 1 and 1.67 at different inlet temperatures, where the experimental data is presented by the black dots with corresponding error bars. The nominal kinetics (POLIMI C1C3 V1412 [83]) is represented by the solid line (—), the optimized kinetics from the* `coliny_direct` *methodology by the dashed line (- -) and the optimized kinetics from the* `coliny_ea` *methodology by the dotted line (···).*

The reason behind why the two optimized mechanisms perform differently lies in the difference between the two algorithms. The `coliny_ea` algorithm starts with a random population of samples over the whole parameter space, and keeps a slight random nature with each new population created. The `coliny_direct` algorithm on the other hand quickly determines the promising regions, and if specific directions in the parameter space result in a drastic increase of the objective function, that direction is not considered promising. This occurs especially for parameters that have a large impact on the rate coefficient, such as the temperature exponent β. Only a small change in β could easily result in a rate coefficient outside the uncertainty bounds, which activates the penalty function, resulting in a large objective function value, i.e. not promising. As `coliny_ea` has a more randomized search approach, it will find combinations where the β parameters are

changed and the rate coefficients are still within the uncertainty bounds, thus considering these solutions as possible candidates. This can be seen in Table 4.3, where the optimized values for `coliny_direct` does not suggest any change in the β parameters, while `coliny_ea` does show some small changes to all the β parameters. The same can partly be said regarding the activation energy E_a as well.

4.6.2 Test case 2: Ignition Delay Time at high pressures using data from a Shock-Tube

For this test case, the experimental targets consist of IDT of methane diluted in carbon dioxide in a ST, at high pressures (100 bar) [112]. The IDT was experimentally evaluated at the moment where the maximum change of the exited species OH^* was measured. However, due to the fact that the experiments were performed at very high pressure, the discrepancy between the OH and OH^* profiles were minimal, and the numerical IDT could therefore be evaluated at the moment of maximum change of OH. This was also confirmed by personal communication with the authors of the paper [112]. The experiments were performed at stoichiometric (ϕ=1) and rich (ϕ=2) conditions. The kinetic mechanism used for this case was the GRI 3.0 [43] mechanism, which consists of 53 species and 325 reactions. Similarly to the previous case, a cumulative sensitivity function was created in order to determine which reactions that should be considered in the optimization. With a threshold of 0.6, 9 reactions and corresponding 20 non-zero parameters were chosen for the optimization, and are reported in Table 4.4. Again, only the non-zero parameters from the 9 reactions were considered.

Table 4.4: *List of the reactions and corresponding kinetic parameters (from the GRI 3.0 [43] mechanism) considered in the optimization for Test case 2.*

Reaction Nr	Reaction Formula	A	β	E_a
32	$H + O_2 + M \Leftrightarrow HO_2 + M$	✓		✓
33	$O_2 + CH_2O \Leftrightarrow HO_2 + HCO$	✓	✓	
53	$H + CH_4 \Leftrightarrow H_2 + CH_3$	✓	✓	✓
116	$2HO_2 \Leftrightarrow O_2 + H_2O_2$	✓		✓
119	$HO_2 + CH_3 \Leftrightarrow OH + CH_3O$	✓		
121	$HO_2 + CH_2O \Leftrightarrow H_2O_2 + HCO$	✓	✓	✓
155	$O_2 + CH_3 \Leftrightarrow O + CH_3O$	✓		✓
156	$O_2 + CH_3 \Leftrightarrow OH + CH_2O$	✓		✓
158 [inf]	$2CH_3\ (+M) \Leftrightarrow C_2H_6\ (+M)$	✓	✓	✓

The optimization was performed using the `coliny_direct` method, and the L2-norm formulation for the objective function (Eq. 2.10) was used. The same settings as mentioned for Test case 1 was used for the `coliny_direct` algorithm (see Table 4.2). The results can be seen in Table 4.5 and Figure 4.4.

It can clearly be seen in Figure 4.4 that the optimized mechanism captures the experimental data very well. This can also be seen in the reduction of the objective function value as seen in Table 4.5. What can also be seen in Table 4.5, is that many of the reaction

Table 4.5: *List of values for the kinetic parameters considered in test case 2. The nominal values refer to the values from the GRI 3.0 [43] mechanism. Also the Obj value is presented at the end of the table for each mechanism. The units of the different kinetic parameters are as follows: A [s - cm^3 - mol], β [-] and E_a [cal/mol].*

Reaction Nr	Parameter	Nominal values	`coliny_direct`
32	A	1.0×10^{14}	4.64×10^{13}
	E_a	40 000	38 960
33	A	2.8×10^{18}	1.30×10^{18}
	β	-0.86	-0.86
53	A	6.6×10^{8}	1.22×10^{9}
	β	1.62	1.62
	E_a	10 800	11 672
116	A	4.2×10^{14}	4.2×10^{14}
	E_a	12 000	12 000
119	A	3.78×10^{13}	2.21×10^{13}
121	A	5.6×10^{6}	5.6×10^{6}
	β	2	2
	E_a	12 000	12 000
155	A	3.56×10^{13}	2.25×10^{13}
	E_a	30 500	30 480
156	A	2.31×10^{12}	1.46×10^{12}
	E_a	20 300	19 691
158	A [inf]	6.77×10^{16}	6.77×10^{16}
	β [inf]	-1.18	-1.18
	E_a [inf]	654	654
Obj [-]		1.37×10^{-2}	5.63×10^{-4}

parameters are not changed during the optimization. This is due to the fact that it is quite a simple test case, with only few experimental targets. However, it still exemplifies the application of `OptiSMOKE++` to IDT from Shock-Tubes.

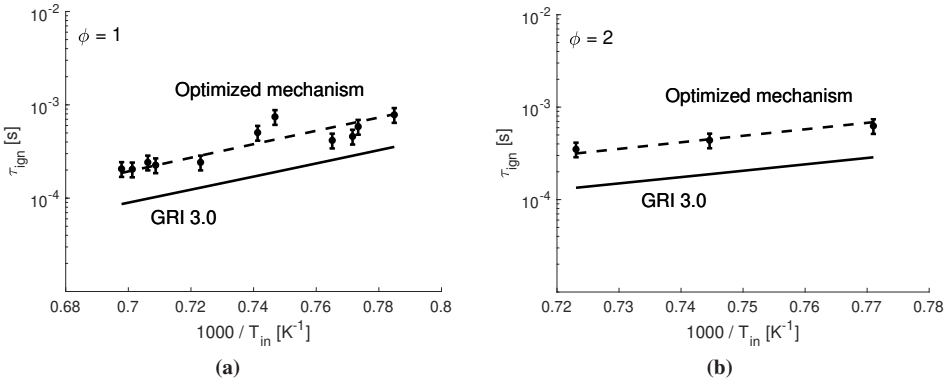

Figure 4.4: *IDT for methane at ϕ= 1 and 2, where the experimental data is presented by the black dots with corresponding error bars. The nominal kinetics (GRI 3.0 [43]) is represented by the solid lines (—) and the optimized mechanism by the dashed lines (- -).*

4.6.3 Test case 3: Methanol oxidation in a Jet Stirred Reactor

In this example, the optimization targets consist of species concentrations of methanol (CH_3OH) oxidation at different temperatures in an iso-thermal JSR [115]. A JSR can be modeled as a Perfectly Stirred Reactor (PSR) in experimental studies. Indeed, the injection occurs through jet nozzles with a high velocity, which ensures instantaneous mixing inside the reactor, thus emulating a PSR. The species concentrations were measured after a fixed residence time (τ=0.05 s), at atmospheric pressure, and at ϕ=0.5 and 1. The injected mixture consisted of 2000 ppm CH_3OH, 6000/3000 ppm O_2 and was balanced out with N_2. The target species for this study were limited to the major species measured (CH_3OH, O_2, CO, CO_2), but a much larger number of species can be handled by `OptiSMOKE++`. The nominal kinetics used for this case was again the POLIMI C1-C3 V1412 [83], and the sensitivity study, for determining which reactions to consider in the optimization, was performed based on each targeted species. A threshold of 0.6 was used on the cumulative sensitivity function, which resulted in the 7 reactions and 17 kinetics parameters listed in Table 4.6. To stay consistent with the performance of the nominal mechanism for other cases, only the non-zero kinetic parameters were considered in the optimization, as can be seen in Table 4.6.

Again the `coliny_direct` method was used in this optimization, with the same settings as specified in Table 4.2. For this test case, the L1-norm formulation of the objective function was used (Eq. 2.13).

As no experimental uncertainty was reported in [115], a standard uncertainty of 1% of the highest measured concentration of respective species was considered for each point, according to recommendations from Olm et al. [85].

A comparison between the nominal and the optimized mechanisms are reported in Figure 4.5 and Table 4.7.

It can clearly be seen that an overall improvement is achieved for each species profile. This can especially be seen for ϕ=1 (Figures 4.5c and 4.5d). For ϕ=0.5 on the other hand,

Table 4.6: *List of the reactions and corresponding kinetic parameters (from the POLIMI C1C3 V1412 [83] mechanism) considered in the optimization for Test case 3.*

Reaction Nr	Reaction Formula	A	β	E_a
1	$O_2 + H \Leftrightarrow O + OH$	✓	✓	✓
4	$OH + HO_2 \Leftrightarrow O_2 + H_2O$	✓		✓
11	$H + HO_2 \Leftrightarrow O_2 + H_2$	✓		✓
13	$2OH\ (+M) \Leftrightarrow H_2O_2\ (+M)$	✓	✓	✓
176	$CH_2OH + M \Leftrightarrow CH_2O + H + M$	✓		✓
410	$CH_3OH + OH \rightarrow H_2O + CH_2OH$	✓	✓	✓
411	$CH_3OH + HO_2 \rightarrow H_2O_2 + CH_2OH$	✓		✓

Table 4.7: *List of values for the kinetic parameters considered in test case 3. The nominal values refer to the values from the POLIMI C1C3 V1412 [83] mechanism. Also the Obj value is presented at the end of the table for each mechanism. The units of the different kinetic parameters are as follows: A [s - cm^3 - mol], β [-] and E_a [cal/mol].*

Reaction Nr	Parameter	Nominal values	`coliny_direct`
1	A	9.6×10^{14}	1.4×10^{15}
	β	-0.2	-0.2
	E_a	16 625	16 625
4	A	5.0×10^{13}	1.08×10^{14}
	E_a	1 000	2 040
11	A	2.5×10^{13}	2.5×10^{13}
	E_a	700	700
13	A	1.3×10^{18}	9.56×10^{17}
	β	-0.90	-0.90
	E_a	-1 700	-1 700
176	A	3.75×10^{14}	1.74×10^{14}
	E_a	25 000	25 000
410	A	9.2×10^{4}	6.77×10^{4}
	β	2.53	2.53
	E_a	-1 000	-1 416
411	A	8.0×10^{13}	4.00×10^{13}
	E_a	19 400	19 400
Obj [-]		1.789×10^{2}	9.43×10^{1}

there are only major improvements for the CO profile (see Figure 4.5b), while the other profiles are very similar, or slightly improved compared to the nominal mechanism.

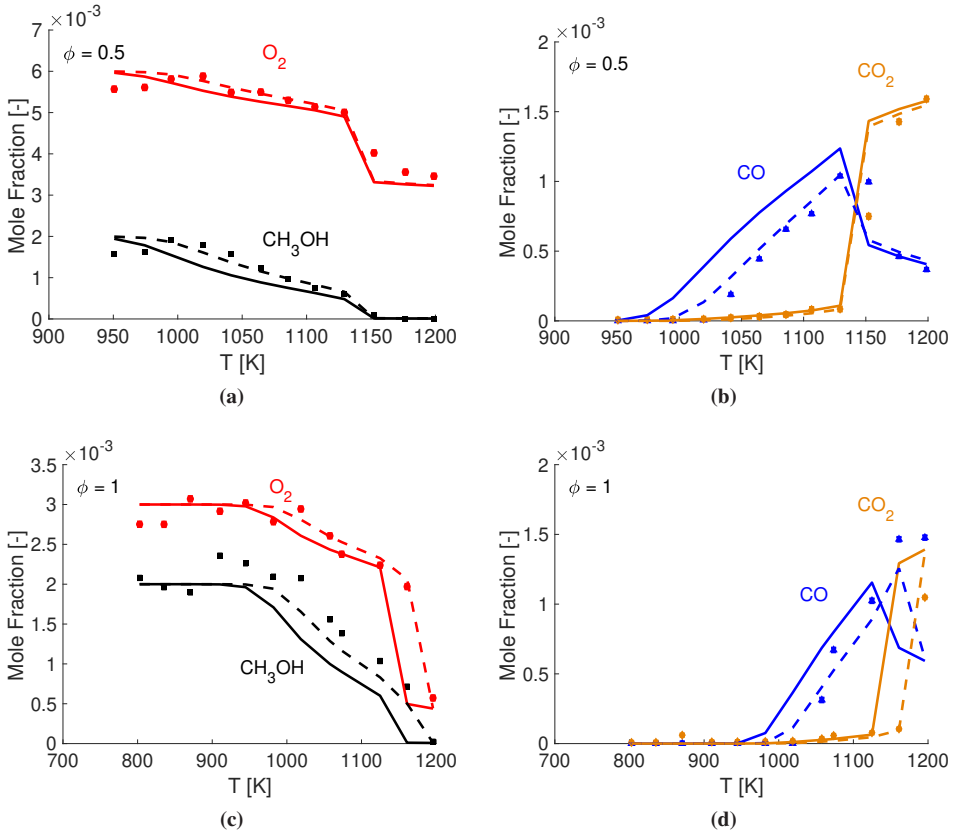

Figure 4.5: *Oxidation of methanol (CH_3OH) at atmospheric pressure in an iso-thermal JSR at different temperatures and at ϕ=0.5 and 1. The experimental data is presented by the scatter, with corresponding error bars. The nominal kinetics (POLIMI C1C3 V1412 [83]) is represented by the solid lines (—) and the optimized kinetics from test case 3 by the dashed lines (- -).*

4.6.4 Test case 4: A combined optimization

In practice, many different targets will be used for optimization, ensuring that the optimized kinetics performs good for a wide range of conditions. The combined optimization of test cases 1 and 3 is therefore used to illustrate this capability of the code. As in test case 1 and 3, the POLIMI C1C3 V1412 [83] mechanism was used. The combination of the non-zero kinetic parameters from Tables 4.1 and 4.6 were used in this optimization. The `coliny_direct` methodology was used for the optimization, with the settings specified in Table 4.2. In order to demonstrate the difference between the two objective function formulations, both the L1-norm (Eq. 2.13) and the L2-norm (Eq. 2.10) formulations were also used. The results are presented in Table 4.8 and Figures 4.6 and 4.7.

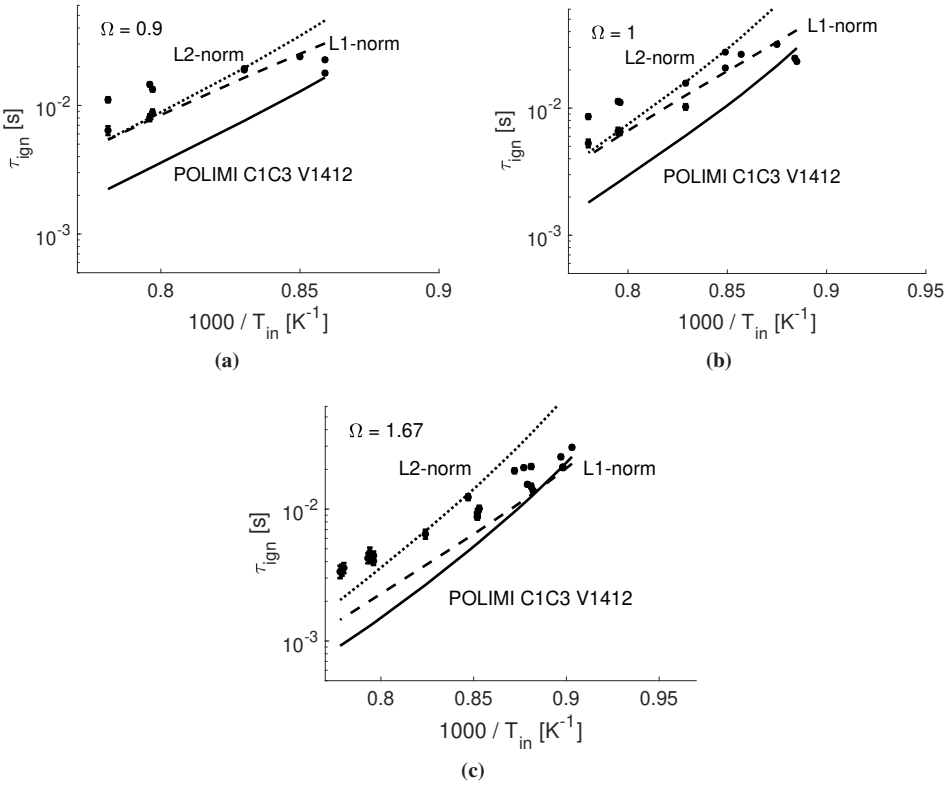

Figure 4.6: *IDT for Ω=0.9, 1 and 1.67 at different inlet temperatures, where the experimental data is presented by the black dots with corresponding error bars. The nominal kinetics is from test case 1 and is represented by the solid line (—). The two mechanisms optimized using the L1 and the L2-norm definitions are represented by the dashed line (- -) and the dotted line (···) respectively.*

The two formulations of the objective function gives the exact same improvements with respect to the experimental targets in test case 3 (see Figure 4.7). Considering that the objective function values for test case 3 are much higher than test case 1, for both L1

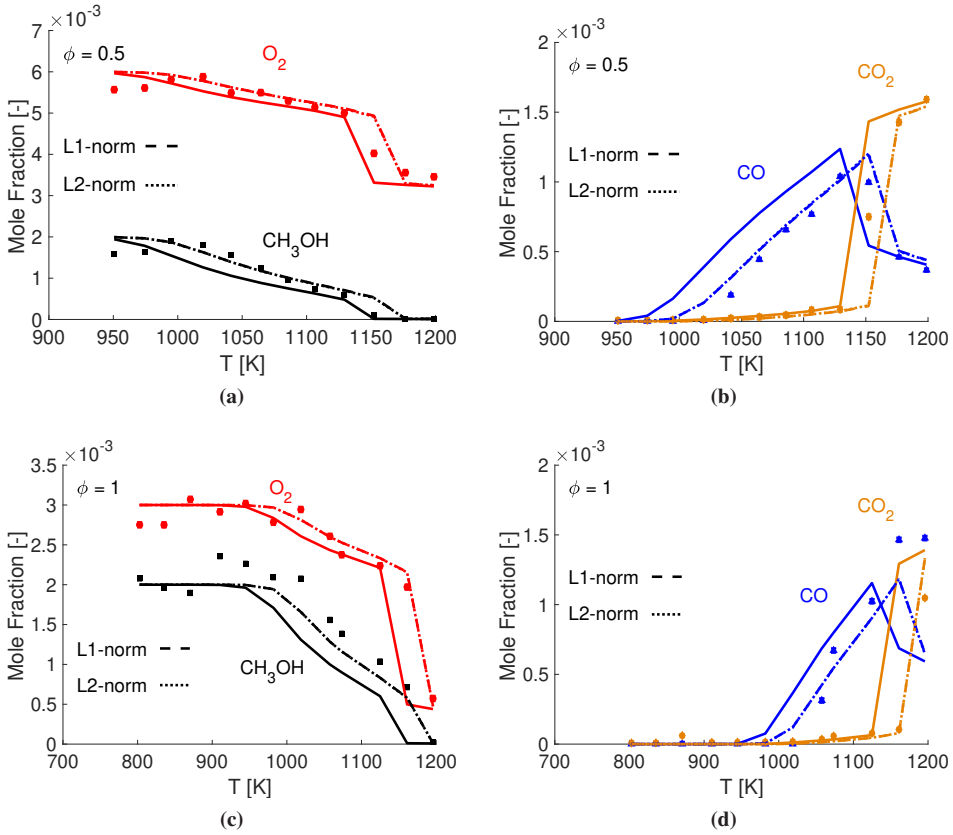

Figure 4.7: *Oxidation of methanol (CH_3OH) at atmospheric pressure in an iso-thermal JSR at different temperatures and at ϕ=0.5 and 1. The experimental data is presented by the scatter, with corresponding error bars. The nominal kinetics is from test case 1 and is represented by the solid lines (—). The two mechanisms optimized using the L1 and the L2-norm definitions are represented by the dashed lines (- -) and the dotted lines (⋯) respectively.*

and L2-norm formulations, the optimizer is first reducing the relative error to these targets. Thereafter, the optimizer tries to find combinations which also improves the objective function values for test case 1. However, for test case 1, the L2-norm formulation tends to over predict the IDT quite drastically at low temperatures (see Figure 4.6). Instead with the L1-norm, some quite significant improvements can be found for Ω=0.9 and 1 (see Figures 4.6a and 4.6b), while only slight improvements can be found for Ω=1.67 (Figure 4.6c). For a more direct comparison, the objective function was calculated using the L1-norm formulation with the mechanisms resulting from the L2-norm optimization, and vice versa. The values are presented in parentheses in Table 4.8. Although the L1-norm objective function value are the same for both the optimized mechanisms, the L2-norm value is even lower for the mechanism optimized using the L1-norm formulation.

Table 4.8: *List of values for the kinetic parameters considered in test case 4. The nominal values refer to the values from the POLIMI C1C3 V1412 [83] mechanism. Also the Obj value is presented at the end of the table for each mechanism. The units of the different kinetic parameters are as follows: A [s - cm^3 - mol], β [-] and E_a [cal/mol].*

Reaction Nr	Parameter	Nominal values	L1-norm	L2-norm
1	A	9.6×10^{14}	8.09×10^{14}	7.06×10^{15}
	β	-0.2	-0.2	-0.2
	E_a	16 625	16 625	16 209
4	A	5.0×10^{13}	5.0×10^{13}	2.5×10^{14}
	E_a	1 000	1 900	1 900
11	A	2.5×10^{13}	1.58×10^{13}	1.58×10^{13}
	E_a	700	700	700
13	A	1.3×10^{18}	9.56×10^{17}	9.56×10^{17}
	β	-0.90	-0.9	-0.9
	E_a	-1 700	-1 700	-1 700
23	A	2.33×10^{34}	3.69×10^{34}	2.33×10^{34}
	β	-5.03	-5.03	-5.03
	E_a	-1 200	-1 200	-1 200
23 [inf]	A	2.50×10^{13}	2.50×10^{13}	1.58×10^{13}
176	A	3.75×10^{14}	1.74×10^{14}	1.74×10^{14}
	E_a	25 000	25 000	25 000
223	A	1.0×10^{12}	5.41×10^{11}	1.85×10^{12}
	E_a	3 000	3 000	3 000
258	A	2.00×10^{12}	9.28×10^{11}	2.00×10^{12}
	E_a	8 000	8 000	8 000
271	A	6.0×10^{12}	1.03×10^{13}	3.51×10^{12}
391	A	2.00×10^{13}	4.31×10^{13}	2.00×10^{13}
	E_a	6 000	6 000	6 000
405	A	3.00×10^{7}	5.54×10^{7}	5.54×10^{7}
	β	2.0	2.0	2.0
	E_a	10 000	10 000	10 000
410	A	9.2×10^{4}	6.77×10^{4}	6.77×10^{4}
	β	2.53	2.53	2.53
	E_a	-1 000	-1 000	-1 000
411	A	8.0×10^{13}	4.01×10^{13}	4.01×10^{13}
	E_a	19 400	19 400	19 400
725	A	2.796×10^{6}	4.43×10^{6}	2.796×10^{6}
	β	2.0	2.0	2.0
	E_a	1 566	1 566	1 566
813	A	3.595×10^{6}	4.89×10^{6}	3.60×10^{6}
	β	2.0	2.0	2.0
	E_a	-238	-238	-238
817	A	3.513×10^{5}	3.513×10^{5}	4.775×10^{5}
	β	2.0	2.0	2.0
	E_a	7 622	7 622	7 622
Obj L1-norm [-]		1.79×10^{2}	9.51×10^{1}	(9.51×10^{1})
Obj L2-norm [-]		1.35×10^{4}	(3.41×10^{3})	3.44×10^{3}

4.6.5 Test case 5: Optimization of Laminar Flame Speed of methane diluted in CO_2

The experimental targets used for this test case consists of LFS data of methane/air diluted with 10% CO_2, at 1 bar and an inlet temperature of 473 K [116]. The experimental measurements were performed for an equivalence ratio between 0.7-1.2. The kinetic mechanism used for this test case was the GRI 3.0 [43] mechanism, and using a threshold of 0.6 on the cumulative sensitivity function resulted in 3 reactions and 7 kinetic parameters, which are listed in Table 4.9.

Table 4.9: *List of the reactions and corresponding kinetic parameters (from the GRI 3.0 [43] mechanism) considered in the optimization for Test case 5.*

Reaction Nr	Reaction Formula	A	β	E_a
38	$H + O_2 \Leftrightarrow O + OH$	✓	✓	✓
109	$OH + C_2H_2 \Leftrightarrow H_2O + C_2H$	✓	✓	✓
145	$O_2 + {}^1CH_2 \Leftrightarrow H_2O + CO$	✓		

Again only the non-zero parameter were used for the optimization. The `coliny_direct` approach was used for this test case, and the L2-norm formulation for the objective function (Eq. 2.10). The results can be seen in Table 4.10 and Figure 4.8.

Table 4.10: *List of values for the kinetic parameters considered in test case 5. The nominal values refer to the values from the GRI 3.0 [43] mechanism. Also the Obj value is presented at the end of the table for each mechanism. The units of the different kinetic parameters are as follows: A [s - cm^3 - mol], β [-] and E_a [cal/mol].*

Reaction Nr	Parameter	Nominal values	`coliny_direct`
38	A	2.65×10^{16}	2.67×10^{16}
	β	-0.67	-0.67
	E_a	17 041	17 180
109	A	3.37×10^{7}	1.52×10^{7}
	β	2.0	2.21
	E_a	14 000	12 999
145	A	1.20×10^{13}	2.90×10^{13}
Obj [-]		1.49×10^{2}	4.67×10^{1}

Even though there are only some minor improvements, the optimized mechanism is able to capture the experimental targets almost perfectly.

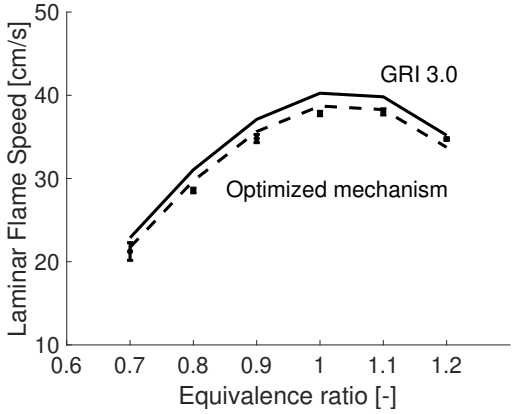

Figure 4.8: *LFS of methane/air diluted with 10% CO_2 at atmospheric pressure and an inlet temperature of 473 K. The experimental data is presented by the black dots with corresponding error bars, and the nominal kinetics (GRI 3.0 [43]) is represented by the solid lines (—) and the optimized mechanism by the dashed lines (- -).*

4.6.6 Runtime and number of evaluations

A comparison between the number of experimental targets, number of uncertain parameters, total number of evaluations, total number of times the penalty function was used and total runtime on one processor for each specific test case is presented in Table 4.11. It should be noted that the runtime for the different test cases depends not only on the number of experimental targets used, or the number of uncertain parameters, but also on the computational expense for the numerical evaluation of the considered facility. This can clearly be seen for test case 5, which has a considerably larger runtime than the other cases as it consists of LFS simulations that are more computationally demanding. The slight difference in the total number of evaluations, found specifically for the cases ran with the `coliny_direct` method, depends on the fact that the optimizer in general finishes one whole iteration before checking for the stopping criteria, and the iterations are not always distributed equally over the complete set of evaluations.

Table 4.11: *List of number of experimental targets, number of uncertain parameters, number of total evaluations, number of times the penalty function was used and finally the total runtime for each specific test case in this chapter.*

Test case	# targets	# parameters	# evaluations	# penalties	Runtime [h]
1 (EA)	34	26	1 000 220	999 023	1.69
1 (DIRECT)	34	26	5 001	1 974	4.29
2 (DIRECT)	14	20	5 021	2 622	0.45
3 (DIRECT)	96	17	5 005	2 992	2.38
4 (DIRECT L1)	122	40	5 013	2 761	5.65
4 (DIRECT L2)	122	40	5 029	2 831	5.58
5 (DIRECT)	6	7	5 001	3 964	44.01

It can be seen from test case 1 that, even though the Evolutionary Algorithm (EA) approach runs for many more evaluations, the runtime is actually lower compared to the DIRECT methodology. This is due to the more random nature of the EA algorithm, which in turn enforces the penalty function to be used a lot more, and the actual good evaluations performed with the EA algorithm is actually less than with the DIRECT algorithm. Interestingly enough the performance of the optimized mechanism with EA is very similar to that of the optimized mechanism with DIRECT, as can be seen in Figure 4.3.

4.7 Optimization of IDT for CH_4 and biomass pyrolysis products

To compare the performance of OptiSMOKE++ with the work performed in Chapter 3, the same set of experimental targets were used in an optimization study. The optimization was performed again using the same kinetic mechanism, i.e. POLIMI C1C3 V1412 [83], and with the same set of kinetic parameters (see Table 3.2). The coliny_direct methodology was used for the optimization, with the L2-norm formulation of the objective function (Eq. 2.10). The performance of the optimized mechanism, together with the nominal and the optimized mechanisms from Chapter 3 can be appreciated in Figures 4.9 and 4.10.

Overall the optimized mechanism from OptiSMOKE++ performs similarly as the optimized mechanism from Chapter 3, i.e. for the methane cases (Figure 4.9) there are no drastic changes. Except for C/O=0.2 (Figure 4.9d) where there are some further improvements achieved by OptiSMOKE++. For the biomass pyrolysis cases (Figure 4.10) the two optimized mechanisms are performing equally good.

The kinetic parameter values are shown in Table 4.12 together with the objective function values. Note that the objective function values with calculated using Eq. 2.10 for a direct comparison with the optimized mechanism from OptiSMOKE++. Comparing the objective function values in Table 4.12, it can actually be seen that the optimized mechanism from OptiSMOKE++ has a slightly higher value. This is mostly due to the slight over prediction of the IDT at C/O=0.1 at low temperatures (Figure 4.9c) for the mechanism from OptiSMOKE++.

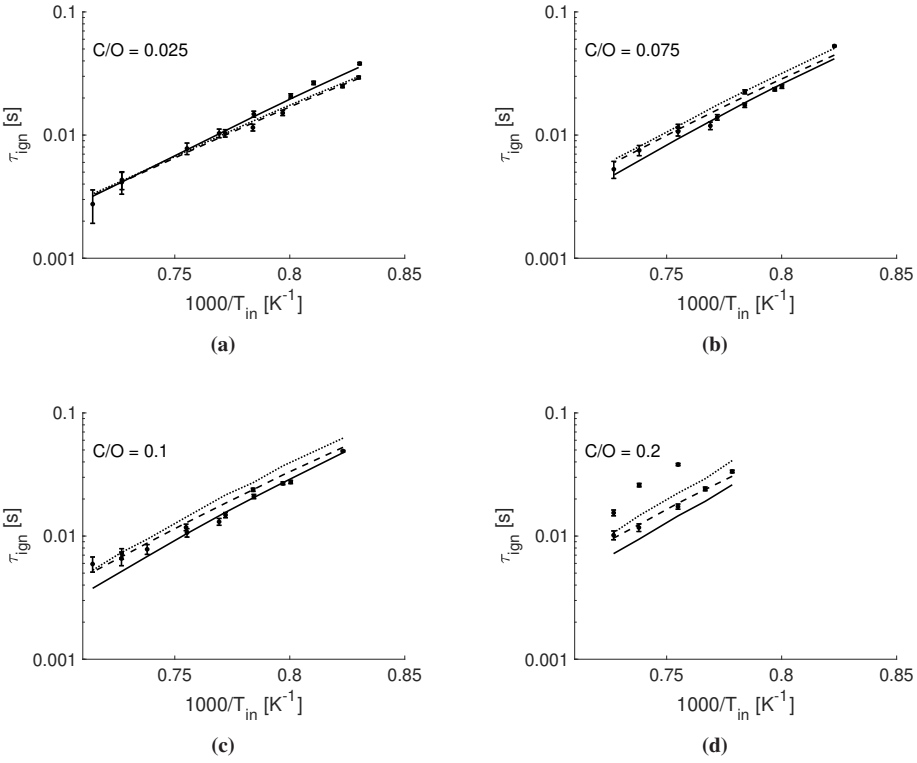

Figure 4.9: *IDT for methane at different inlet temperatures for C/O = 0.025-0.2. Experimental data are represented by points with corresponding error bars, while simulation results for the POLIMI mechanism are presented by the solid lines (—), the optimized mechanism from Chapter 3 by the dashed lines (- -) and the optimized mechanism from* `OptiSMOKE++` *by the dotted lines (⋯).*

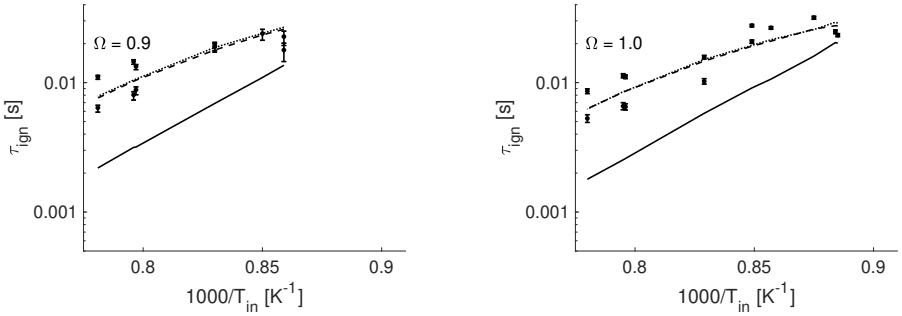

(a) **(b)**

Figure 4.10: *IDT for biomass pyrolysis products at different inlet temperatures for Ω = 0.9 and 1. Experimental data are represented by points with corresponding error bars, while simulation results for the POLIMI mechanism are presented by the solid lines (—), the optimized mechanism from Chapter 3 by the dashed lines (- -) and the optimized mechanism from* `OptiSMOKE++` *by the dotted lines (⋯).*

Table 4.12: *Nominal and optimized kinetic parameters, together with the corresponding objective function values calculated using Eq 2.10. The nominal values are from the POLIMI C1-C3 [83], while the two optimized mechanisms are from Chapter 3 and the* `OptiSMOKE++`*. The units of the different kinetic parameters are as follows: A [s - cm^3 - mol], β [-] and E_a [cal/mol].*

Reaction Nr	Parameter	Nominal values	Chapter 3	OptiSMOKE++
1	A	9.6×10^{14}	6.1×10^{14}	6.4×10^{14}
	β	-0.2	-0.2	-0.2
	E_a	16 625	16 556	16 625
271	A	6.0×10^{12}	2.56×10^{13}	2.79×10^{13}
405	A	3.0×10^{7}	7.54×10^{7}	6.80×10^{7}
	β	2	2	2
	E_a	10 000	10 139	10 000
Obj [-]		36.48×10^{-3}	2.82×10^{-3}	2.99×10^{-3}

4.8 Concluding remarks

The development of an efficient toolbox, for the optimization of a large number of kinetic parameters, with respect to different experimental targets, has been presented in this chapter. This was realized by coupling the DAKOTA toolkit with the OpenSMOKE++ framework. The toolbox consists of different features, which has been showcased in five different test cases, and these features are;

— Possibility to use experimental targets from different facilities, i.e. Batch Reactors, PFRs, PSRs, ST, RCMs and premixed laminar flames. Experimental data from different facilities can also be used simultaneously.

— Different optimization methodologies available in the DAKOTA toolkit can be employed.

— Two different definitions of the objective function has been implemented. The user can therefore choose the objective function definition most suitable for the case at hand. The benefit of using the L1-norm definition was highlighted, especially when considering experimental targets of different nature.

— The approach described in Fürst et al. [82] (see 2.2) has been implemented for calculating the upper and lower bounds for each kinetic parameter, based on the uncertainty limits of the rate coefficient.

— In order to arrive with a feasible kinetic mechanism, i.e. physically viable kinetic parameters, OptiSMOKE++ utilizes a penalty function which forcefully increases the objective function value when a set of kinetic parameters gives a rate coefficient outside the uncertainty bounds. This ensures that the optimizer choose an optimal point which still gives a physically viable rate coefficient value.

Combining all these features allowed OptiSMOKE++ to find a combination of parameters, which showed large improvements with respect to the nominal mechanisms used in each case.

To further evaluate the performance of OptiSMOKE++, the same optimization study that was performed in Chapter 3 was carried out with OptiSMOKE++. The results showed that the optimized mechanism from OptiSMOKE++ gave very similar performance overall compared to the mechanism from Chapter 3.

Based on the knowledge gathered from the work performed in both in this and in Chapter 3, the optimization of a kinetic mechanism, using many uncertain kinetic parameters, can be performed. What remains is to combine the two, and optimize a kinetic mechanism with respect to a large set of data, using OptiSMOKE++, for MILD conditions.

CHAPTER 5

Optimization of a kinetic mechanism for propane MILD combustion

As a final application, the optimization of a kinetic mechanism with respect to MILD combustion for a large set of experimental data was performed. Propane was chosen as the fuel, as it is both representative of the thermochemical and combustion properties of larger hydrocarbons, and due to the availability of a large database focused on MILD combustion of propane.

5.1 Experimental database

The experimental data used in this work consists of IDT of propane from two different publications [16, 117], and species measurements from a JSR [17, 118]. The IDT data consisted of different inlet temperatures, equivalence ratios, dilution ratios and diluent species. The species measurements similarly considered the effect of inlet temperature, equivalence ratio and diluent species. The dilution ratio for the JSR data was always kept to 90%, and was balanced out with N_2. The experimental conditions are summarized in Table 5.1.

The IDT data were measured at atmospheric pressure in a 1.4 m long PFR with an inner diameter of 0.01 m. The reactor was enclosed inside a heater, which ensured that the surrounding temperature was the same as the inlet temperature of the reactor (in order to reduce the heat losses). The overall heat transfer coefficient was calculated to 100.4 W/(m^2K) in [117]. The temperature profile was measured with thermocouples of type N,

Table 5.1: *Experimental data used for the optimization of propane kinetics in MILD conditions.*

Type	T [K]	ϕ [-]	Dilution	Nr of experiments	Ref
IDT	850-1250	0.1-2.67	90-97% N_2	431	[117]
IDT	850-1250	0.1-2.67	90-95% CO_2 & 90% H_2O	197	[16]
Speciation	720-1100	0.5-1.5	90% N_2 + CO_2	182	[17]
Speciation	720-1100	0.5-1.5	90% N_2 + H_2O	278	[118]

placed every 0.05 m along the axis of the reactor. The moment of ignition was identified at the location where a temperature increase of 10 K, with respect to the inlet temperature, was measured. The IDT was calculated by dividing the distance with the flow velocity, which in turn was calculated by dividing the flow rate with the cross area of the reactor. Based on the spacing between the thermocouples, and the flow velocity, an experimental error could be estimated as $(0.05/2)/v_i$, where v_i is the flow velocity for condition i.

The species profiles were evaluated in a non-isothermal quartz reactor of spherical shape with a volume (V) of 113 cm^3. The reactor was located inside two electrical fiber ovens, allowing the surrounding temperature to be the same as the inlet temperature, thus minimizing heat losses. Nonetheless, as the temperature inside the reactor increases due to chemical reactions, an overall heat transfer coefficient of 54.392 W/(m^2K) was specified according to [17,118]. All the experiments were performed at a pressure (P) of 1.1 atm and at a fixed residence time (τ_{res}) of 0.5 s. However, due to the thermal expansion inside the reactor, the volumetric flow rate (V/τ_{res}) cannot be considered constant. What is however constant is the mass flow rate ($\dot{m}$), which can be calculated based on the volumetric flow rate and the density of the mixture (ρ_{mix}), i.e. $\dot{m} = V/\tau_{res}/\rho_{mix}$, where the ρ_{mix} was calculated as $\rho_{mix} = \sum_i (M_i x_i) P/RT$, with M_i being the molar mass and x_i the mole fraction of species i, P the pressure, R the ideal gas constant and T the temperature.

The following species were measured in the two works; O_2, H_2, CO, CH_4, C_2H_2, C_2H_4, C_2H_6, C_3H_4 and C_3H_8 in [17] and O_2, H_2, CO, CO_2, CH_4, C_2H_2, C_2H_4 and C_2H_6 in [118].

However, due to an oscillating behavior, reported both in the experiments and simulations of these conditions, the experimental data from the the JSR were not included as targets for the optimization. The numerical oscillations resulted in infeasibly large simulation times for these data, and as the optimization process requires thousands of evaluations, it was not viable to use these data as targets for the optimization. They were instead used as a validation of the optimized mechanism, to evaluate if any major performance changes had occurred after the optimization.

5.2 Optimization strategy

The optimization was performed in a step-by-step approach similarly as done in Olm et al. [59], adding a new set of data with each optimization step, and keeping the targets from the previous step. The uncertain reactions were determined using a cumulative impact factor (see 2.1.2 and 2.1.3), where one cumulative function was created for each set of data,

and for each added data set, the reactions not previously considered in the optimization were added. This gradually increased the amount of reactions considered in the optimization, but as many of the most impactful reactions were the same for the different data sets, the increase was not that drastic with each new data set added to the optimization.

The optimization was performed using the `OptiSMOKE++` tool, described in Chapter 4. In an attempt to combine the features of both the EA (see 2.5.2) and the DIRECT (see 2.5.1) approaches, the optimization was first performed with the DIRECT approach, and then with the EA approach to add more randomness to the optimization. By doing so, the strengths of the two approaches are combined, and a better solution can be found. This is indeed what the developer of the DIRECT algorithm D. R. Jones suggests in [92], i.e. combining the DIRECT algorithm with another optimizer for the best performance. Although Jones suggests that the DIRECT algorithm should be combined with a good local optimizer, in this case another global optimizer was used for refining the search. This ensures that no global optimum was overseen.

The specific settings used for the two algorithms were as specified in Table 5.2.

Table 5.2: *List of specific settings used for the optimization of propane.*

`coliny_direct`		`coliny_ea`	
Max function evaluations	15 000	Max function evaluations	1 000 000
Max iterations	15 000	Max iterations	1 000 000
Convergence tolerance	10^{-8}	Convergence tolerance	10^{-8}
Solution target	10^{-6}	Solution target	10^{-6}
Seed	1000	Seed	1000
Global balance parameter	0.1	Population size	300
		Mutation rate	0.6
		Crossover rate	0.4
		Replacement size	10

The Nr of experiments in Table 5.1 refers specifically to the combination of inlet temperatures, equivalence ratios, dilution ratios and diluent species used in the experiments. However, these numbers are not strictly distributed between the different conditions equally, and some conditions consist of more experimental points than others. It is therefore important to divide the objective function with the number of experimental data in each dataset, as discussed in 2.3. This removes any persisting bias towards data sets which consist of more experimental data points, and an overall improvement for the complete set of data can be achieved.

The L2-norm definition of the objective function (Eq. 2.10) was used in this work, but no major difference in the results would be expected if the L1-norm (Eq. 2.13) definition would have been used.

5.3 Results

The first set of data considered in this optimization, was the data from [117], which consists of IDT of propane with N_2 as diluent. As mentioned in both [117] and [16], the

POLIMI C1C3 LT [83] mechanism was performing well for the conditions at hand, which is why it was used for this optimization study. The sensitivity study was performed with respect to temperature, and the resulting cumulative impact factor study resulted in the list of reactions presented in Table 5.3 for the IDT data. This set of reactions was determined using a threshold (ϵ) of 0.3, i.e. 70% of the impact can be represented with these reactions, for the specific cases.

Table 5.3: *Reactions with cumulative impact factor values above the threshold of 0.3 for the IDT of propane in MILD conditions. the specific conditions.*

		Diluent species		
Reaction Nr	Formula	N_2	CO_2	H_2O
1	$O_2 + H \Leftrightarrow O + OH$	✓	✓	✓
4	$OH + HO_2 \Leftrightarrow O_2 + H_2O$			✓
12	$2HO_2 \Leftrightarrow O_2 + H_2O_2$	✓		✓
23	$2CH_3$ (+M) $\Leftrightarrow C_2H_6$ (+M)	✓		
23 [inf]	$2CH_3$ (+M) $\Leftrightarrow C_2H_6$ (+M)	✓	✓	✓
27	$CH_3 + C_2H_5$ (+M) $\Leftrightarrow C_3H_8$ (+M)			✓
27 [inf]	$CH_3 + C_2H_5$ (+M) $\Leftrightarrow C_3H_8$ (+M)	✓	✓	✓
161	$O_2 + CH_4 \Leftrightarrow HO_2 + CH_3$	✓	✓	✓
271	$HO_2 + CH_3 \Leftrightarrow OH + CH_3O$	✓	✓	✓
391	$C_2H_4 + OH \Leftrightarrow H_2O + C_2H_3$	✓	✓	✓
407	$C_3H_8 + H \Leftrightarrow H_2 + n\text{-}C_3H_7$	✓	✓	✓
412	$C_3H_8 + HO_2 \Leftrightarrow H_2O_2 + n\text{-}C_3H_7$	✓		✓
413	$C_3H_8 + HO_2 \Leftrightarrow H_2O_2 + iso\text{-}C_3H_7$	✓		✓
525	$CH_3 + CH_3OO \rightarrow 2CH_3O$	✓		
904	$C_3H_8 + OH \rightarrow H_2O + n\text{-}C_3H_7$	✓	✓	✓
933	$C_3H_8 + OH \rightarrow H_2O + iso\text{-}C_3H_7$	✓	✓	✓

Many of these reactions can also be found in the optimization of methane and biomass pyrolysis products (see Table 3.2 and Table 4.1). These reactions seems to be highly influential particularly in MILD conditions. In fact, the oxidation of CH_3 through reactions R271 and R525 are particularly important for the ignition of propane at low temperatures according to Sabia et al. [117].

The influence of reaction R1 on ignition has already been mentioned in Chapter 3. This branching reaction creates two highly reactive radicals, namely O and OH, which participate strongly in other reactions in the ignition process.

At intermediate to high temperatures (T_{in}>1000 K), the influence of the recombination of CH_3 through reaction R23, becomes significant, as is shown in [16], where it was shown that this particular reaction showed very high influence to the ignition at high temperatures, regardless the equivalence ratio. This lowers the reactivity of the system, which also changes the slope of the IDT curve, indicating a so-called Negative Temperature Coefficient (NTC) behavior.

At low temperatures, the reactions R412, R413, R904 and R933 describe how propane (C_3H_8) undergo dehydrogenation by reacting with OH and HO_2 radicals to form normal- and iso-propyl (n-C_3H_7 and iso-C_3H_7) [117]. Although the normal- and iso-propyl radicals are highly reactive species, further reactions involving these radical were not included

in the optimization study mainly because the sensitivity analysis were performed at the moment of ignition of the different conditions. Reactions including the normal- and iso-propyl radicals are more important in the post-ignition segment and did therefore not show up in the sensitivity analysis.

According to Table 5.3, the dilution of CO_2 does not add any other important reactions that influence the IDT, that was not already important for dilution with N_2. However, as both reactions R23 and R27 are influenced by third bodies, the third body efficiency of CO_2 were included as an uncertain parameter for these two reactions. The upper and lower limits for the third body efficiencies were assumed $\pm$50% of the nominal value.

For the cases diluted with H_2O, only reactions R4 and R27 (low pressure limit) are added, where R4 directly involves H_2O through the reverse reaction step, and R27 again is a third body reaction. The third body efficiencies of H_2O was therefore also included in the optimization, for both reactions R23 and R27.

Only the non-zero parameters of the above mentioned reactions were used in the optimization. This is done in order to not drastically change the behavior of the mechanism, which is validated for a wide range of conditions. The number of uncertain parameters for the different cases therefore adds up to: 29, 31 and 38.

The complete comparison between the nominal and optimized mechanism can be found in Appendix B, but some key results are presented and discussed below.

A comparison of the performance of the optimized mechanism with respect to the nominal for stoichiometric conditions can be found in Figure 5.1 at all the different dilution ratios and diluent species. Interestingly enough, at stoichiometric conditions at 90% N_2 dilution (Figure 5.1a), the optimized mechanism is showing larger tendencies towards a NTC behavior, which is also supported by the experimental findings [117]. With increasing dilution ratio, and with CO_2 and H_2O as diluent, this behavior is no longer found, but large improvements in these conditions can be found nonetheless. However, due to the strong effect on the IDT at higher dilution ratios (95-97%) and at rich conditions ($\phi > 1$), the major improvements can be found there.

A comparison between the kinetic parameter values of the nominal and optimized mechanisms can be found in Table 5.4, together with the objective function values for the two mechanisms. It can be noticed that the objective function value of the optimized mechanism is lowered by roughly four times, with respect to the nominal mechanism. This reduction is mostly achieved by changes in the pre-exponential factors of the uncertain reactions, and only small changes are applied to the temperature exponents and activation energies. This is mainly due to the fact that a shift towards larger IDT values were enough as the slope of the nominal mechanism in the $\log(\tau)$ vs 1000/T space was good to start with. A more apparent NTC trend, at close to and at stoichiometric conditions, could be achieved with only small changes to some temperature exponents and activation energies. Another interesting fact is that although the conditions considered are highly diluted with third body species, such as CO_2 and H_2O, the optimized mechanism presents no changes to these values. Even for reaction R27, for which the nominal values are only put to the standard, i.e. 1. This indicates that the effect of the third bodies are not that impactful for these reactions. Indeed, Sabia et al. [16] discussed mainly the effect of third body efficiencies of CO_2 and H_2O for reactions such as H + O_2 + M $\Leftrightarrow$ HO_2 + M and H_2O_2 + M $\Leftrightarrow$ OH + OH +M. As these reactions are not included in the optimization study, the influence of third body efficiencies were not that significant. Larger improvements could possibly be

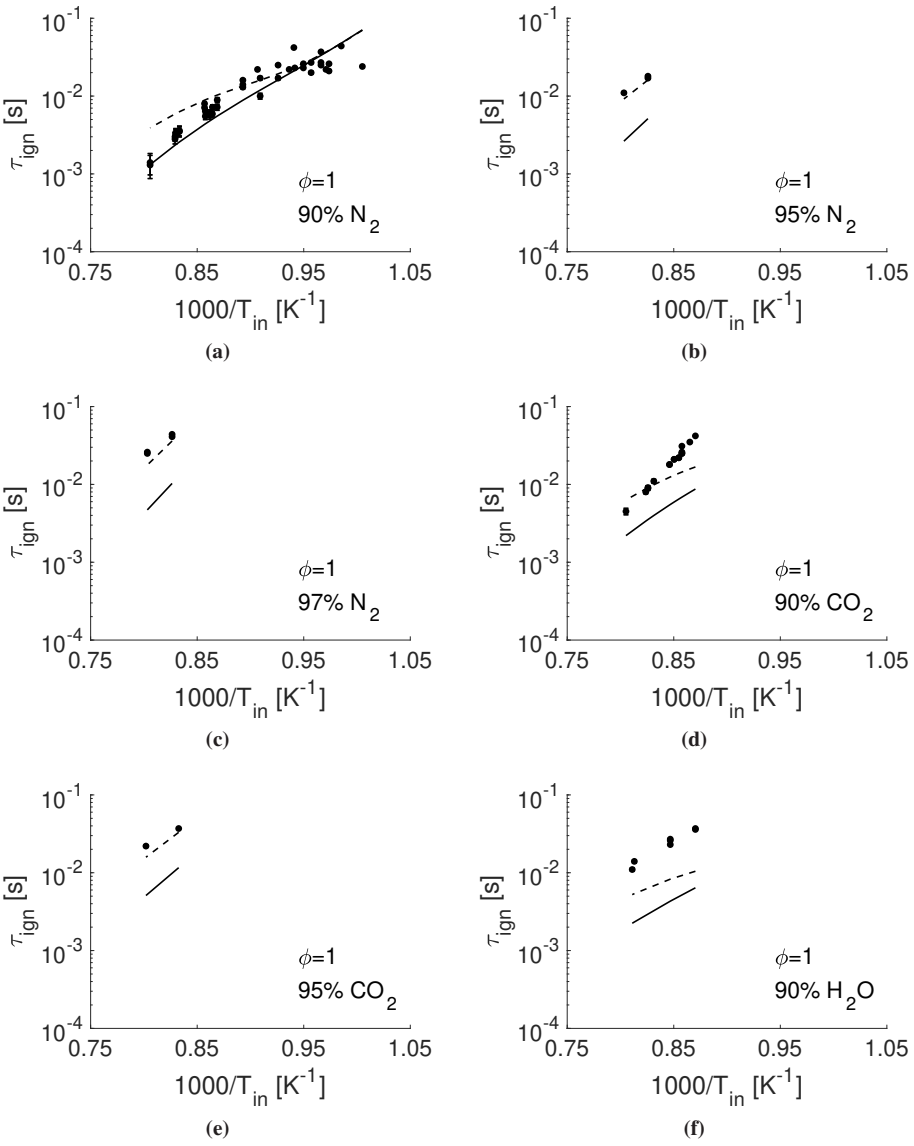

Figure 5.1: *IDT for propane diluted with 90-97% N_2, 90-95% CO_2 and 90% H_2O at different inlet temperatures for ϕ = 1. Experimental data (from [16, 117]) are represented by points with corresponding error bars, and the simulation results for the POLIMI mechanism are presented by the solid lines (—) and the optimized mechanism by the dashed lines (- -).*

found if such influential third body efficiencies were included in the optimization, and the approach of selecting the uncertain kinetic parameters could be improved.

Table 5.4: *Comparison between the values for the kinetic parameters considered in the optimization. The nominal values refer to the values from the POLIMI C1C3 V1412 [83] mechanism. Also the Obj value is presented at the end of the table for the two mechanisms. The units of the different kinetic parameters are as follows: A [s - cm^3 - mol], β [-], E_a [cal/mol] and M [-].*

Reaction Nr	Parameter	Nominal values	Optimized values
1	A	9.6×10^{14}	6.71×10^{14}
	β	-0.2	-0.21
	E_a	16 625	16 513
4	A	5.0×10^{13}	3.71×10^{13}
	E_a	1 000	1 047
12	A	2.11×10^{12}	4.35×10^{12}
23	A	2.33×10^{34}	4.65×10^{34}
	β	-5.03	-5.04
	E_a	-1 200	-837
	M_{CO_2}	3	3
	M_{H_2O}	5	5
23 [inf]	A	2.5×10^{13}	4.53×10^{13}
27	A	6.8×10^{61}	5.88×10^{61}
	β	-13.42	-13.55
	E_a	6 000	6 063
	M_{CO_2}	1	1
	M_{H_2O}	1	1
27 [inf]	A	9.6×10^{14}	4.93×10^{14}
	β	-0.50	-0.50
161	A	9.0×10^{13}	9.0×10^{13}
	E_a	56 000	56 088
271	A	6.0×10^{12}	7.07×10^{12}
391	A	2.0×10^{13}	3.72×10^{13}
	E_a	6 000	7 040
407	A	1.27×10^{14}	2.11×10^{14}
	E_a	10 500	10 283
412	A	4.2×10^{13}	1.91×10^{13}
	E_a	20 400	21 988
413	A	1.4×10^{13}	3.26×10^{13}
	E_a	17 700	19 127
525	A	3.0×10^{13}	9.49×10^{13}
	E_a	-1 200	-1 197
904	A	3.195×10^{6}	6.39×10^{6}
	β	2.0	2.0
	E_a	-498.69	-989.02
933	A	7.988×10^{5}	4.00×10^{6}
	β	2.0	2.0
	E_a	-1 798	-1 548
Obj [-]		8.56×10^{-1}	2.31×10^{-1}

5.3.1 Validation against JSR data

As previously mentioned, the experimental data from [17,118] were used as validation targets. As a whole, the performance of the optimized mechanism is similar as the nominal one, as can be seen in some species profiles presented in Figures 5.2-5.4. The complete set of profiles can be found in Appendix B. Although the objective function value was reduced from 2.51 $\times 10^7$ to 1.10 $\times 10^7$ (using the L2-norm Eq. 2.10), only slight differences can be noticed in peak values for species such as propene (C_3H_6) and ethylene (C_2H_4). However, for the major species, such as O_2, CO, CO_2 and C_3H_8, there are no major differences between the two mechanisms, and the general trend of the experiments are predicted. The major discrepancy between the experimental data and the simulations can be found for methyl acetylene (C_3H_4) (see Figures B8g and B9g), where both the mechanisms are over predicting the molar fractions drastically. However, as this was the same for the nominal mechanism, no major difference is found with the optimized mechanism.

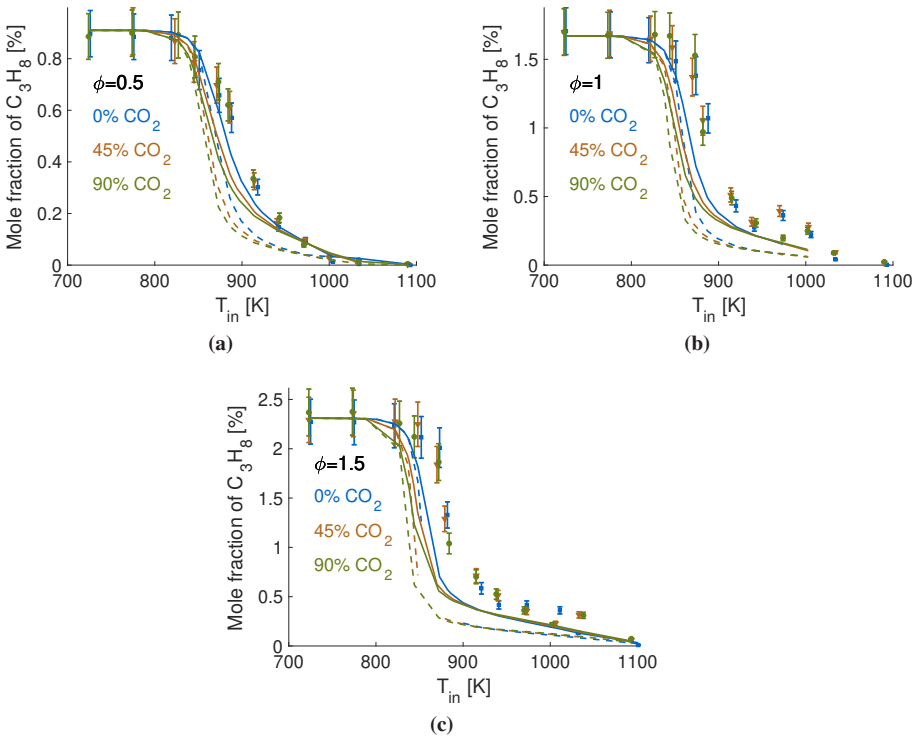

Figure 5.2: *JSR C_3H_8 measurements for propane oxidation diluted with CO_2 and N_2 at different inlet temperatures for ϕ = 0.5-1.5. Experimental data (from [17]) are represented by points with corresponding error bars, and the simulation results for the POLIMI mechanism are presented by the solid lines (—) and the optimized mechanism by the dashed lines (- -).*

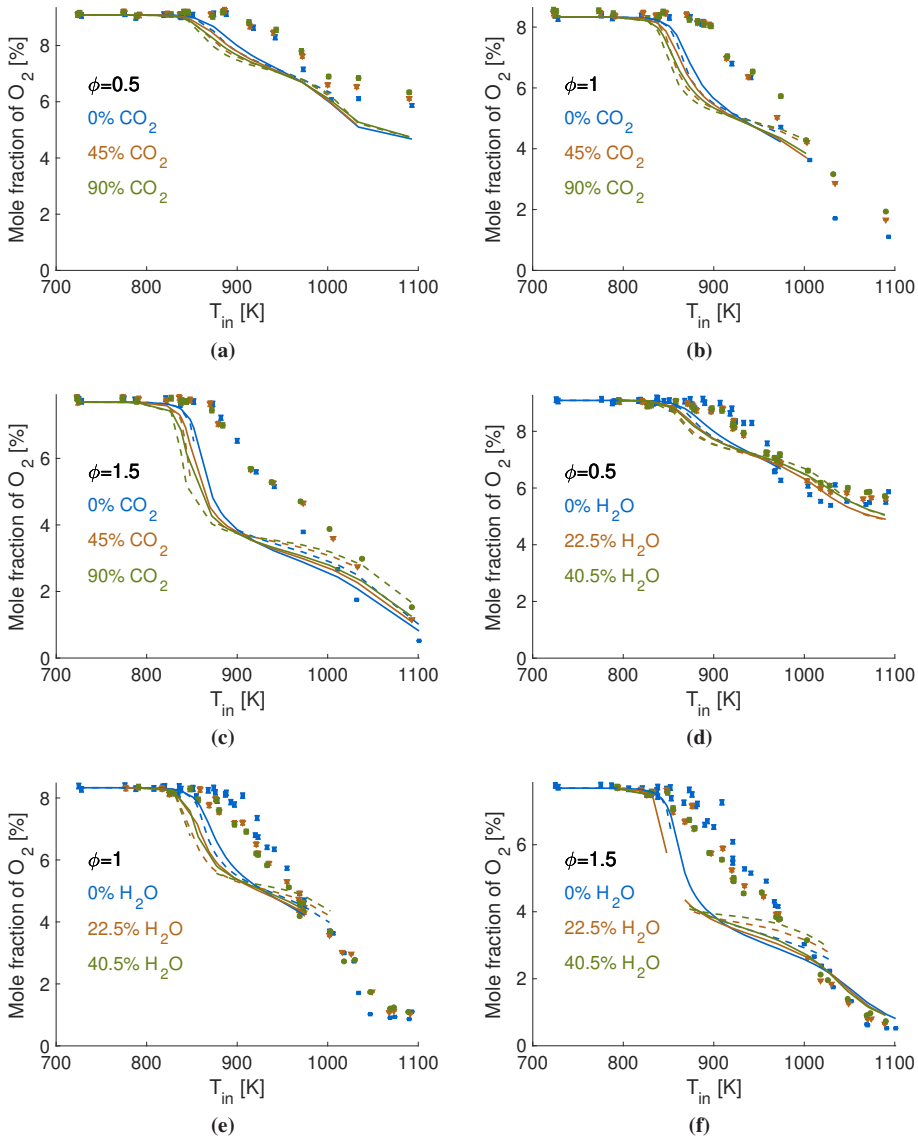

Figure 5.3: *JSR O_2 measurements for propane oxidation diluted with CO_2, H_2O and N_2 at different inlet temperatures for ϕ = 0.5-1.5. Experimental data (from [17, 118]) are represented by points with corresponding error bars, and the simulation results for the POLIMI mechanism are presented by the solid lines (—) and the optimized mechanism by the dashed lines (- -).*

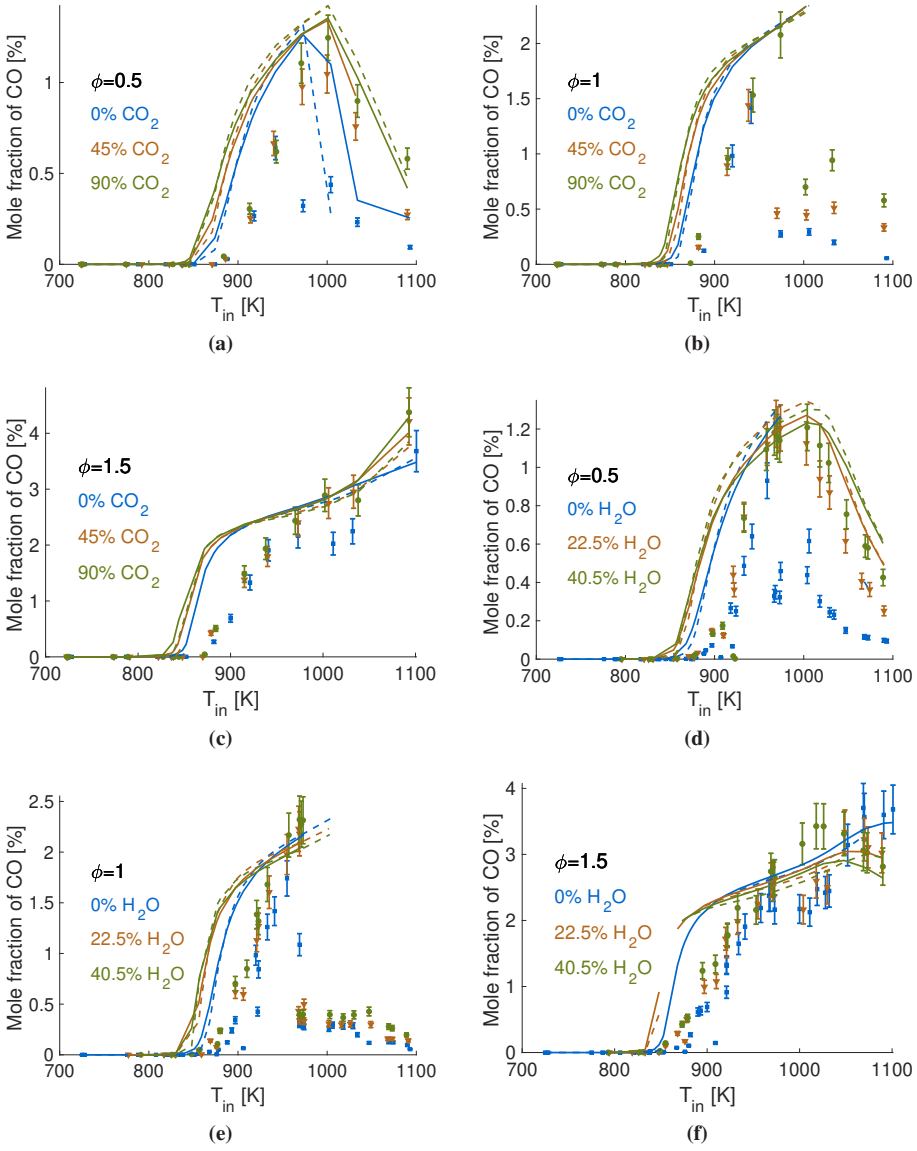

Figure 5.4: *JSR CO measurements for propane oxidation diluted with CO_2, H_2O and N_2 at different inlet temperatures for ϕ = 0.5-1.5. Experimental data (from [17, 118]) are represented by points with corresponding error bars, and the simulation results for the POLIMI mechanism are presented by the solid lines (—) and the optimized mechanism by the dashed lines (- -).*

5.4 Concluding remarks

The application of optimization of a chemical mechanism with respect to a large set of experimental targets in MILD combustion has been presented in this chapter. Propane was used as the targeted fuel, as a large database of MILD combustion of propane was available in the form of Ignition Delay Times (IDTs) and species measurements form a Jet Stirred Reactor (JSR). However, due to numerical instabilities in the simulation of the JSR data, these were only used as a final validation of the optimized mechanism, rather than optimization targets. Nonetheless, more than 600 experimental targets of IDT were used for the optimization. The optimization was performed in a step-by-step approach, where the each step consisted of adding another data set to the optimization, still keeping the previous experiments as targets. The uncertain reactions were determined using a cumulative impact factor for each separate data set. The kinetic parameters of the reactions which showed a cumulative impact factor above the threshold of 0.3 were used in the optimization. With each step, the reactions which were not already considered in the optimization, were added to the optimization. However, as many of the reactions were in common for the different data sets, the amount of uncertain parameters did not increase that drastically with each step. The total amount of 38 uncertain parameters were used in the optimization contemporary. The optimization was performed with the toolbox `OptiSMOKE++`, described in Chapter 4. By using two different optimization approaches, namely `coliny_direct` and `coliny_ea`, the optimization was achieved using the benefits of both these methods. The `coliny_direct` was used to quickly arrive at a good potential optimum, and the `coliny_ea` method was used to find further improvements using the more randomized approach of Evolutionary Algorithm (EA).

Based on the results from this chapter, the following conclusions can be made:

— The optimized mechanism showed large improvements, especially for IDT at high equivalence ratios, and at high dilution ratios.

— The optimized mechanism showed a change in curvature at lower temperatures and equivalence ratios close to and at stoichiometric conditions, indicating a so called Negative Temperature Coefficient (NTC) behavior, which is also something that was found in the experiments.

— The suggested changes to the kinetic parameters consisted mainly of changing the pre-exponential factors of the uncertain reactions. Considering that the nominal mechanism showed good trends with respect to the IDT, a shift towards larger IDT values was achieved by only changing these parameters.

— Some slight changes to the temperature exponents and activation energies was enough to change the aforementioned curvature at close to and at stoichiometric conditions towards a NTC behavior.

Additionally, the validation against the JSR data showed that the optimized mechanism performed very similarly as the nominal mechanism. The only major difference was found in the peak predictions of C_3H_6 and C_2H_4, which were slightly higher for the optimized mechanism. However, the major species profiles were very similar for the two mechanisms.

Although the performance of the optimized mechanism is quite satisfactory, there are still room for improvements, especially at the conditions diluted with H_2O. As the effect

of third body efficiencies was not influential for the reactions considered, further improvements could be found if reactions where the third body efficiencies are impactful were included. However, the optimized mechanism from this work can easily be used as a starting point for further optimization.

CHAPTER 6

Conclusions

Considering that for MILD combustion simulations, the usage of detailed kinetics is important, a large part of the prediction uncertainty in numerical simulations can be allocated only to the kinetics. Additionally, as existing detailed mechanisms have been developed and validated against conventional combustion targets, their performance with respect to MILD conditions is not optimal. Due to the increased presence of combustion products and higher temperature of the reacting mixture, MILD combustion behaves chemically differently compared to conventional conditions. To reduce the uncertainty and improve the performance of detailed kinetic mechanisms with respect to MILD combustion, the application of Uncertainty Quantification (UQ) and Optimization techniques has been performed in this work.

The first application of this was focused on the optimization of detailed kinetics with respect to Ignition Delay Time (IDT) of methane and biomass pyrolysis products. The optimization was performed using Surrogate Models (SMs) for representing the response of changing the uncertain kinetic parameters. In this work, the amount of uncertain parameters was directly reduced by performing a forward UQ study to determine which reactions that had only minor influence on the conditions considered. Such a study would become even more crucial as the number of experimental targets increase, which directly increases the amount of reactions that show high sensitivity towards the experiments. The prior uncertainty ranges of each kinetic parameter were determined using a novel approach developed in this work. The approach uses the extreme points of the uncertainty band of the rate coefficient, i.e. at T_{min} and T_{max}, and by finding the curve, with two unknown parameters, that intercepts these points, the extreme values of the kinetic parameters can be

determined. This approach has proven to be suitable, as it presents a somewhat conservative estimation of the limits of the kinetic parameters, which in turn allows for optimization of the mechanism with only minor changes to the overall behavior. Physically viable values of the rate coefficients were assured by only evaluating the parameter combinations that did not provide rate coefficient values outside of the uncertainty bounds. The optimal point, out of all the evaluated parameter combinations, provided quite drastic improvements for the IDT of biomass pyrolysis products, as well as for C/O=0.2 and for high temperatures for the other methane cases. To ensure that no drastic reduction in performance of the mechanism was found for conventional conditions, the optimized mechanism was compared to the nominal for IDT of methane-air mixtures at different pressures. Interestingly enough, it was even found that the optimized mechanism is outperforming the nominal mechanism at low pressures (1 atm).

This first application of optimization towards MILD experimental targets proved successful. However, with an increasing amount of experimental targets, the approach of using SMs would quickly become infeasible. With an increasing number of experimental targets also the amount of uncertain kinetic parameters that should be considered in the optimization would increase. This would directly increase the complexity of the mechanism response to each change in the parameters, and it would become increasingly difficult to build accurate SMs for the optimization. An efficient toolbox for the optimization of kinetic mechanisms, with respect to a large number of uncertain parameters and experimental targets was therefore developed. Rather than using SMs for representing the behavior of changes in the mechanism, this tool tightly coupled an optimization toolkit (`DAKOTA`) with a simulation code (`OpenSMOKE++`) for simulations of detailed kinetics in reactive systems. By doing so, this new tool, called `OptiSMOKE++`, is able to use sophisticated optimization algorithms, which determines potential optimal parameter combinations in the parameter space based on information from previous evaluations. The global optimum can therefore be found, using a relatively small amount of simulations. The tool was created in a way that the user has flexibility in the choice of the optimization approach, experimental targets, objective function formulation and uncertain kinetic parameters. Depending on the choice of optimization approach, the tool seems to be remarkably suitable for optimizing kinetic mechanisms, considering a large amount of uncertain parameters simultaneously.

The tool (`OptiSMOKE++`) was finally used for the optimization of a kinetic mechanism with respect to MILD combustion, considering a large amount of experimental data, and quite a significant amount of uncertain kinetic parameters. The fuel considered was propane, and a large set of IDT at a wide range of equivalence ratios, inlet temperatures, dilution ratios and diluent species were considered as targets for the optimization. Large improvements could be found for rich conditions, as well as for high dilution ratios. These improvements could be found by mostly changing the pre-exponential factors of the uncertain reactions. As indeed the nominal mechanism showed a good tendency towards the IDT, the shift towards larger IDT values was achieved with just this change. However, by changing only slightly the temperature exponents and activation energies for the considered reactions, the optimized mechanism was able to show an increased Negative Temperature Coefficient (NTC) behavior at close to and at stoichiometric conditions with N_2 as diluent, which was also found experimentally. For the conditions diluted with H_2O, only small improvements were found, but considering that the reactions used in the opti-

mization showed no direct impact of the third body efficiencies of either H_2O or CO_2, further improvements could be achieved if more reactions were included in the optimization. Specifically reactions where the third body efficiency has a larger influence. Considering that the approach applied in this work only considers the sensitivity of the pre-exponential factor towards the simulation results, the effect of the third body efficiencies were not emphasised in the selection process of the uncertain parameters. This is definitely something that could be improved in the approach used in this work. The optimized mechanism was also validated against species measurements from the oxidation of propane in MILD conditions in a Jet Stirred Reactor (JSR). The performance of the optimized mechanism was very similar to the nominal mechanism, which were able to capture the general trends in the species profiles. Only the prediction of the peak values of C_3H_6 and C_2H_4 were slightly higher for the optimized mechanism, but the profiles of the major species were very similar.

As a final remark, it can be said that the performance of existing detailed chemical mechanisms can be improved with respect to MILD combustion by applying the optimization strategies put forth in this work. Through the development of the `OptiSMOKE++` toolbox, an optimization study considering a large set of experimental targets, as well as many uncertain kinetic parameters simultaneously, can be performed.

Future perspectives

The work performed in this thesis has been focusing on the application of optimization strategies on existing detailed kinetic mechanism that have not necessarily been validated against the conditions considered as targets, i.e. MILD combustion. However, as a further application of the tools developed here, it would be very interesting to look towards optimizing new reaction pathways determined for larger fuels. These reaction pathways are nowadays normally determined using high level theoretical calculations consisting of; *ab-initio* electronic structure theory, transition state theory, classical trajectory simulations and master equations [119, 120]. These methods are able to quite accurately determine the rate constants for new reaction pathways, but as with any methodology, there still exists a correlated uncertainty. By optimizing these new pathways, within their specific uncertainty bounds, significant improvements can be found much faster than by redoing the quite computationally expensive theoretical calculations mentioned above.

Another interesting aspect that was already mentioned is the determination of influential kinetic parameters. As the dimensionality of the problem increases, i.e. more experimental data is considered, more reactions will show large sensitivities with respect to some specific condition. If all the kinetic parameters should always be considered in an optimization study, the amount of uncertain parameters will increase drastically. If instead only the most influential parameters can be determined *a priori*, the convergence of the optimization will be much faster, and more detail can be put on only the important parameters.

Nomenclature

Acronyms

Acronym	Description
ANN	Artificial Neural Network
B2B-DC	Bound-to-Bound Data Collaboration
CDC	Colorless Distributed Combustion
CFD	Computational Fluid Dynamics
DAKOTA	Design Analysis Kit for Optimization and Terascale Applications
DIRECT	DIviding RECTangles
EA	Evolutionary Algorithm
EGR	Exhaust Gas Recirculation
FLOX	Flameless Oxidation
GA	Genetic Algorithm
GLS	Generalized Least Squares
GP	Gaussian Process interpolation
HDMR	High-Dimensional Model Representation
HiTAC	High Temperature Air Combustion
IDT	Ignition Delay Time
JSR	Jet Stirred Reactor
LAD	Least Absolute Deviation
LFS	Laminar Flame Speed
LHS	Latin Hypercube Sampling
LS	Least Squares
MILD	Moderate of Intense Low-oxygen Dilution
MLE	Maximum Likelihood Estimation
MUM-PCE	Method of Uncertainty Minimization using Polynomial Chaos Expansions
Norm	Normalized
Nr	Number
NTC	Negative Temperature Coefficient

PCE	Polynomial Chaos Expansion
PFR	Plug Flow Reactor
PSR	Perfectly Stirred Reactor
QoI	Quantity of Interest
RCM	Rapid Compression Machine
SM	Surrogate Model
ST	Shock-Tube
UQ	Uncertainty Quantification

Roman symbols

Symbol	Unit	Description
a		Coefficient
A	s - cm^3 - mol	Pre-exponential factor
b		Coefficient
$b(\mathbf{x})$		Polynomial function
c		Coefficient
C	s	Computational cost
C_0	s	Computational overhead
Da		Damköhler number
E_a	cal/mol	Activation energy
f		Uncertainty parameter
$f(\mathbf{x})$		Regression function
$\mathbf{g}$		Set of constants
I		Impact factor
k	s^{-1}	Reaction rate coefficient
K		Number of species
$\dot{m}$	kg/s	Mass flow rate
M	kg/mol	Molar mass
N		Number of experimental data points
Obj		Objective function
P	atmosphere (atm)	Pressure
$\mathbf{r}$		Correlation vector
R	1.987 cal/K/mol	Ideal gas constant
S		Sensitivity coefficient
T	K	Temperature
v	m/s	Velocity
V	m^3	Volume
x		Function parameter/mole fraction
X		Number of standard deviations
$\mathbf{X}$		Parameter vector
y		Absolute value of QoI
$y(\mathbf{x})$		Model representation
Y		QoI
$Z(\mathbf{x})$		Residual function

Greek symbols

Symbol	Unit	Description
α		Weighing factor
β		Temperature exponent
γ		Correlation function degree
ϵ		Cut-off threshold
ε		Relative experimental error
θ		Hyper-parameters for the correlation function
ρ	kg/m^3	Density
σ		Standard deviation
τ	s	Time
ϕ		Equivalence ratio
Ψ		Correlation function
$\mathbf{\Psi}$		Correlation matrix
Ω		Oxygen ratio

Subscripts

Symbol	Description
0	Nominal
d	Number of dimensions in the parameter space
exp	Experimental
i	Index
ign	Ignition delay
in	Inlet
j	Index
max	Maximum
min	Minimum
mix	Mixture
p	Number of polynomial functions
res	Residence
$stat$	Statistical

Superscripts

Symbol	Description
$*$	Prediction point
exp	Experimental value
n	Number of observations
sim	Simulation value

List of Figures

List of Figures

List of Tables

Appendices

Appendix A: Prior uncertainty range evaluation

This appendix presents the forward Uncertainty Quantification (UQ) study that was performed in combination with the work of Chapter 3. The reactions considered were the following; R1 (O_2 + H $\Leftrightarrow$ O + OH), R229 (O_2 + CH_3 $\Leftrightarrow$ O + CH_3O), R271 (HO_2 + CH_3 $\Leftrightarrow$ OH + CH_3O, R405 (CH_4 + H $\Leftrightarrow$ H_2 + CH_3) and R513 (CH_3OO $\Leftrightarrow$ CH_2O + OH). The reaction numbers refer to the order they appear in the POLIMI mechanism [83]. The prior uncertainty range for each reaction (represented by the grey area in Figures A1-A10) was determined using the specific uncertainty ranges of the kinetic parameters, and when all three parameters (A, β and E_a) were given for a specific reaction, a set of samples were used to determine the potential uncertainty range with respect to the experimental targets [18, 93]. It should be noted that this study was only performed on each single reaction, and that the combined effect of changing the kinetic parameters from more than one reaction was not evaluated.

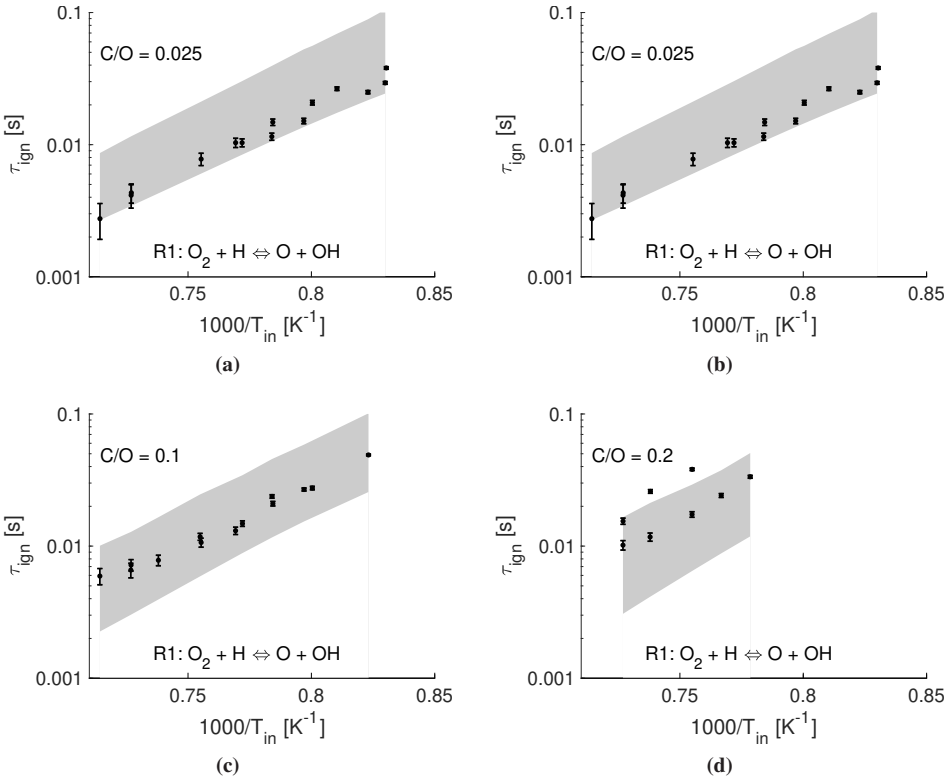

Figure A1: *Prior uncertainty range for reaction R1 (O_2 + H ⇔ O + OH) for methane at C/O = 0.025-0.2. Experimental data are represented by points with corresponding error bars.*

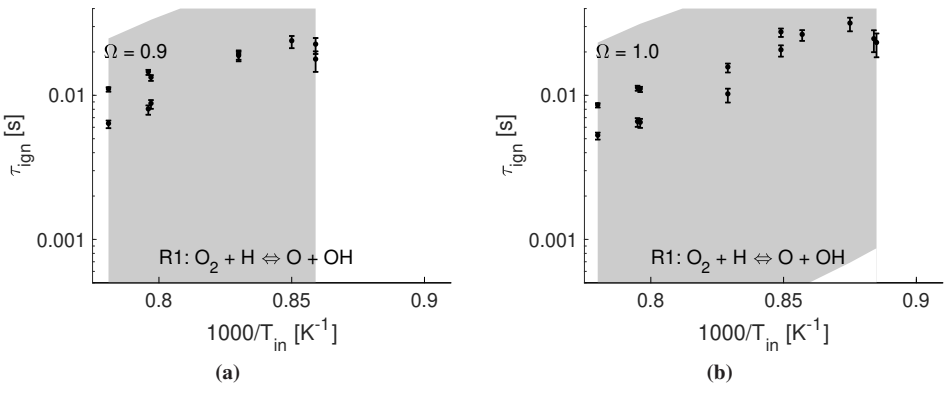

Figure A2: *Prior uncertainty range for reaction R1 (O_2 + H ⇔ O + OH) for biomass pyrolysis products at Ω = 0.9 and 1. Experimental data are represented by points with corresponding error bars.*

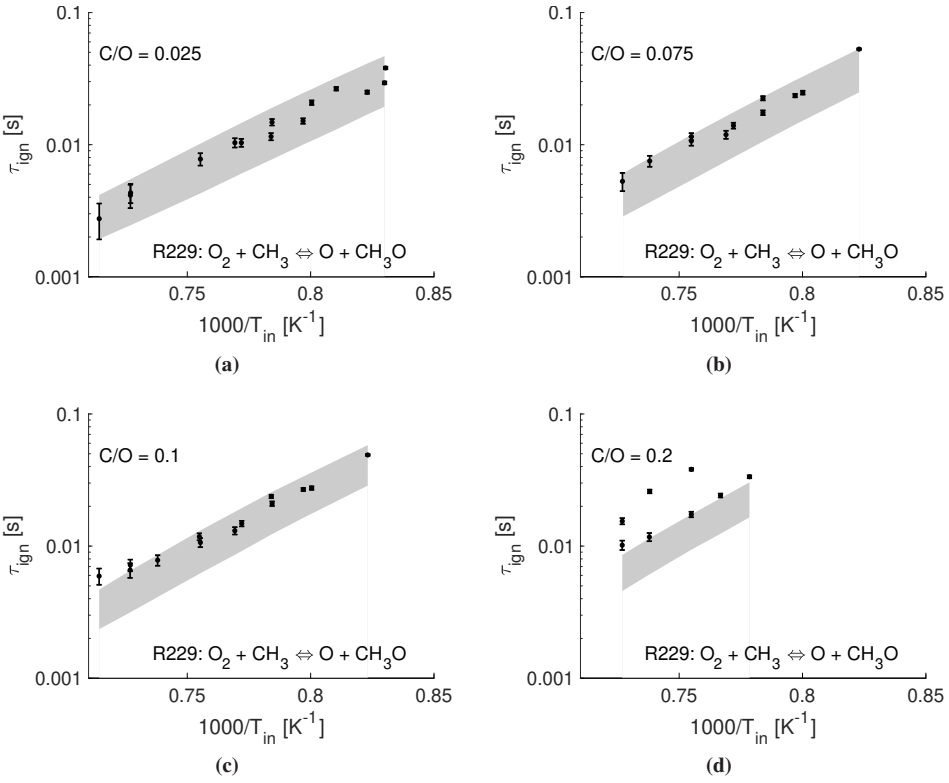

Figure A3: *Prior uncertainty range for reaction R229 (O_2 + CH_3 ⇔ O + CH_3O) for methane at C/O = 0.025-0.2. Experimental data are represented by points with corresponding error bars.*

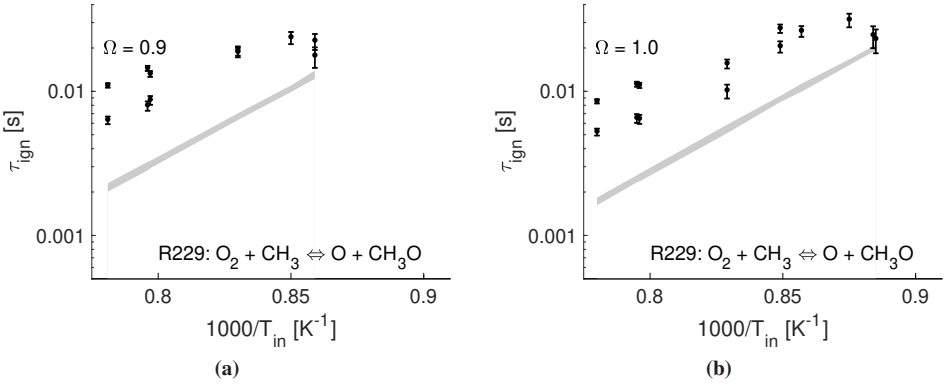

Figure A4: *Prior uncertainty range for reaction R229 (O_2 + CH_3 ⇔ O + CH_3O) for biomass pyrolysis products at Ω = 0.9 and 1. Experimental data are represented by points with corresponding error bars.*

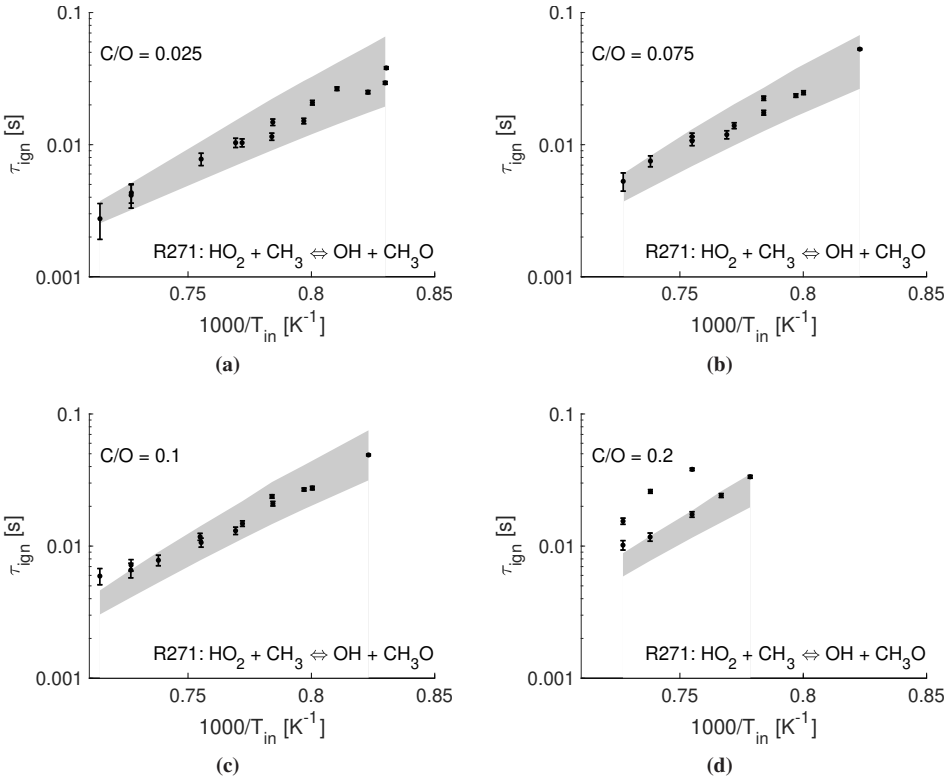

Figure A5: *Prior uncertainty range for reaction R271 (HO_2 + CH_3 ⇔ OH + CH_3O) for methane at C/O = 0.025-0.2. Experimental data are represented by points with corresponding error bars.*

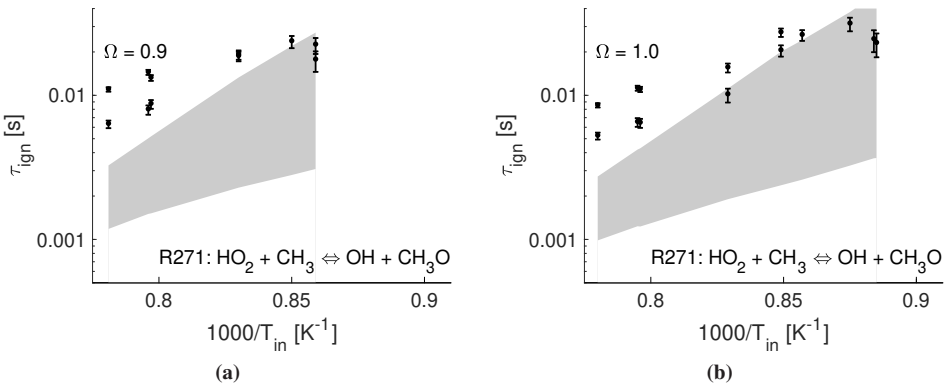

Figure A6: *Prior uncertainty range for reaction R271 (HO_2 + CH_3 ⇔ OH + CH_3O) for biomass pyrolysis products at Ω = 0.9 and 1. Experimental data are represented by points with corresponding error bars.*

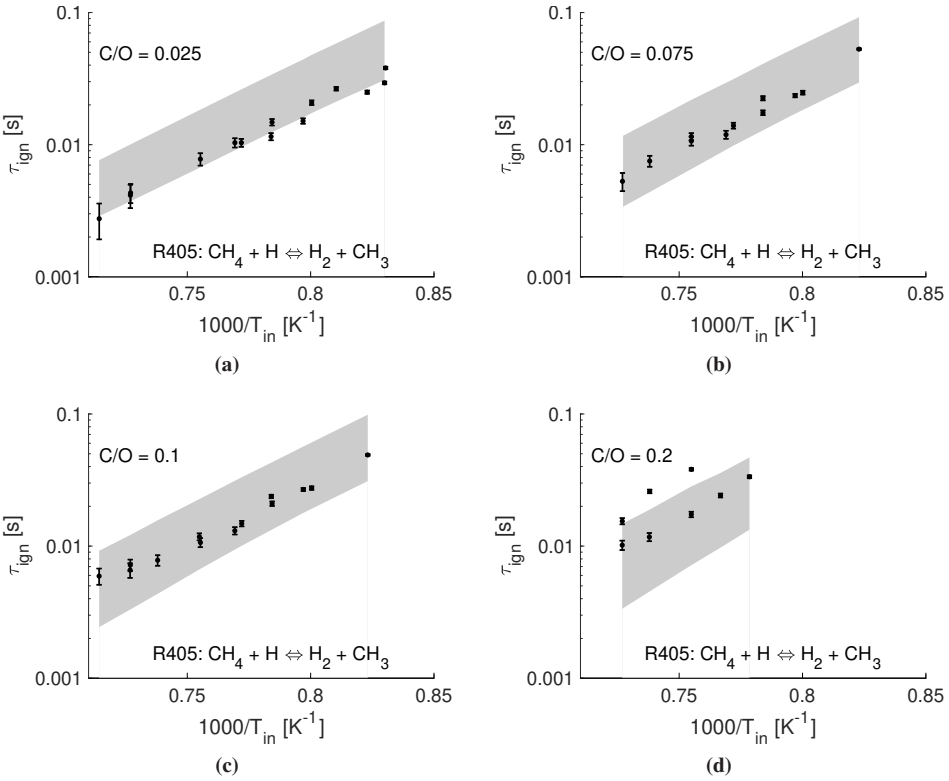

Figure A7: *Prior uncertainty range for reaction R405 (CH_4 + H ⇔ H_2 + CH_3) for methane at C/O = 0.025-0.2. Experimental data are represented by points with corresponding error bars.*

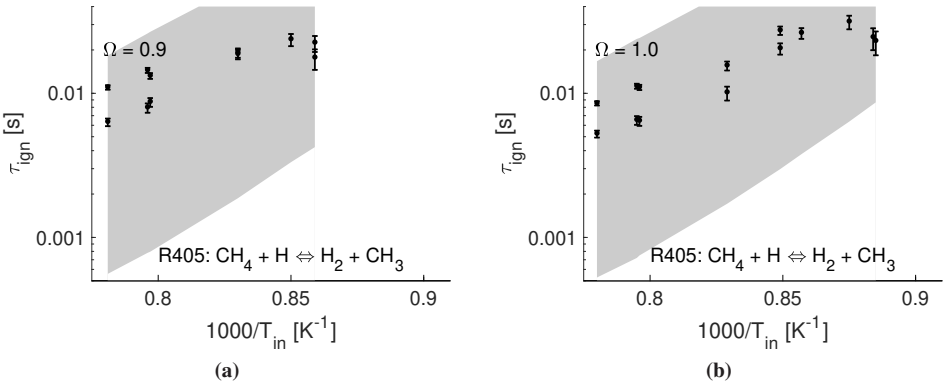

Figure A8: *Prior uncertainty range for reaction R405 (CH_4 + H ⇔ H_2 + CH_3) for biomass pyrolysis products at Ω = 0.9 and 1. Experimental data are represented by points with corresponding error bars.*

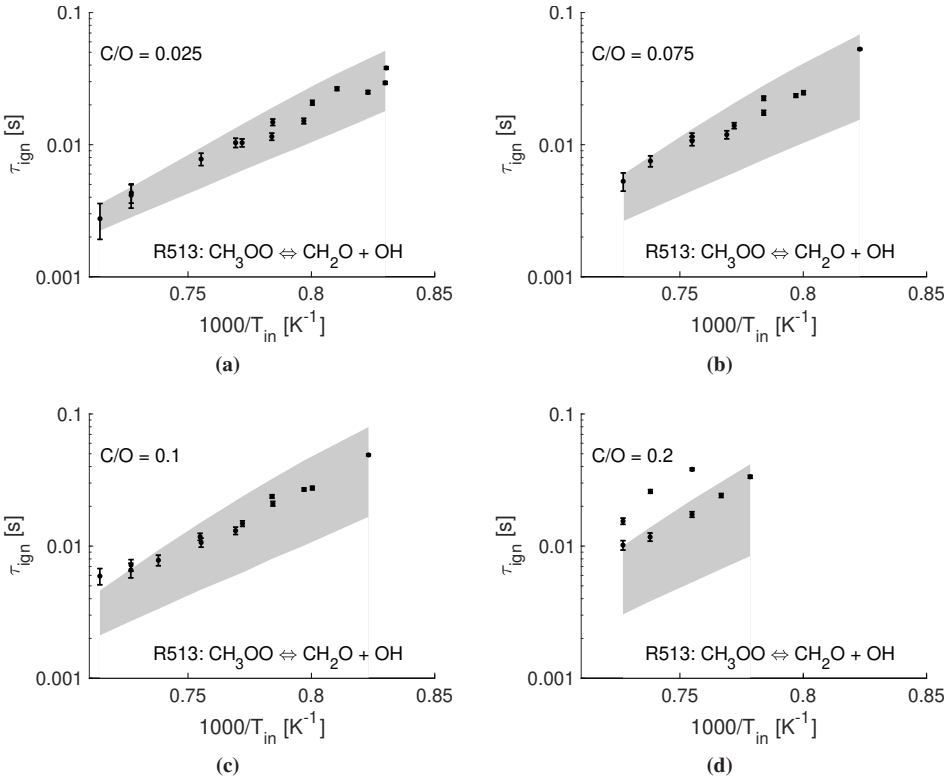

Figure A9: *Prior uncertainty range for reaction R513 ($CH_3OO \Leftrightarrow CH_2O + OH$) for methane at C/O = 0.025-0.2. Experimental data are represented by points with corresponding error bars.*

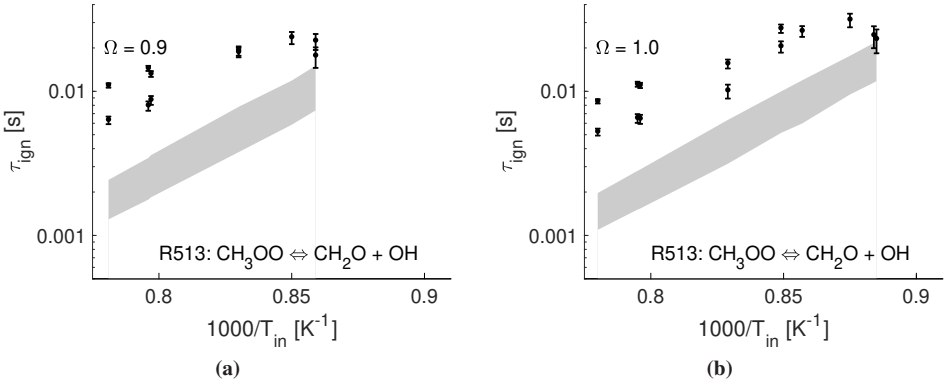

Figure A10: *Prior uncertainty range for reaction R513 ($CH_3OO \Leftrightarrow CH_2O + OH$) for biomass pyrolysis products at Ω = 0.9 and 1. Experimental data are represented by points with corresponding error bars.*

Appendix B: Propane optimization results

This appendix presents the results from the optimization performed in Chapter 5. The figures are divided into sections based on their type, and the nominal mechanism (POLIMI C1C3 LT [83]) is represented by the solid lines in the figures, and the optimized mechanism by the dashed lines.

Ignition Delay Time of propane in MILD conditions

The experimental data are from [16, 117], and consists of IDT of propane at different inlet temperatures, equivalence ratios, dilution percentages and diluent species.

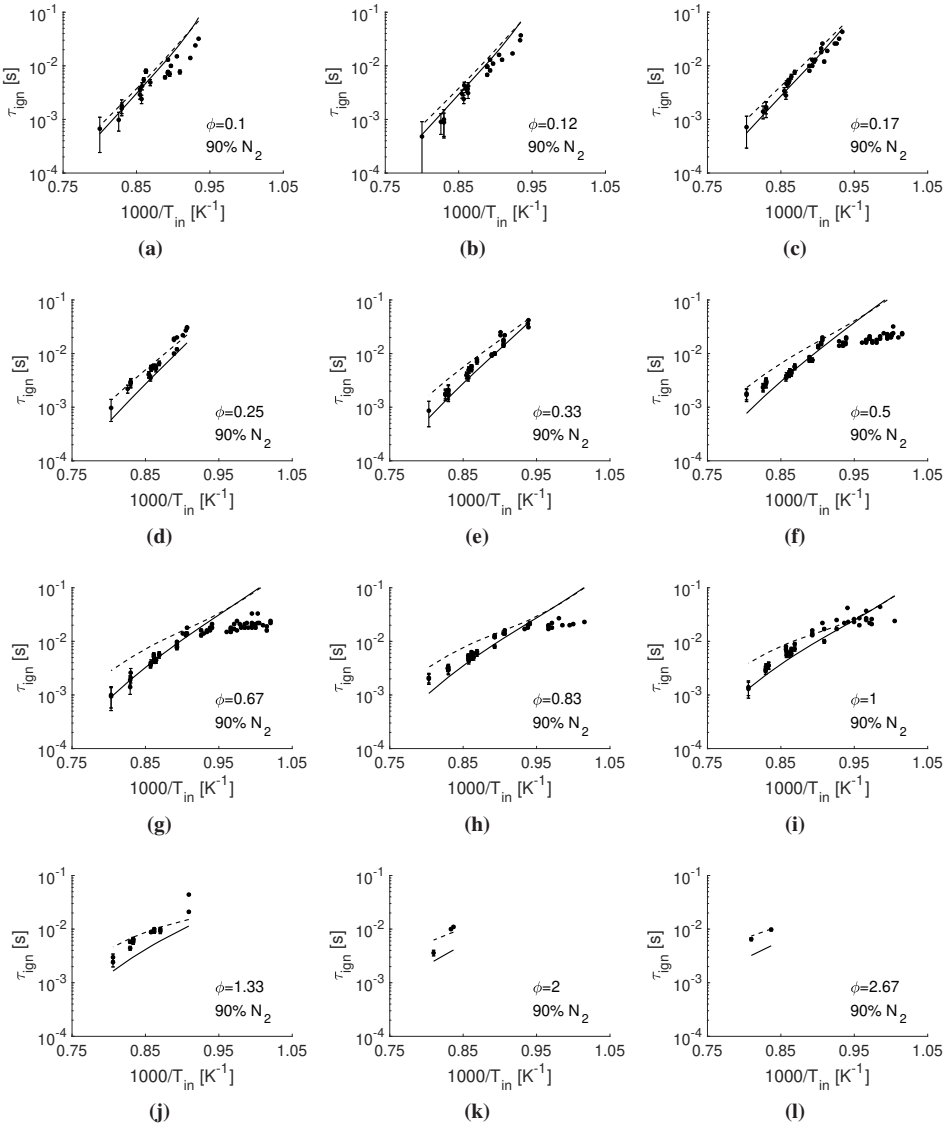

Figure B1: *IDT for propane diluted with 90% N_2 at different inlet temperatures for ϕ = 0.1-2.67. Experimental data (from [117]) are represented by points with corresponding error bars, and the simulation results for the POLIMI mechanism are presented by the solid lines (—) and the optimized mechanism by the dashed lines (- -).*

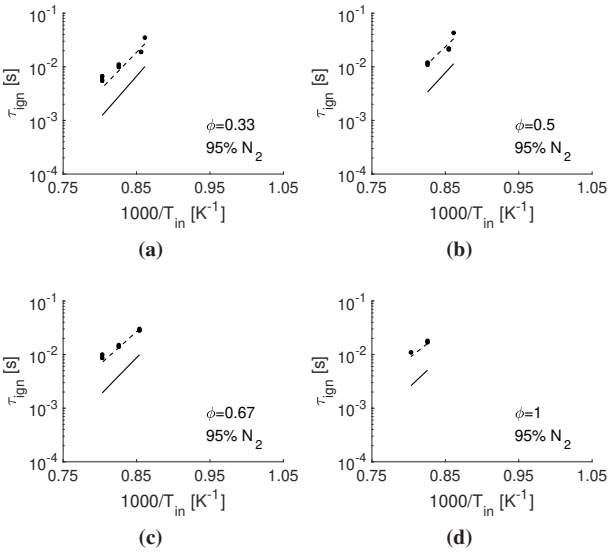

Figure B2: *IDT for propane diluted with 95% N_2 at different inlet temperatures for ϕ = 0.33-1. Experimental data (from [117]) are represented by points with corresponding error bars, and the simulation results for the POLIMI mechanism are presented by the solid lines (—) and the optimized mechanism by the dashed lines (- -).*

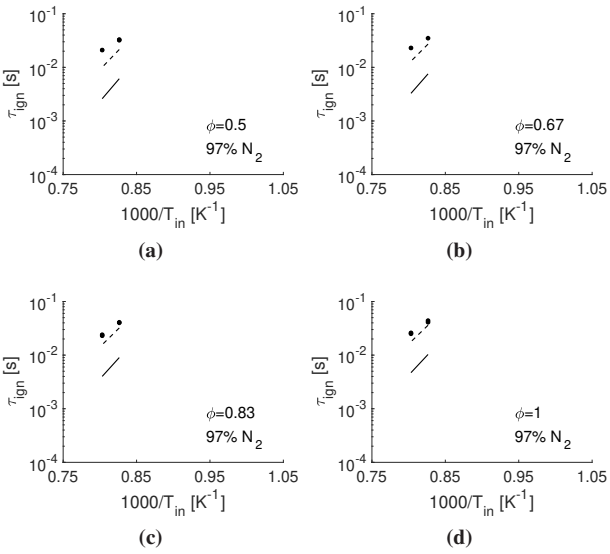

Figure B3: *IDT for propane diluted with 97% N_2 at different inlet temperatures for ϕ = 0.5-1. Experimental data (from [117]) are represented by points with corresponding error bars, and the simulation results for the POLIMI mechanism are presented by the solid lines (—) and the optimized mechanism by the dashed lines (- -).*

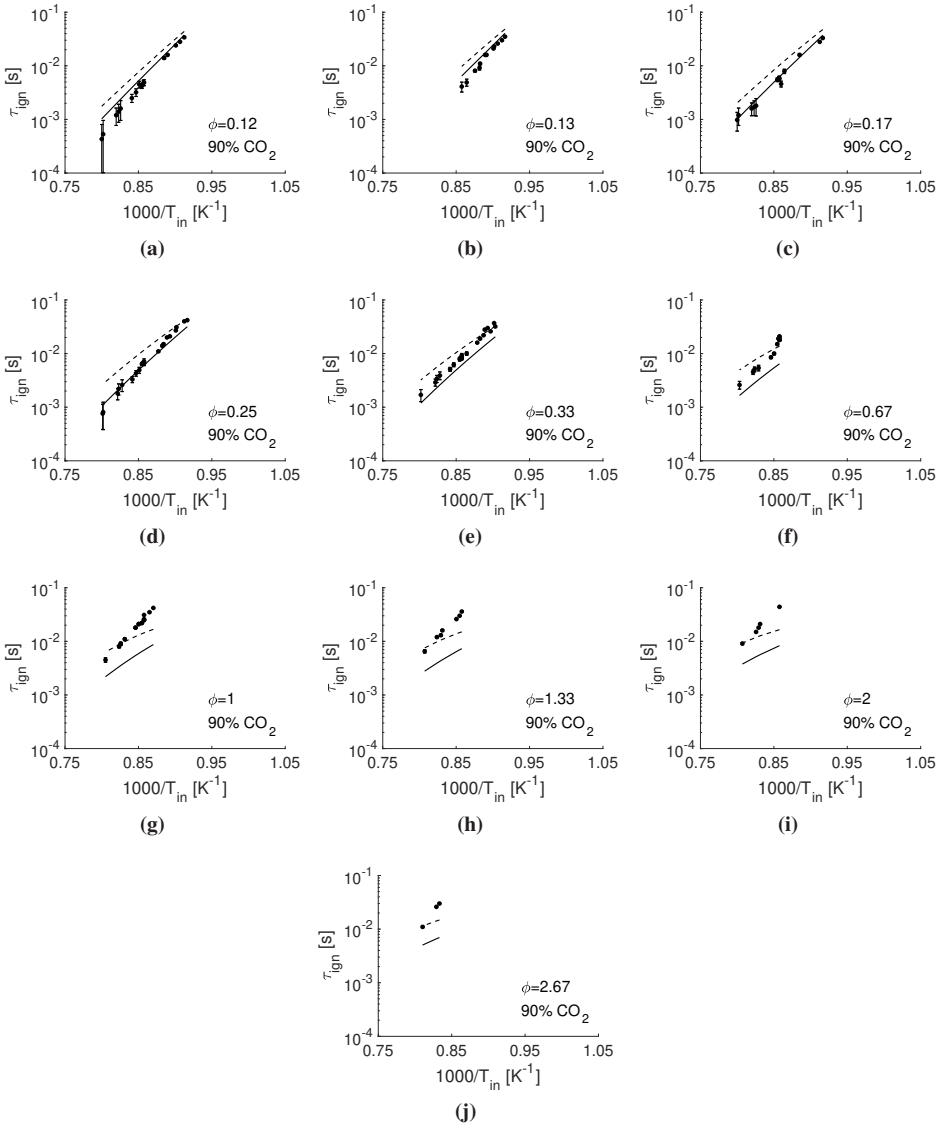

Figure B4: *IDT for propane diluted with 90% CO_2 at different inlet temperatures for ϕ = 0.12-2.67. Experimental data (from [16]) are represented by points with corresponding error bars, and the simulation results for the POLIMI mechanism are presented by the solid lines (—) and the optimized mechanism by the dashed lines (- -).*

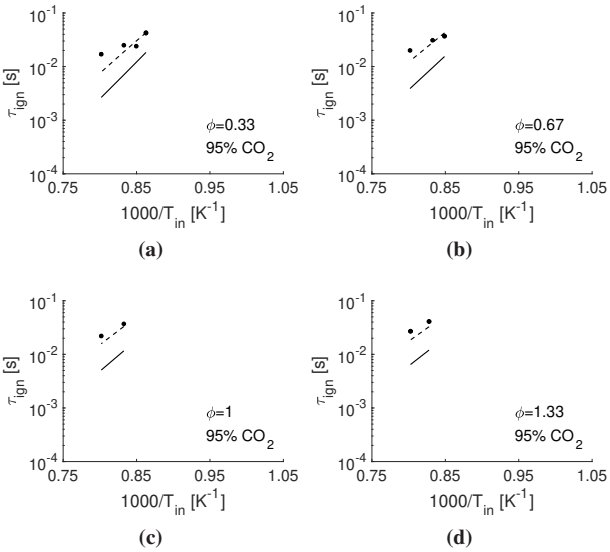

Figure B5: *IDT for propane diluted with 95% CO_2 at different inlet temperatures for ϕ = 0.33-1.33. Experimental data (from [16]) are represented by points with corresponding error bars, and the simulation results for the POLIMI mechanism are presented by the solid lines (—) and the optimized mechanism by the dashed lines (- -).*

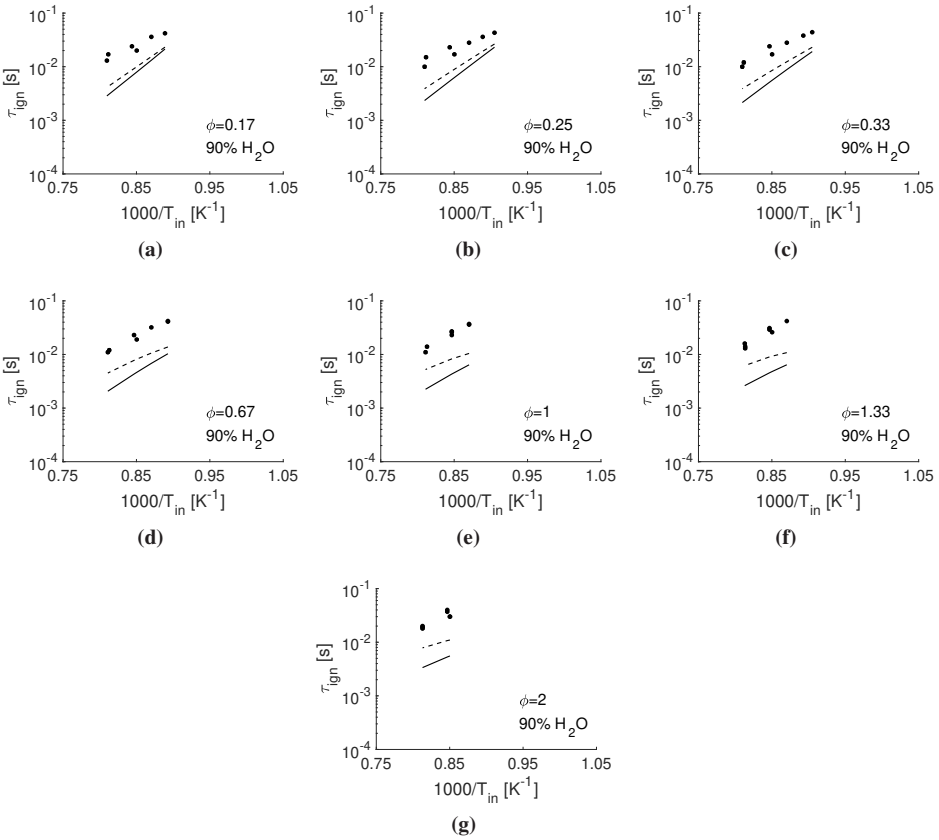

Figure B6: *IDT for propane diluted with 90% H_2O at different inlet temperatures for ϕ = 0.17-2. Experimental data (from [16]) are represented by points with corresponding error bars, and the simulation results for the POLIMI mechanism are presented by the solid lines (—) and the optimized mechanism by the dashed lines (- -).*

Species mole fractions from a Jet Stirred Reactor

The experimental data [17, 118] are divided into different figures based on equivalence ratio (0.5, 1 and 1.5), diluent species (CO_2 and H_2O) and measured species. In each figure the different dilution ratios for CO_2 and H_2O are represented by the different colors. The lines represent the simulation results, and where the lines are cut, numerical oscillations were observed.

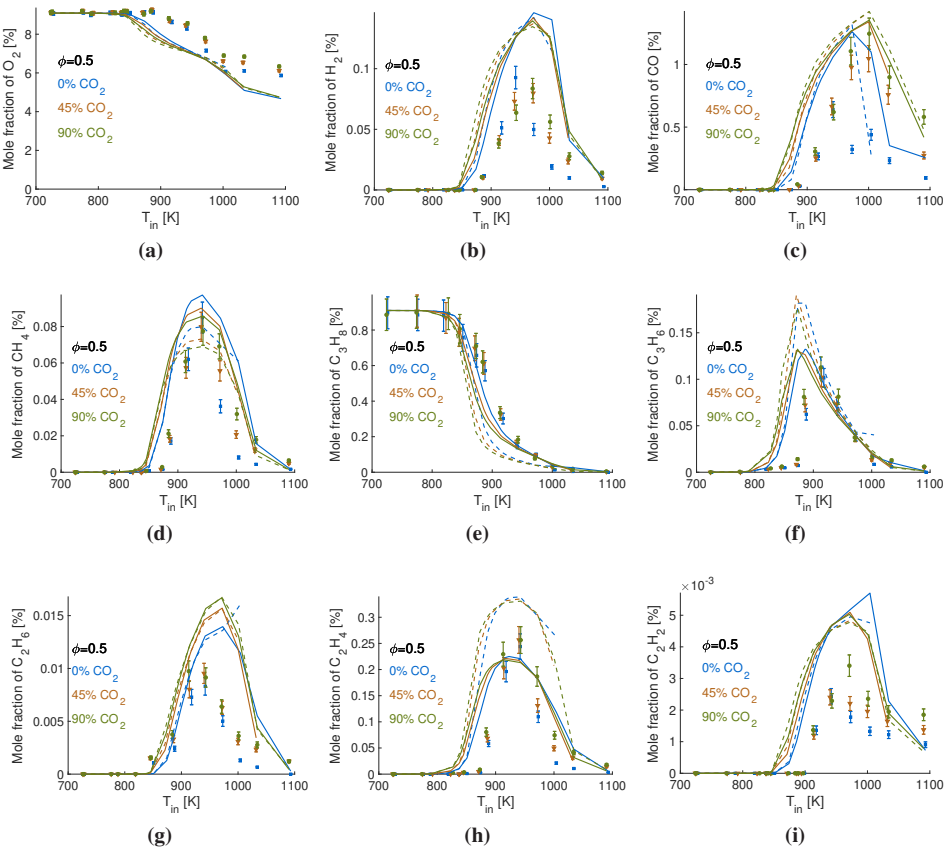

Figure B7: *JSR species measurements for propane oxidation diluted with CO_2 and N_2 at different inlet temperatures for ϕ = 0.5. Experimental data (from [17]) are represented by points with corresponding error bars, and the simulation results for the POLIMI mechanism are presented by the solid lines (—) and the optimized mechanism by the dashed lines (- -).*

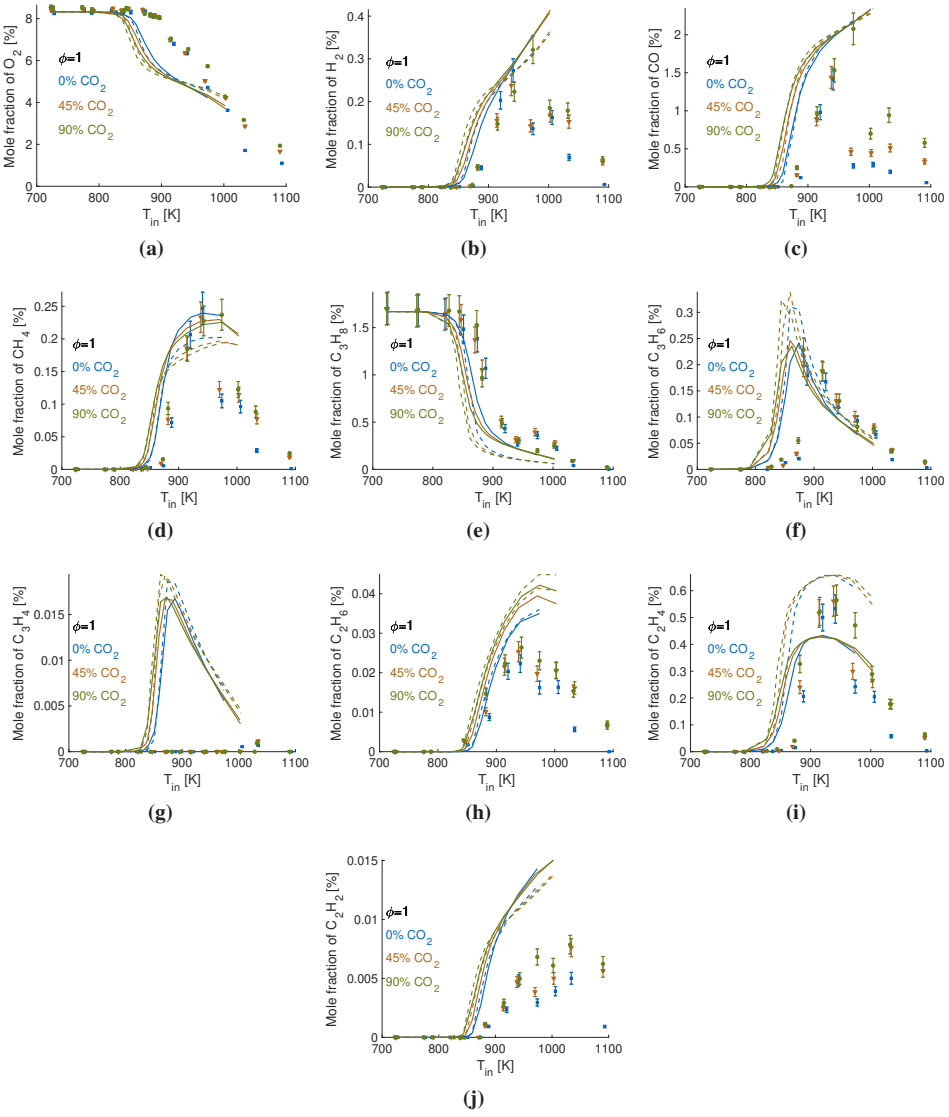

Figure B8: *JSR species measurements for propane oxidation diluted with CO_2 and N_2 at different inlet temperatures for $\phi = 1$. Experimental data (from [17]) are represented by points with corresponding error bars, and the simulation results for the POLIMI mechanism are presented by the solid lines (—) and the optimized mechanism by the dashed lines (- -).*

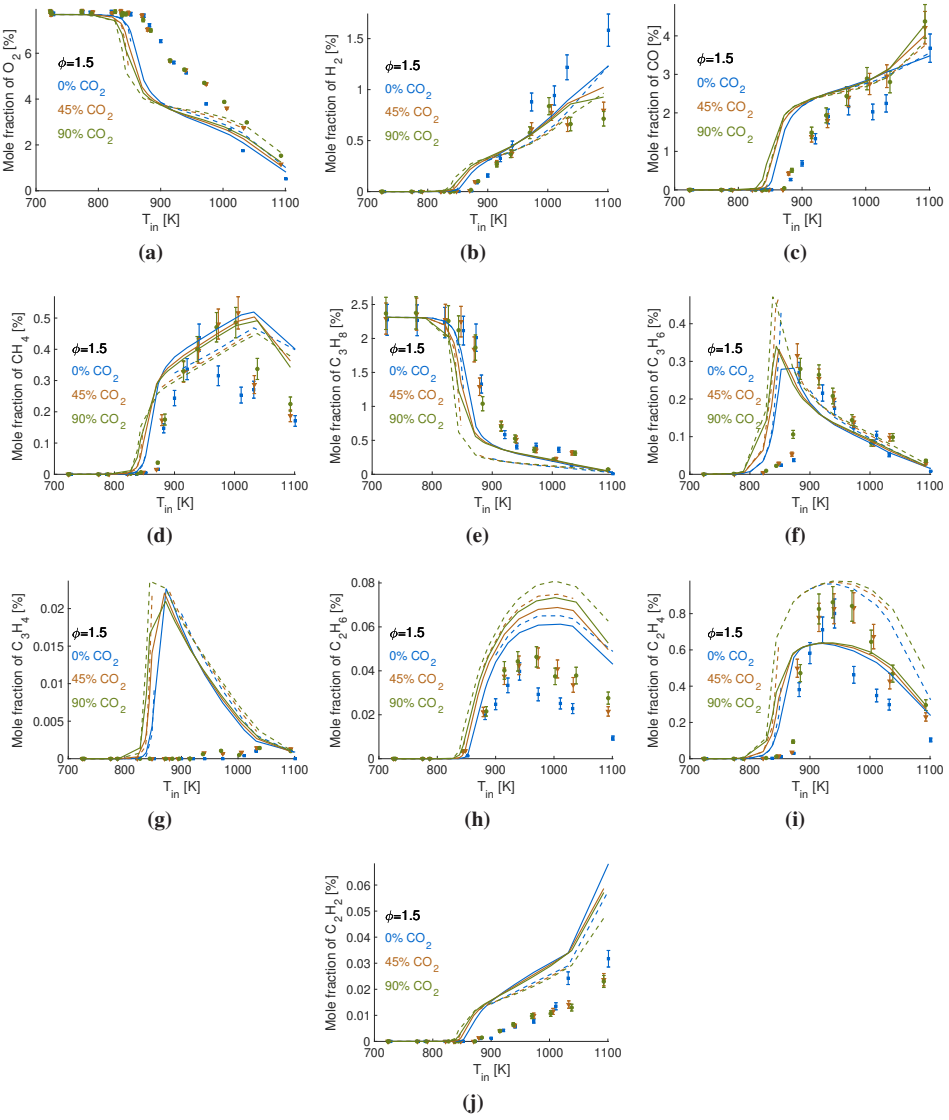

Figure B9: *JSR species measurements for propane oxidation diluted with CO_2 and N_2 at different inlet temperatures for ϕ = 1.5. Experimental data (from [17]) are represented by points with corresponding error bars, and the simulation results for the POLIMI mechanism are presented by the solid lines (—) and the optimized mechanism by the dashed lines (- -).*

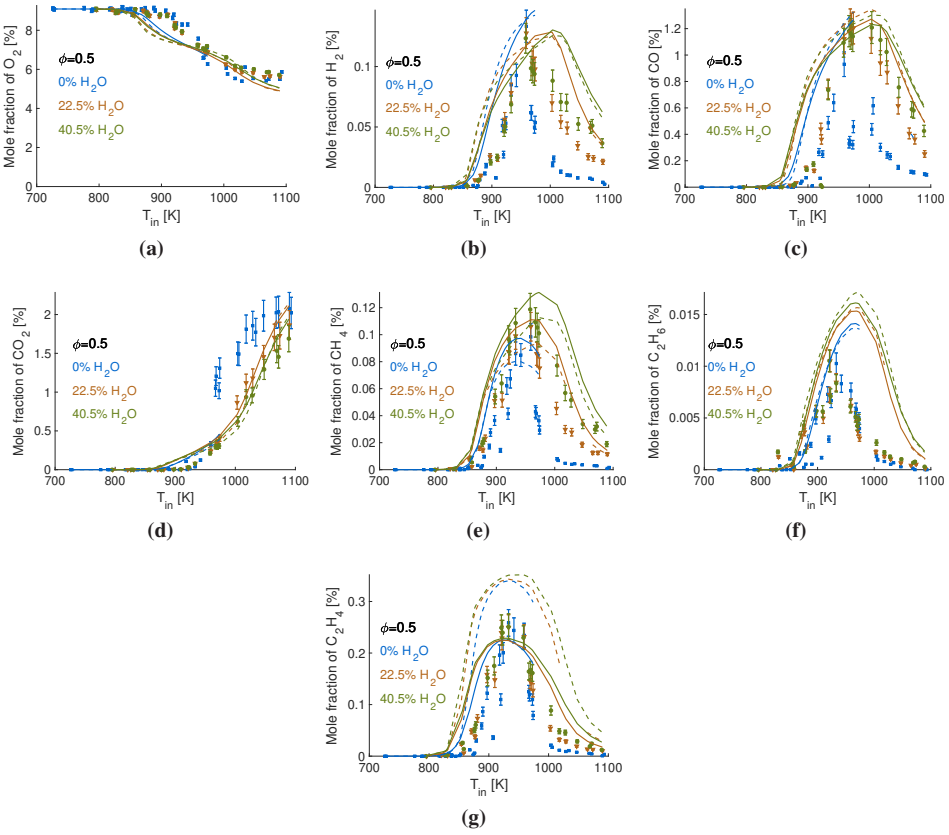

Figure B10: *JSR species measurements for propane oxidation diluted with H_2O and N_2 at different inlet temperatures for ϕ = 0.5. Experimental data (from [118]) are represented by points with corresponding error bars, and the simulation results for the POLIMI mechanism are presented by the solid lines (—) and the optimized mechanism by the dashed lines (- -).*

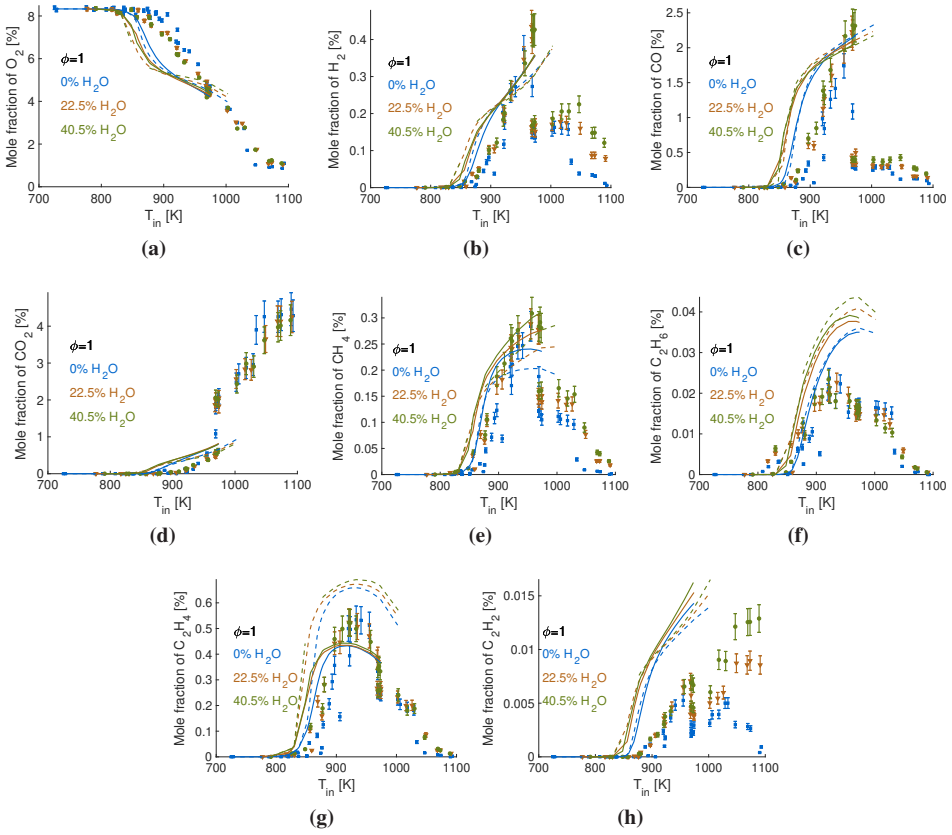

Figure B11: *JSR species measurements for propane oxidation diluted with H_2O and N_2 at different inlet temperatures for ϕ = 1. Experimental data (from [118]) are represented by points with corresponding error bars, and the simulation results for the POLIMI mechanism are presented by the solid lines (—) and the optimized mechanism by the dashed lines (- -).*

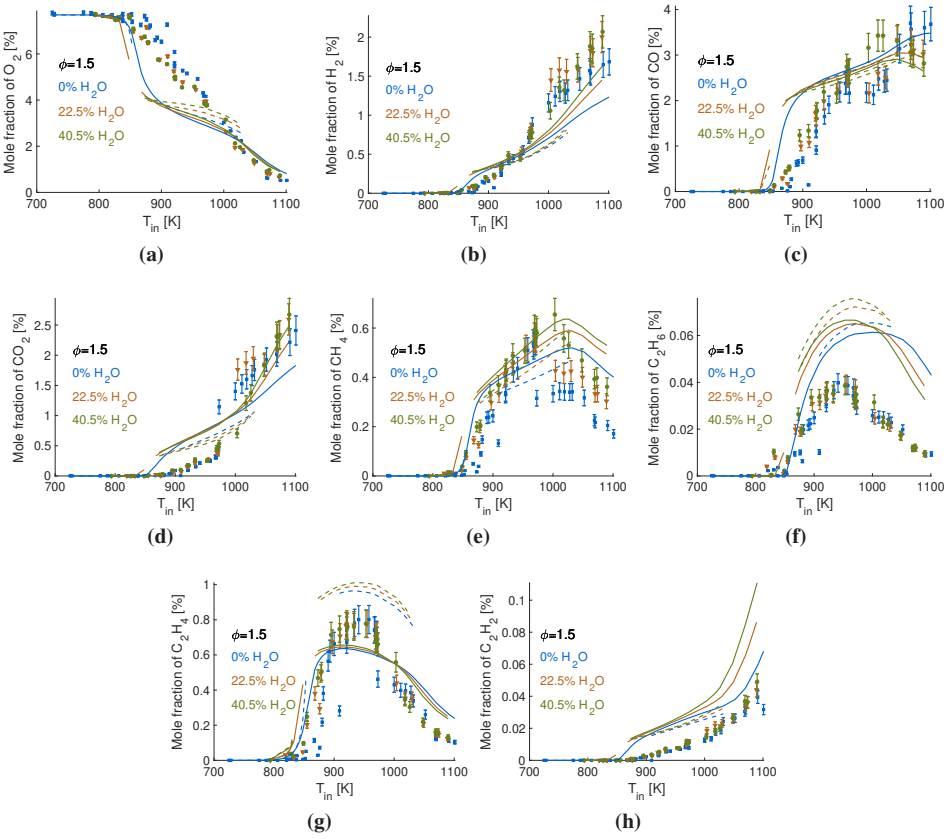

Figure B12: *JSR species measurements for propane oxidation diluted with H_2O and N_2 at different inlet temperatures for ϕ = 1.5. Experimental data (from [118]) are represented by points with corresponding error bars, and the simulation results for the POLIMI mechanism are presented by the solid lines (—) and the optimized mechanism by the dashed lines (- -).*

Bibliography

[1] G. Baumbach, *Air Quality Control*. Berlin, Heidelberg: Springer Berlin Heidelberg, 1996.

[2] A. Cavaliere and M. de Joannon, "Mild Combustion," *Progress in Energy and Combustion Science*, vol. 30, no. 4, pp. 329–366, 2004.

[3] J. A. Wünning and J. G. Wünning, "Flameless Oxidation To Reduce Thermal No-Formation," *Progress in Energy and Combustion Science*, vol. 23, pp. 81–94, 1997.

[4] H. Tsuji, A. K. Gupta, T. Hasegawa, M. Katsuki, K. Kishimoto, and M. Morita, *High Temperature Air Combustion*. CRC Press, dec 2002.

[5] V. K. Arghode and A. K. Gupta, "Effect of flow field for colorless distributed combustion (CDC) for gas turbine combustion," *Applied Energy*, vol. 87, pp. 1631–1640, may 2010.

[6] A. Frassoldati, T. Faravelli, and E. Ranzi, "Kinetic modeling of the interactions between NO and hydrocarbons at high temperature," *Combustion and Flame*, vol. 135, no. 1-2, pp. 97–112, 2003.

[7] P. Glarborg, J. A. Miller, B. Ruscic, and S. J. Klippenstein, "Modeling nitrogen chemistry in combustion," *Progress in Energy and Combustion Science*, vol. 67, pp. 31–68, 2018.

[8] T. Lu and C. K. Law, "Toward accommodating realistic fuel chemistry in large-scale computations," *Progress in Energy and Combustion Science*, vol. 35, no. 2, pp. 192–215, 2009.

[9] B. Andersson, R. Andersson, L. Håkansson, M. Mortensen, R. Sudiyo, and B. van Wachem, *Computational Fluid Dynamics for Engineers*. Cambridge University Press, 2011.

[10] T. Turányi and A. S. Tomlin, *Analysis of Kinetic Reaction Mechanisms*. Springer, 2015.

[11] "NUI Galway - Mechanism Downloads." http://c3.nuigalway.ie/combustionchemistrycentre/mechanismdownloads/.

[12] "GRI-Mech." http://combustion.berkeley.edu/gri-mech/.

[13] "CRECK Modeling Group - Kinetics." http://creckmodeling.chem.polimi.it/menu-kinetics.

[14] "Chemical-Kinetic Mechanisms for Combustion Applications." http://web.eng.ucsd.edu/mae/groups/combustion/mechanism.html.

[15] L. Wang, Z. Liu, S. Chen, C. Zheng, and J. Li, "Physical and Chemical Effects of CO_2 and H_2O Additives on Counter flow Diffusion Flame Burning Methane," *Energy & Fuels*, vol. 27, no. 12, pp. 7602–7611, 2013.

[16] P. Sabia, M. Lubrano, P. Giudicianni, G. Sorrentino, and R. Ragucci, "CO_2 and H_2O effect on propane auto-ignition delay times under mild combustion operative conditions," *Combustion and Flame*, vol. 162, no. 3, pp. 533–543, 2015.

[17] M. Lubrano Lavadera, P. Sabia, G. Sorrentino, R. Ragucci, and M. de Joannon, "Experimental study of the effect of CO_2 on propane oxidation in a Jet Stirred Flow Reactor," *Fuel*, vol. 184, pp. 876–888, 2016.

[18] P. Sabia, M. Lubrano Lavadera, G. Sorrentino, P. Giudicianni, R. Ragucci, and M. De Joannon, "H_2O and CO_2 Dilution in MILD Combustion of Simple Hydrocarbons," *Flow, Turbulence and Combustion*, vol. 96, no. 2, pp. 433–448, 2016.

[19] H. Wang and D. A. Sheen, "Combustion kinetic model uncertainty quantification, propagation and minimization," *Progress in Energy and Combustion Science*, vol. 47, pp. 1–31, 2015.

[20] T. Turányi, "Lecture 1-3 uncertainty of data and parameters," July 2016. http://garfield.chem.elte.hu/COST_Training_School_2016/overheads/Turanyi_1-3_Uncertainty_of_Data_and_Parameters.pdf.

[21] M. T. Reagan, H. N. Najm, R. G. Ghanem, and O. M. Knio, "Analysis of parametric uncertainty propagation in detailed combustion chemistry," *Computational Fluid and Solid Mechanics*, pp. 1501–1505, 2003.

[22] M. T. Reagan, H. N. Najm, P. P. Pébay, O. M. Knio, and R. G. Ghanem, "Quantifying uncertainty in chemical systems modeling," *International Journal of Chemical Kinetics*, vol. 37, pp. 368–382, jun 2005.

[23] H. N. Najm, B. J. Debusschere, Y. M. Marzouk, S. Widmer, and O. Le Maitre, "Uncertainty quantification in chemical systems," *INTERNATIONAL JOURNAL FOR NUMERICAL METHODS IN ENGINEERIN*, vol. 80, pp. 789–814, 2009.

[24] J. Prager, H. N. Najm, K. Sargsyan, C. Safta, and W. J. Pitz, "Uncertainty quantification of reaction mechanisms accounting for correlations introduced by rate rules and fitted Arrhenius parameters," *Combustion and Flame*, vol. 160, no. 9, pp. 1583–1593, 2013.

[25] T. Turányi, L. Zalotai, S. Dóbé, and T. Bérces, "Effect of the uncertainty of kinetic and thermodynamic data on methane flame simulation results," *Physical Chemistry Chemical Physics*, vol. 4, no. 12, pp. 2568–2578, 2002.

[26] I. G. Zsély, J. Zádor, and T. Turányi, "Uncertainty analysis of updated hydrogen and carbon monoxide oxidation mechanisms," *Proceedings of the Combustion Institute*, vol. 30, no. 1, pp. 1273–1281, 2005.

[27] J. Zádor, I. G. Zsély, T. Turányi, M. Ratto, S. Tarantola, and A. Saltelli, "Local and Global Uncertainty Analyses of a Methane Flame Model," *The Journal of Physical Chemistry A*, vol. 109, pp. 9795–9807, nov 2005.

[28] J. Zádor, I. G. Zsély, and T. Turányi, "Local and global uncertainty analysis of complex chemical kinetic systems," *Reliability Engineering and System Safety*, vol. 91, no. 10-11, pp. 1232–1240, 2006.

[29] I. G. Zsély, J. Zádor, and T. Turányi, "Uncertainty analysis of NO production during methane combustion," *International Journal of Chemical Kinetics*, vol. 40, pp. 754–768, nov 2008.

[30] T. Ziehn and A. S. Tomlin, "A global sensitivity study of sulfur chemistry in a premixed methane flame model using HDMR," *International Journal of Chemical Kinetics*, vol. 40, pp. 742–753, nov 2008.

[31] T. Ziehn, K. J. Hughes, J. F. Griffiths, R. Porter, and A. S. Tomlin, "A global sensitivity study of cyclohexane oxidation under low temperature fuel-rich conditions using HDMR methods," *Combustion Theory and Modelling*, vol. 13, pp. 589–605, sep 2009.

[32] R. T. Skodje, A. S. Tomlin, S. J. Klippenstein, L. B. Harding, and M. J. Davis, "Theoretical Validation of Chemical Kinetic Mechanisms: Combustion of Methanol," *The Journal of Physical Chemistry A*, vol. 114, pp. 8286–8301, aug 2010.

[33] S. J. Klippenstein, L. B. Harding, M. J. Davis, A. S. Tomlin, and R. T. Skodje, "Uncertainty driven theoretical kinetics studies for CH_3OH ignition: HO_2+CH_3OH and O_2+CH_3OH," *Proceedings of the Combustion Institute*, vol. 33, no. 1, pp. 351–357, 2011.

[34] M. J. Davis, R. T. Skodje, and A. S. Tomlin, "Global Sensitivity Analysis of Chemical-Kinetic Reaction Mechanisms: Construction and Deconstruction of the Probability Density Function," *The Journal of Physical Chemistry A*, vol. 115, pp. 1556–1578, mar 2011.

[35] M. Frenklach and D. E. Bornside, "Shock-initiated ignition in methane-propane mixtures," *Combustion and Flame*, vol. 56, no. 1, pp. 1–27, 1984.

[36] M. Frenklach, "Systematic optimization of a detailed kinetic model using a methane ignition example," *Combustion and Flame*, vol. 58, no. 1, pp. 69–72, 1984.

[37] M. J. Frenklach, Michael and Wang, Hai and Rabinowitz, "Optimization and analysis of large chemical kinetic mechanisms using the solution mapping method - Combustion of methane," *Progress in Energy and Combustion Science*, vol. 18, pp. 47–73, 1992.

[38] M. Frenklach, A. Packard, and P. Seiler, "Prediction uncertainty from models and data," in *Proceedings of the 2002 American Control Conference (IEEE Cat. No.CH37301)*, vol. 5, pp. 4135–4140 vol.5, IEEE, 2002.

[39] M. Frenklach, A. Packard, P. Seiler, and R. Feeley, "Collaborative data processing in developing predictive models of complex reaction systems," *International Journal of Chemical Kinetics*, vol. 36, no. 1, pp. 57–66, 2004.

[40] M. Frenklach, "Transforming data into knowledge-Process Informatics for combustion chemistry," *Proceedings of the Combustion Institute*, vol. 31 I, pp. 125–140, 2007.

[41] M. Frenklach, H. Wang, C.-L. Yu, M. Goldenberg, C. Bowman, R. Hanson, D. Davidson, E. Chang, G. Smith, D. Golden, W. Gardiner, and V. Lissianski, "GRI-Mech 1.2." http://combustion.berkeley.edu/gri-mech/new21/version12/text12.html.

[42] C. Bowman, R. Hanson, D. Davidson, W. J. Gardiner, V. Lissianski, G. Smith, D. Golden, M. Frenklach, and M. Goldenberg, "GRI-Mech 2.11." http://combustion.berkeley.edu/gri-mech/new21/version21/text21.html.

[43] G. P. Smith, D. M. Golden, M. Frenklach, N. W. Moriarty, B. Eiteneer, M. Goldenberg, C. T. Bowman, R. K. Hanson, S. Song, W. C. J. Gardiner, V. V. Lissianski, and Z. Qin, "GRI-Mech 3.0." http://combustion.berkeley.edu/gri-mech/version30/text30.html.

[44] D. A. Sheen, X. You, H. Wang, and T. Løvås, "Spectral uncertainty quantification, propagation and optimization of a detailed kinetic model for ethylene combustion," *Proceedings of the Combustion Institute*, vol. 32 I, no. 1, pp. 535–542, 2009.

[45] D. A. Sheen and H. Wang, "The method of uncertainty quantification and minimization using polynomial chaos expansions," *Combustion and Flame*, vol. 158, no. 12, pp. 2358–2374, 2011.

[46] D. A. Sheen, C. M. Rosado-Reyes, and W. Tsang, "Kinetics of H atom attack on unsaturated hydrocarbons using spectral uncertainty propagation and minimization techniques," *Proceedings of the Combustion Institute*, vol. 34, no. 1, pp. 527–536, 2013.

[47] Y. Xin, D. A. Sheen, H. Wang, and C. K. Law, "Skeletal reaction model generation, uncertainty quantification and minimization: Combustion of butane," *Combustion and Flame*, vol. 161, no. 12, pp. 3031–3039, 2014.

[48] O. Park, P. S. Veloo, D. A. Sheen, Y. Tao, F. N. Egolfopoulos, and H. Wang, "Chemical kinetic model uncertainty minimization through laminar flame speed measurements," *Combustion and Flame*, vol. 172, pp. 136–152, 2016.

[49] Y. Tao, G. P. Smith, and H. Wang, "Critical kinetic uncertainties in modeling hydrogen/carbon monoxide, methane, methanol, formaldehyde, and ethylene combustion," *Combustion and Flame*, vol. 195, pp. 18–29, 2018.

[50] Y. Tao and H. Wang, "Joint probability distribution of Arrhenius parameters in reaction model optimization and uncertainty minimization," *Proceedings of the Combustion Institute*, vol. 37, no. 1, pp. 817–824, 2019.

[51] L. Cai and H. Pitsch, "Mechanism optimization based on reaction rate rules," *Combustion and Flame*, vol. 161, no. 2, pp. 405–415, 2014.

[52] L. Cai and H. Pitsch, "Optimized chemical mechanism for combustion of gasoline surrogate fuels," *Combustion and Flame*, vol. 162, no. 5, pp. 1623–1637, 2015.

[53] L. Cai, H. Pitsch, S. Y. Mohamed, V. Raman, J. Bugler, H. Curran, and S. M. Sarathy, "Optimized reaction mechanism rate rules for ignition of normal alkanes," *Combustion and Flame*, vol. 173, pp. 468–482, 2016.

[54] F. vom Lehn, L. Cai, and H. Pitsch, "Impact of thermochemistry on optimized kinetic model predictions: Auto-ignition of diethyl ether," *Combustion and Flame*, vol. 210, pp. 454–466, dec 2019.

[55] I. Zsély, T. Varga, T. Nagy, M. Cserháti, T. Turányi, S. Peukert, M. Braun-Unkhoff, C. Naumann, and U. Riedel, "Determination of rate parameters of cyclohexane and 1-hexene decomposition reactions," *Energy*, vol. 43, pp. 85–93, jul 2012.

[56] T. Varga, T. Nagy, C. Olm, I. Zsély, R. Pálvölgyi, É. Valkó, G. Vincze, M. Cserháti, H. Curran, and T. Turányi, "Optimization of a hydrogen combustion mechanism using both direct and indirect measurements," *Proceedings of the Combustion Institute*, vol. 35, no. 1, pp. 589–596, 2015.

[57] T. Varga, C. Olm, T. Nagy, I. G. Zsély, É. Valkó, R. Pálvölgyi, H. J. Curran, and T. Turányi, "Development of a Joint Hydrogen and Syngas Combustion Mechanism Based on an Optimization Approach," *International Journal of Chemical Kinetics*, vol. 48, no. 8, pp. 407–422, 2016.

[58] C. Olm, T. Varga, É. Valkó, S. Hartl, C. Hasse, and T. Turányi, "Development of an Ethanol Combustion Mechanism Based on a Hierarchical Optimization Approach," *International Journal of Chemical Kinetics*, vol. 48, pp. 423–441, aug 2016.

[59] C. Olm, T. Varga, É. Valkó, H. J. Curran, and T. Turányi, "Uncertainty quantification of a newly optimized methanol and formaldehyde combustion mechanism," *Combustion and Flame*, vol. 186, pp. 45–64, 2017.

[60] V. Samu, T. Varga, K. Brezinsky, and T. Turányi, "Investigation of ethane pyrolysis and oxidation at high pressures using global optimization based on shock tube data," *Proceedings of the Combustion Institute*, vol. 36, no. 1, pp. 691–698, 2017.

[61] V. Samu, T. Varga, I. Rahinov, S. Cheskis, and T. Turányi, "Determination of rate parameters based on NH_2 concentration profiles measured in ammonia-doped methane-air flames," *Fuel*, vol. 212, pp. 679–683, jan 2018.

[62] T. Turányi, T. Nagy, I. G. Zsély, M. Cserháti, T. Varga, B. T. Szabó, I. Sedyó, P. T. Kiss, A. Zempléni, and H. J. Curran, "Determination of rate parameters based on both direct and indirect measurements," *International Journal of Chemical Kinetics*, vol. 44, pp. 284–302, may 2012.

[63] W. Polifke, W. Geng, and K. Döbbeling, "Optimization of Rate Coefficients for Simplified Reaction Mechanisms with Genetic Algorithms," *Combustion and Flame*, vol. 113, pp. 119–134, apr 1998.

[64] S. Harris, L. Elliott, D. Ingham, M. Pourkashanian, and C. Wilson, "The optimisation of reaction rate parameters for chemical kinetic modeling of combustion using genetic algorithms," *Computer Methods in Applied Mechanics and Engineering*, vol. 190, pp. 1065–1090, nov 2000.

[65] L. Elliott, D. B. Ingham, A. G. Kyne, N. S. Mera, M. Pourkashanian, and C. W. Wilson, "Multiobjective Genetic Algorithm Optimization for Calculating the Reaction Rate Coefficients for Hydrogen Combustion," *Industrial & Engineering Chemistry Research*, pp. 1215–1224, 2003.

[66] L. Elliott, D. Ingham, A. Kyne, N. Mera, M. Pourkashanian, and C. W. Wilson, "Incorporation of physical bounds on rate parameters for reaction mechanism optimization using genetic algorithms," *Combustion Science and Technology*, vol. 175, pp. 619–648, apr 2003.

[67] L. Elliott, D. B. Ingham, A. G. Kyne, N. S. Mera, M. Pourkashanian, and C. W. Wilson, "Genetic algorithms for optimisation of chemical kinetics reaction mechanisms," *Progress in Energy and Combustion Science*, vol. 30, pp. 297–328, 2004.

[68] L. Elliott, D. B. Ingham, A. G. Kyne, N. S. Mera, M. Pourkashanian, and C. W. Wilson, "Reaction Mechanism Reduction and Optimization Using Genetic Algorithms," *Industrial & Engineering Chemistry Research*, pp. 658–667, 2005.

[69] F. Perini, J. L. Brakora, R. D. Reitz, and G. Cantore, "Development of reduced and optimized reaction mechanisms based on genetic algorithms and element flux analysis," *Combustion and Flame*, vol. 159, pp. 103–119, 2012.

[70] N. Sikalo, O. Hasemann, C. Schulz, and A. Kempf, "A Genetic Algorithm-Based Method for the Optimization of Reduced Kinetics Mechanisms," *International Journal of Chemical Kinetics*, pp. 2028–2055, 2015.

[71] J. P. Kim, U. Schnell, and G. Scheffknecht, "Comparison of different global reaction mechanisms for MILD combustion of natural gas," *Combustion Science and Technology*, vol. 180, no. 4, pp. 565–592, 2008.

[72] L. Wang, Z. Liu, S. Chen, and C. Zheng, "Comparison of different global combustion mechanisms under hot and diluted oxidation conditions," *Combustion Science and Technology*, 2012.

[73] Y. Tu, W. Yang, and H. Liu, "A Refined Global Reaction Mechanism for Gently Preheated MILD Combustion of Methane," *Energy and Fuels*, vol. 31, no. 9, pp. 10144–10157, 2017.

[74] F. Hu, P. Li, J. Guo, Z. Liu, L. Wang, J. Mi, B. Dally, and C. Zheng, "Global reaction mechanisms for MILD oxy-combustion of methane," *Energy*, 2018.

[75] J. Si, G. Wang, P. Li, and J. Mi, "Optimization of Global Reaction Mechanism for MILD Combustion of Methane Using Artificial Neural Network (ANN)," *Energy & Fuels*, p. acs.energyfuels.9b04413, feb 2020.

[76] É. Valkó, T. Varga, A. S. Tomlin, Á. Busai, and T. Turányi, "Investigation of the effect of correlated uncertain rate parameters via the calculation of global and local sensitivity indices," *Journal of Mathematical Chemistry*, vol. 56, no. 3, pp. 864–889, 2018.

[77] B. Sudret, "Global sensitivity analysis using polynomial chaos expansions," *Reliability Engineering & System Safety*, vol. 93, pp. 964–979, jul 2008.

[78] I. Sobol', "Global sensitivity indices for nonlinear mathematical models and their Monte Carlo estimates," *Mathematics and Computers in Simulation*, vol. 55, pp. 271–280, feb 2001.

[79] D. Coppitters, W. De Paepe, and F. Contino, "Surrogate-assisted robust design optimization and global sensitivity analysis of a directly coupled photovoltaic-electrolyzer system under techno-economic uncertainty," *Applied Energy*, vol. 248, pp. 310–320, aug 2019.

[80] K. Verleysen, D. Coppitters, A. Parente, W. De Paepe, and F. Contino, "How can power-to-ammonia be robust? Optimization of an ammonia synthesis plant powered by a wind turbine considering operational uncertainties," *Fuel*, vol. 266, p. 117049, apr 2020.

[81] J. Warnatz, "Resolution of gas phase and surface combustion chemistry into elementary reactions," *Proceedings of the Combustion Institute*, pp. 553–579, 1992.

[82] M. Fürst, P. Sabia, M. Lubrano Lavadera, G. Aversano, M. de Joannon, A. Frassoldati, and A. Parente, "Optimization of Chemical Kinetics for Methane and Biomass Pyrolysis Products in Moderate or Intense Low-Oxygen Dilution Combustion," *Energy & Fuels*, vol. 32, pp. 10194–10201, oct 2018.

[83] E. Ranzi, A. Frassoldati, R. Grana, A. Cuoci, T. Faravelli, A. P. Kelley, and C. K. Law, "Hierarchical and comparative kinetic modeling of laminar flame speeds of hydrocarbon and oxygenated fuels," *Progress in Energy and Combustion Science*, vol. 38, pp. 468–501, aug 2012.

[84] S. G. Davis, A. V. Joshi, H. Wang, and F. Egolfopoulos, "An optimized kinetic model of H_2/CO combustion," *Proceedings of the Combustion Institute*, vol. 30, pp. 1283–1292, jan 2005.

[85] C. Olm, I. G. Zsély, T. Varga, H. J. Curran, and T. Turányi, "Comparison of the performance of several recent syngas combustion mechanisms," *Combustion and Flame*, vol. 162, no. 5, pp. 1793–1812, 2015.

[86] N. Wiener, "The Homogeneous Chaos," *American Journal of Mathematics*, vol. 60, p. 897, oct 1938.

[87] D. G. Krige, "A statistical approach to some basic mine valuation problems on the Witwatersrand," *Journal of the Chemical Metallurgical & Society of South Mining Africa*, vol. 52, no. 6, pp. 119–139, 1951.

[88] C. E. Rasmussen and C. K. I. Williams, eds., *Gaussian processes for machine learning.* The MIT Press, 2004.

[89] H. Rabitz, Ö. F. Aliş, J. Shorter, and K. Shim, "Efficient input-output model representations," *Computer Physics Communications*, vol. 117, pp. 11–20, mar 1999.

[90] I. Couckuyt, A. Forrester, D. Gorissen, F. De Turck, and T. Dhaene, "Blind Kriging: Implementation and performance analysis," *Advances in Engineering Software*, vol. 49, no. 1, pp. 1–13, 2012.

[91] D. R. Jones, C. D. Perttunen, and B. E. Stuckman, "Lipschitzian optimization without the Lipschitz constant," *Journal of Optimization Theory and Applications*, vol. 79, pp. 157–181, oct 1993.

[92] D. R. Jones, "DIRECT Global Optimization Algorithm," in *Encyclopedia of Optimization* (C. A. Floudas and P. M. Pardalos, eds.), pp. 431–440, Boston, MA: Springer US, 2009.

[93] P. Sabia, M. de Joannon, A. Picarelli, and R. Ragucci, "Methane auto-ignition delay times and oxidation regimes in MILD combustion at atmospheric pressure," *Combustion and Flame*, vol. 160, no. 1, pp. 47–55, 2013.

[94] C. J. Mueller, M. P. B. Musculus, M. Lyle, W. J. Pitz, and C. K. Westbrook, "The Oxygen Ratio: A Fuel-Independent Measure of Mixture Stoichiometry," tech. rep., Lawrence Livermore National Laboratory, 2003.

[95] A. Cuoci, A. Frassoldati, T. Faravelli, and E. Ranzi, "OpenSMOKE++: An object-oriented framework for the numerical modeling of reactive systems with detailed kinetic mechanisms," *Computer Physics Communications*, vol. 192, pp. 237–264, 2015.

[96] W. K. Metcalfe, S. M. Burke, S. S. Ahmed, and H. J. Curran, "A Hierarchical and Comparative Kinetic Modeling Study of C_1-C_2 Hydrocarbon and Oxygenated Fuels," *International Journal of Chemical Kinetics*, vol. 45, pp. 638–675, oct 2013.

[97] C.-w. Zhou, Y. Li, E. O. Connor, K. P. Somers, S. Thion, C. Keesee, O. Mathieu, E. L. Petersen, T. A. Deverter, M. A. Oehlschlaeger, G. Kukkadapu, C.-j. Sung, M. Alrefae, F. Khaled, A. Farooq, P. Dirrenberger, P.-a. Glaude, F. Battin-leclerc, J. Santner, Y. Ju, T. Held, F. M. Haas, F. L. Dryer, and H. J. Curran, "A comprehensive experimental and modeling study of isobutene oxidation," *Combustion and Flame*, vol. 167, pp. 353–379, 2016.

[98] D. Healy, D. M. Kalitan, C. J. Aul, E. L. Petersen, G. Bourque, and H. J. Curran, "Oxidation of C_1 - C_5 Alkane Quinternary Natural Gas Mixtures at High Pressures," *Energy & Fuels*, no. 18, pp. 1521–1528, 2010.

[99] V. P. Zhukov, "Verification , Validation and Testing of Kinetic Models of Hydrogen Combustion in Fluid Dynamic Computations," *4th European Conference for Aerospace Sciences (EUCASS)*, vol. 2012, 2011.

[100] D. L. Baulch, C. T. Bowman, C. J. Cobos, R. A. Cox, T. Just, J. A. Kerr, M. J. Pilling, D. Stocker, J. Troe, W. Tsang, R. W. Walker, and J. Warnatz, "Evaluated Kinetic Data for Combustion Modeling: Supplement II," *Journal of Physical and Chemical Reference Data*, vol. 34, no. 3, pp. 757–1397, 2005.

[101] J. A. Manion, R. E. Huie, R. D. Levin, D. R. J. Burgess, V. L. Orkin, W. Tsang, W. S. McGivern, J. W. Hudgens, V. D. Knyazev, D. B. Atkinson, E. Chai, A. M. Tereza, C.-Y. Lin, T. C. Allison, W. G. Mallard, F. Westley, J. T. Herron, R. F. Hampson, and D. H. Frizzell, "NIST Chemical Kinetics Database," 2015. http://kinetics.nist.gov/.

[102] I. Couckuyt, T. Dhaene, and P. Demeester, "ooDACE Toolbox: A Flexible Object-Oriented Kriging Implementation," *Journal of Machine Learning Research*, vol. 15, pp. 3183–3186, 2014.

[103] E. Hu, X. Li, X. Meng, Y. Chen, Y. Cheng, Y. Xie, and Z. Huang, "Laminar flame speeds and ignition delay times of methane-air mixtures at elevated temperatures and pressures," *Fuel*, vol. 158, pp. 1–10, 2015.

[104] J. Zhang, L. Wei, X. Man, X. Jiang, Y. Zhang, E. Hu, and Z. Huang, "Experimental and Modeling Study of n-Butanol Oxidation at High Temperature," *Energy & Fuels*, vol. 26, no. 6, pp. 3368–3380, 2012.

[105] B. M. Adams, M. S. Ebeida, M. S. Eldred, G. Geraci, J. D. Jakeman, K. A. Maupin, J. A. Monschke, L. P. Swiler, J. A. Stephens, D. M. Vigil, T. M. Wildey, W. J. Bohnhoff, K. R. Dalbey, J. P. Eddy, R. W. Hooper, K. T. Hu, P. D. Hough, E. M. Ridgway, and A. Rushdi, "Dakota, A Multilevel Parallel Object-Oriented Framework for Design Optimization, Parameter Estimation, Uncertainty Quantification, and Sensitivity Analysis: Version 6.5 User's Manual," 2014.

[106] B. M. Adams, M. S. Ebeida, M. S. Eldred, G. Geraci, J. D. Jakeman, K. A. Maupin, J. A. Monschke, L. P. Swiler, J. A. Stephens, D. M. Vigil, T. M. Wildey, W. J. Bohnhoff, K. R. Dalbey, J. P. Eddy, R. W. Hooper, K. T. Hu, P. D. Hough, E. M. Ridgway, and A. Rushdi, "Dakota, A Multilevel Parallel Object-Oriented Framework for Design Optimization, Parameter Estimation, Uncertainty Quantification, and Sensitivity Analysis: Version 6.5 Reference Manual," 2014.

[107] "The DAKOTA project: Large-scale engineering optimization and uncertainty analysis." https://dakota.sandia.gov/.

[108] W. R. Elwasif, D. E. Bernholdt, S. Pannala, S. Allu, and S. S. Foley, "Parameter Sweep and Optimization of Loosely Coupled Simulations Using the DAKOTA Toolkit," in *2012 IEEE 15th International Conference on Computational Science and Engineering*, pp. 102–110, IEEE, dec 2012.

[109] R. A. Hansel, C. N. Brock, B. C. Paikoff, A. R. Tackett, and D. G. Walker, "Automated generation of highly accurate , efficient and transferable pseudopotentials," *Computer Physics Communications*, vol. 196, pp. 267–275, 2015.

[110] C. N. Brock, B. C. Paikoff, M. I. Sallih, A. R. Tackett, and D. G. Walker, "Force-based optimization of pseudopotentials for non-equilibrium configurations," *Computer Physics Communications*, vol. 201, pp. 106–118, 2016.

[111] N. V. Petrukhin, N. N. Grishin, and S. M. Sergeev, "Ignition delay time - an important fuel property," *Chemistry and Technology of Fuels and Oils*, vol. 51, pp. 581–584, Jan 2016.

[112] M. Karimi, B. Ochs, Z. Liu, D. Ranjan, and W. Sun, "Measurement of methane autoignition delays in carbon dioxide and argon diluents at high pressure conditions," *Combustion and Flame*, vol. 204, pp. 304–319, 2019.

[113] A. K. Das, C. J. Sung, Y. Zhang, and G. Mittal, "Ignition delay study of moist hydrogen/oxidizer mixtures using a rapid compression machine," *International Journal of Hydrogen Energy*, vol. 37, no. 8, pp. 6901–6911, 2012.

[114] N. Bourgeois, S. S. Goldsborough, H. Jeanmart, and F. Contino, "CFD simulations of Rapid Compression Machines using detailed chemistry: Evaluation of the 'crevice containment' concept," *Combustion and Flame*, vol. 189, pp. 225–239, 2018.

[115] U. Burke, W. K. Metcalfe, S. M. Burke, K. A. Heufer, P. Dagaut, and H. J. Curran, "A detailed chemical kinetic modeling, ignition delay time and jet-stirred reactor study of methanol oxidation," *Combustion and Flame*, vol. 165, pp. 125–136, mar 2016.

[116] B. C. Duva, L. E. Chance, and E. Toulson, "Effect of CO2 Dilution on the Laminar Burning Velocities of Premixed Methane/Air Flames at Elevated Temperature," *Journal of Engineering for Gas Turbines and Power*, vol. 142, mar 2020.

[117] P. Sabia, M. D. Joannon, M. Lubrano, and P. Giudicianni, "Autoignition delay times of propane mixtures under MILD conditions at atmospheric pressure," *Combustion and Flame*, vol. 161, no. 12, pp. 3022–3030, 2014.

[118] M. Lubrano Lavadera, P. Sabia, M. de Joannon, A. Cavaliere, and R. Ragucci, "Propane oxidation in a Jet Stirred Flow Reactor. The effect of H_2O as diluent species," *Experimental Thermal and Fluid Science*, no. January, 2018.

[119] S. J. Klippenstein, "From theoretical reaction dynamics to chemical modeling of combustion," *Proceedings of the Combustion Institute*, vol. 36, no. 1, pp. 77–111, 2017.

[120] C. Cavallotti, M. Pelucchi, Y. Georgievskii, and S. J. Klippenstein, "EStokTP: Electronic Structure to Temperature- and Pressure-Dependent Rate Constants-A Code for Automatically Predicting the Thermal Kinetics of Reactions," *Journal of Chemical Theory and Computation*, vol. 15, no. 2, pp. 1122–1145, 2019.

List of publications

International Journals

M. Fürst , P. Sabia , M.L. Lavadera , G. Aversano , M. de Joannon , A. Frassoldati and A. Parente, Optimization of chemical kinetics for methane and biomass pyrolysis products in moderate or intense low-oxygen dilution combustion, Energy Fuels 32 (10) (2018) 10194-10201

M. Ferrarotti, **M. Fürst**, E. Cresci, W. de Paepe and A. Parente, Key modeling aspects in the simulation of a quasi-industrial 20 kW moderate or intense low-oxygen dilution combustion chamber, Energy Fuels 32 (10) (2018) 10228-10241

R. Longo, **M. Fürst**, A. Bellemans, M. Ferrarotti, M. Derudi and A. Parente, CFD dispersion study based on a variable Schmidt formulation for flows around different configurations of ground-mounted buildings, Building and Environment 154 (2019) 336-347

In preparation for International Journals

M. Fürst , A. Bertolino, A. Cuoci, T. Faravelli , A. Frassoldati and A. Parente, `OptiSMOKE++`: A toolbox for optimization of chemical kinetic mechanisms, (2020)